



Applications and multidisciplinary perspective on 3D printing techniques: Recent developments and future trends

Amir A. Elhadad^a, Ana Rosa-Sainz^b, Raquel Cañete^c, Estela Peralta^c, Belén Begines^d,
Mario Balbuena^b, Ana Alcudia^d, Y. Torres^{b,*}

^a Department of Pre-Clinical Oral Health Sciences, College of Dental Medicine, QU-Health, Qatar University, Qatar

^b Departamento de Ingeniería y Ciencia de los Materiales y del Transporte, Escuela Politécnica Superior, Universidad de Sevilla, 41011 Seville, Spain

^c Departamento de Ingeniería del Diseño, Escuela Politécnica Superior, Universidad de Sevilla, Seville 41011, Spain

^d Departamento de Química Orgánica y Farmacéutica, Facultad de Farmacia, Universidad de Sevilla, 41012 Seville, Spain



ARTICLE INFO

Keywords:

Additive manufacturing
3D/4D printing
Smart materials
Bioprinting
Tissue regeneration

ABSTRACT

In industries as diverse as automotive, aerospace, medical, energy, construction, electronics, and food, the engineering technology known as 3D printing or additive manufacturing facilitates the fabrication of rapid prototypes and the delivery of customized parts. This article explores recent advancements and emerging trends in 3D printing from a novel multidisciplinary perspective. It also provides a clear overview of the various 3D printing techniques used for producing parts and components in three dimensions. The application of these techniques in bioprinting and an up-to-date comprehensive review of their positive and negative aspects are covered, as well as the variety of materials used, with an emphasis on composites, hybrids, and smart materials. This article also provides an updated overview of 4D bioprinting technology, including biomaterial functions, bioprinting materials, and a targeted approach to various tissue engineering and regenerative medicine (TERM) applications. As a foundation for anticipated developments for TERM applications that could be useful for their successful usage in clinical settings, this article also examines present challenges and obstacles in 4D bioprinting technology. Finally, the article also outlines future regulations that will assist researchers in the manufacture of complex products and in the exploration of potential solutions to technological issues.

1. Introduction

In the last three decades, additive manufacturing (AM) technology has advanced significantly and is currently being used in a variety of sectors. This technology has been referenced by an array of labels, including rapid prototyping (RP), layered manufacturing (LM), and solid free-form fabrication (SFF) [1]. Recently, AM applications have greatly increased in a variety of industries, including the biomedicine, energy, automobile, aerospace, and automotive industries [2]. For aerospace systems, where complex layouts and materials such as titanium alloys, nickel superalloys, and high temperature refractories are routinely used, AM offers an economical alternative to conventional production techniques [2,3]. In this sense, several structural and operational automotive elements, such as engine exhausts, drive shafts, gearbox parts, and braking devices for low-volume automobiles, can also be produced at a lower cost through the use of AM. The biomedical sciences are increasingly utilizing 3D printing (3DP), proving its usefulness for

numerous research and medical applications. The manufacture of implants for bones, biological scaffolds, artificial organs, medicine devices, microvasculature networks, and biological chips is without a doubt among the most significant uses of AM [4,5].

The 3DP manufacturing process is based primarily on computer-aided design (CAD), which is later divided into layers by appropriate software and fed to a 3D printer to proceed with computer-aided manufacture (CAM) [6]. Charles W. Hull registered the first patent for the 3D printer on 8 August 1984; however, it was named an apparatus for the production of 3D objects by Stereolithography (SLA) [7]. He defined this process as the "printing" of consecutive layers of material on top of one another to produce a 3D object. Hull's technique required directing ultraviolet (UV) rays onto liquid photopolymers, which are curable liquids [7]. Subsequently, he continued acquiring patents for AM, including one for the standard tessellation language format (STL), which integrates the CAD with the 3D printer [8]. Since then, SLA has remained the most popular AM technique despite going through many

* Corresponding author.

E-mail address: ytorres@us.es (Y. Torres).

changes and the introduction of several new types of printers [9]. When Scott Crump obtained a patent for fused deposition modeling (FDM) in 1992, the manufacturing industry underwent an evolution. Components are produced by extruding material, typically a thermoplastic polymer in the form of a filament, through a nozzle that is computer controlled on an XY platform [10]. Michael Cima and Emanuel Sachs, two professors at the Massachusetts Institute of Technology, did not receive their patent for the "3D printer" until 1993. With the use of an inkjet printhead and a binder application method, their invention could be used to print objects composed of plastic, metal, and ceramic.

Table 1 shows the four main components of the effective parameters in AM: input, method, materials, and applications. When AM is addressed, the word "input" typically refers to the digital design files (like CAD files) that the printer uses. Although numerous methods have been established for AM systems, they typically fall into four categories: (1) slicing and connecting, (2) melting and hardening or combining, (3) joining or binding, and (4) photocuring. The last kind can be further classified into a single laser beam and a double laser beam [11]. There are several different types of materials that can be used in AM systems, including solid, liquid and powder [11]. Pellets, wires, and laminates are examples of solid materials. Paper, polymer, wax, resins, metals, and ceramics are some common materials used in AM. Applications are divided into three groups in a variety of industries: manufacturing and tooling, engineering and analysis, and design [11].

Global awareness of 3DP is increasing as it develops and has a transformative impact on how items are manufactured in a variety of fields, including healthcare and medical [12], aerospace and transportation [13], food industry [14], digital art, textiles and clothing [15], and architecture and construction design [16]. Considering many aspects of AM and the critical variables that could influence the production properties is essential in order to choose the ideal type of AM for particular applications. **Fig. 1** describes the most recent 3DP procedures, as well as the application and custom characteristics of the final products.

2. Classification of 3D printing techniques

One of the most problematic aspects of the various AM methods available for 3DP is that the authors' categorization of the diverse approaches varies slightly depending on the literature. Each technique may also be subcategorized according to the technology on which the equipment is built, giving a complicated and perhaps misleading picture of the global issue. It is typical to encounter scientific papers that refer to the same AM approach under several titles, making it difficult to

correlate information and obtain a comprehensive grasp of AM. However, the most widely used classification is the one offered by the ISO/ASTM 52900:2015 standard, which differentiates AM processes into seven major classes: (1) Vat Photopolymerization (VP); (2) Material Jetting (MJ); (3) Binder Jetting (BJ); (4) Powder Bed Fusion (PBF); (5) Material Extrusion (ME); (6) Directed Energy Deposition (DED); and (7) Sheet Lamination (SL) [17,18]. **Fig. 2** shows a schematic representation of AM processes classified according to ISO/ASTM 52900: 2015 standard [17,18].

To construct an object, the printing method includes image acquisition, image processing, and 3DP, as illustrated in **Fig. 3** [19,20]. The stage of image acquiring includes imaging the object to be printed using X-rays, computed tomography (CT), or magnetic resonance imaging (MRI) [20]. The second stage involves image processing employing software capable of segmenting images and producing a 3D CAD surface model in STL format using a 20 triangle mesh [21]. Once the image processing step is finished, the slicer program receives the STL file and begins to slice it in layers [22], according to the parameters determined by the 3DP technique and the material used. Using the 3D model, a software generates a tool path plan in the form of a g-code file, providing the printer with the motion path required to deposit ink at the correct location and time [23]. After that, the 3DP builds the object layer-by-layer until it produces a construct that may require physical or chemical cross-linking for structural stability.

When comparing AM to subtractive manufacturing (cutting, drilling, micromachining, etc.) and formative manufacturing techniques (casting, forging, welding, etc.), ISO/ASTM 52900:2015 standard defines AM as the process of integrating materials to produce parts from 3D model data, typically layer-by-layer [24]. When compared to more conventional subtractive manufacturing, typically involves cutting the required shape from a block of material, layer-by-layer fabrication drastically reduces material waste and enables the fabrication of complicated geometries [25].

2.1. Material Jetting (MJ)

Material Jetting (MJ), as illustrated in **Fig. 4**, uses micronozzles to deposit a thin layer of photopolymer or wax-like materials on the surface of the build platform [26]. With this technology, a layer of liquid is initially printed on the build plate, and then it is UV-hardened. The building plate is lowered so that the following layer could be printed on top. The polymer layer is photopolymerized with UV light, and the 3D object is built up layer-by-layer [26]. Multiple materials can be produced at once using one or more printer heads. The rationale is that each

Table 1
Input, materials, methods and application of additive manufacturing.

INPUT		MATERIAL		
CAD Model surface or solid	Physical object	Laminates, pellets, wire	Powder	Liquid
STL, IGES, OBJ, AMF, 3MF, others	Point data from digitizer	Paper, resins, powders (nylon, alumide), ABS, PLA, PC, Wax, graphite, graphene, Metals, ceramics, carbon fiber, others.		
Slice and layer data, speed, inside fill				
ADDITIVE MANUFACTURING				
Cutting and glueing/ joining	Single laser beam	Photo-curing	Design	Engineering and analysis
Joining/binding	Two laser beam		Manufacturing	
Melting and solidifying fusing	Masked lamp		Aerospace, automotive, medical/healthcare, food, consumer product industries, others	
METHOD		APPLICATIONS		

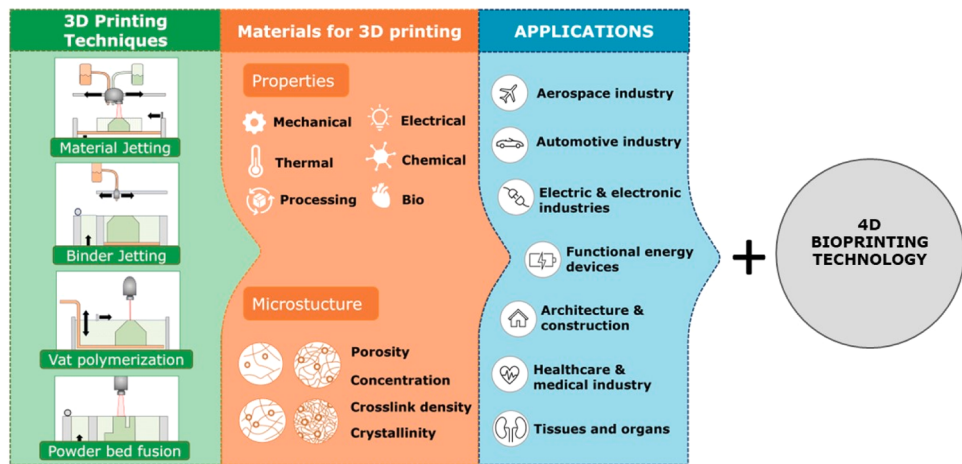


Fig. 1. The most recent 3D printing procedures, as well as the application and customized properties of the final products.

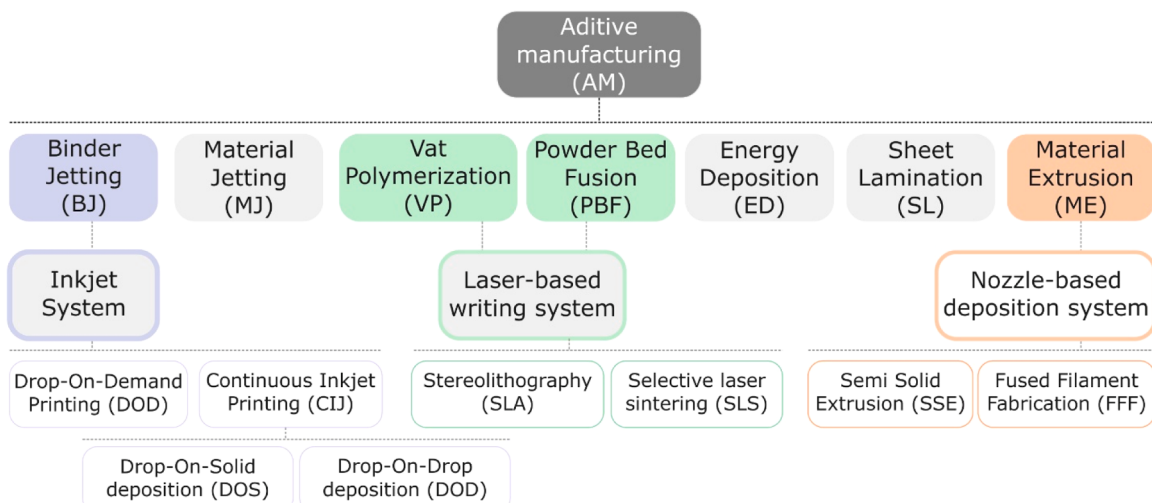


Fig. 2. An overview of the techniques used in additive manufacturing according to ISO/ASTM 52900:2015 [17,18].

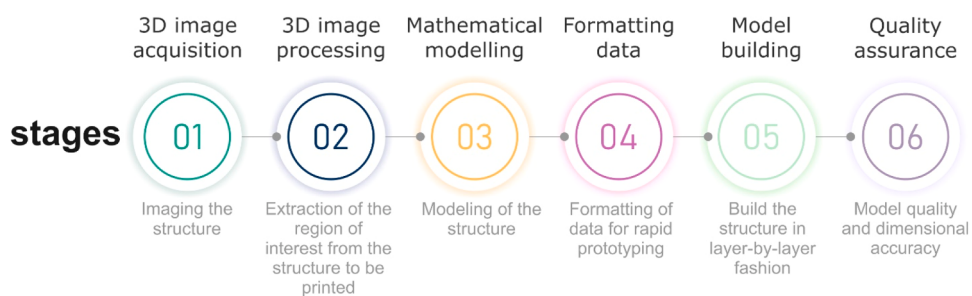


Fig. 3. Schematic of the various phases in the three-dimensional printing process.

of the several nozzle arrays functions as a distinct channel. The utilization of micronozzles enables multi-material printing and the employing of soluble supports to stabilize the printed object if it has a difficult shape. The supporting material is simply removed after the 3D impression and the finished product is obtained with a very good surface finish remaining. The printers used by MJ can produce layers with a thickness of 50–25 µm, and the manufactured items have a high resolution [27,28]. MJ technology offers higher productivity, a larger range of part sizes, and a wider availability of materials than other techniques such as Vat Photopolymerization. In a standard practical MJ system, the

materials are deposited by fifty up to hundreds MJ nozzles [28].

Compared to other processes, the mechanism of MJ is significantly easier because printing machines do not need complicated components. High manufacturing speed is another advantage of this method [29]. In fact, the ability of this method to manufacture parts so quickly with high resolution and adequate surface polish depends on hundreds or thousands of nozzles [29,30]. Additionally, the ability to print both multi-material and multicolour items distinguishes it from other AM technologies. In comparison, the most significant drawbacks or restrictions of MJ could be listed as high prices, poor mechanical

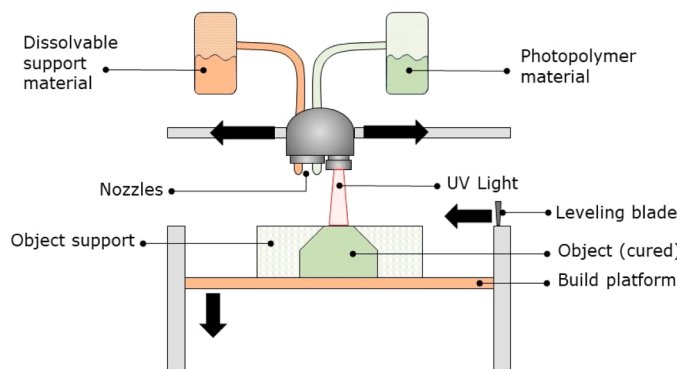


Fig. 4. Schematic diagram of Material Jetting (MJ).

characteristics (photopolymers cured with UV tend to lose mechanical characteristics over time), restricted durability and material selection. Besides, MJ also finds limitations in biomedical applications due to the UV light used to cure the photopolymeric materials [30].

There are two basic types of MJ that may be distinguished based on how droplets are produced and released: continuous stream (MJ-CS, Fig. 5a) and drop on demand (MJ-DOD, Fig. 5b).

2.1.1. Continuous-Stream mode (MJ-CS)

In MJ-CS mode (Fig. 5a), the fluid flow is split into droplets upon release from the nozzle by a continuous column of fluid under constant pressure. Vibration, disturbance, or jet modulation may cause this splitting [31]. The droplets travel through a charging zone to control the speed of deposition before being diverted to their destinations by high-voltage deflection plates. The plus side of this approach is its rapid rate of deposition, which may find application in medicinal labeling [31]. The drawbacks, however, include the need for the material employed to be able to transfer charge and the expense of recycling of or reusing the deflected droplets after the fluid is released [31].

2.1.2. Drop-on-demand mode (MJ-DOD)

In contrast to continuous operation, MJ-DOD (Fig. 5b) produces distinct droplets immediately from the nozzle [31]. Pressure increases within each nozzle cause droplets to develop at specific times as a result of thermal, piezoelectric, electrostatic, acoustic or other actuators [31]. The liquid material is continuously blasted out of the nozzle in continuous mode, where it breaks into individual droplets after leaving the spray head. To ensure that the jet separates into discrete drops of consistent size, vibrations can, for example, regulate the time of splitting. After leaving the nozzle, the material droplets must be redirected in the required direction to ensure that they are sprayed only onto the structure at the intended place. As a result, the droplets either already possess an electric charge or first pass through a charged field before receiving one. In a deflecting field, the particles are then redirected to the desired point. The MJ-DOD approach has the advantage of producing considerably smaller droplets, which allows for better resolution of

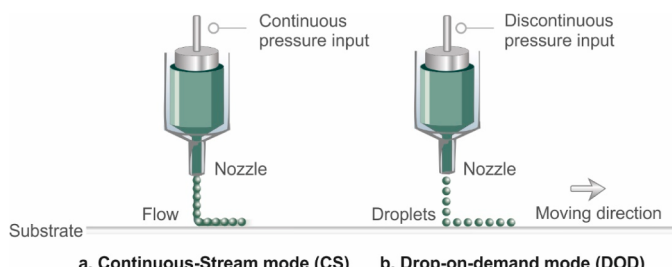


Fig. 5. Material Jetting deposition modes: (a) continuous (b) and drop-on demand droplet.

the latter object, while MJ-CS can manufacture droplets much faster than MJ-DOD. Another issue is that unwanted drops must be discarded or reinserted into the system, which could waste material or cause the repurposed substance to lose its sterility [32].

2.2. Binder Jetting (BJ)

As stated by Saches et al., Binder Jetting technology (BJ) is an integration of the MJ-AM and PBF-AM techniques [33]. BJ, often known as inkjet printing, is the second most common 3DP method used in the construction sector [34]. The setup has two chambers: one is a powder tank, while the other is a platform for construction [35]. The method binds particles, which might be made of polymers [36], ceramics [37], metals [38], or composites [39], according to a 3D model employing a number of nozzles to deliver a liquid binder to the powder bed. Fig. 6 shows the layout of a BJ system.

While acting as a bonding agent, the binder is applied to the print bed initially in a thin film, and then is carefully coated on the powder layer in accordance with the pattern of the current layer. Subsequently, this procedure is repeated layer by layer until the final design is created, as illustrated in Fig. 7 [35]. This 3DP technology does not involve high temperatures or a laser since the powder particles are bound by the liquid binder rather than sintering or melting, allowing the production of large parts at reasonable cost [40]. The item produced (also known as the "green body") is removed from the building platform for additional post-processing when the bonding process is complete [41]. To improve the physical characteristics of the final product, the "green body" must undergo energy-based consolidation [41].

For metallic parts in particular, post-processing is a challenging phase in BJ that needs to be properly handled. The "green body" must be de-binded for 6–12 h before being heated at a specific temperature for a specific amount of time, depending on the type of metal. Consolidation, infiltration, and sintering are all stages of heat treatment. The BJ process can be described in general terms as follows [42]:

- **Printing.** Regardless of the cutting-edge materials being produced, the current BJ process is identical to that of its older iteration [42].
- **Curing cycle.** In BJ, which uses the build box, the powder bed and the parts produced are frequently cured simultaneously to eliminate the remaining binder in the manufactured piece [43]. Binder system, printed component design, component wall thicknesses, powder bed, and printed job box height all have an impact on the curing temperature and duration [43]. Typically, a curing phase is used to enhance the binding between the binder and the powders through further polymerization and crosslinking [44]. A binder is sprayed by jetting, and it dries while printing. In contrast, curing involves heating the entire building box for eight hours in an oven at 185–200°C to strengthen the mechanical characteristics of the printed components [44].

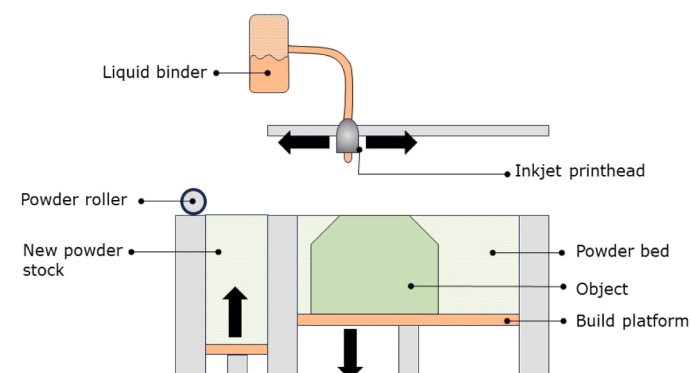


Fig. 6. Schematic diagram of Binder Jetting (BJ).

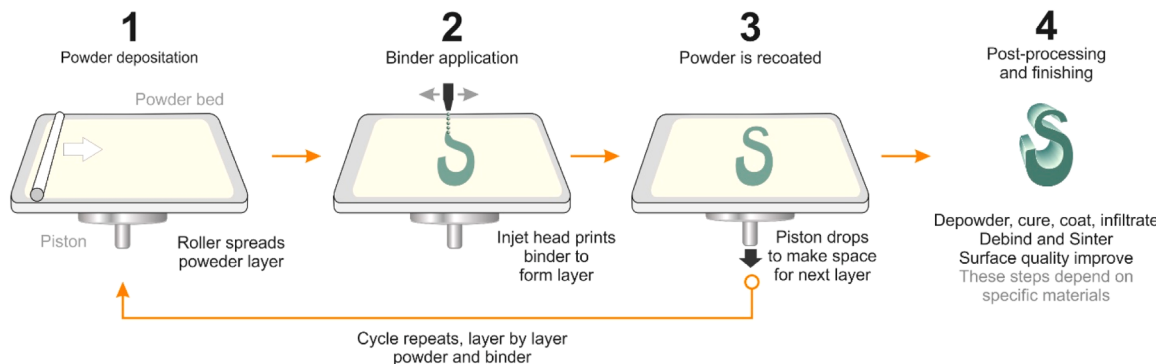


Fig. 7. Binder Jetting 3D printing process.

- **De-powdering.** After curing, the “green body” must be cleaned of extra or loose powder to make them durable enough to handle [44].
- **Measuring the “green body” strength** after the curing and de-powdering phases.

1. **Pyrolysis or Burnout step.** Binder-jetted parts are exposed to a burning cycle as soon as the cured green items are ready for densification.
2. **Impacts of residual matter and material chemistry.** Once the binder has been gasified or degraded and most of the green component has been eliminated, there may occasionally still be some oxygen and carbon left [45].
3. **Sintering and/or Infiltration.** After curing and de-powdering, the relative density of the “green body” is typically between 50% and 60%. To achieve the desired density along with the targeted mechanical properties, further densification can be performed using a variety of methods [45].

1. **Infiltration.** The remaining porosity can be completely eliminated, and the full density can be reached with almost no dimensional modifications by infiltrating an alloy (such as bronze with steel) with a lower melting temperature than the 3DP matrix.
2. **Sintering.** The alternative method for densifying BJ components is sintering, a process during which BJ pieces shrink in order to remove its printing-induced porosity. The sintering environment, powder shape, powder composition, surface area, and pressurized spray deposition (PSD) all have an impact on the kinetics and densification of the sintering. The dynamics and linear shrinkage of densification are both impacted by PSD. Given that shrinkage, microstructure, porosity, and phase formation in the final product can be affected by PSD.

Finishing. BJ pieces typically have an average surface roughness of 6 µm (Ra) after sintering, and post-processing is essential to enhance surface finish [45]. The two processes that are most frequently used to improve surface quality are bead blasting and tumble polishing; however, additional processes, including plating, machining, extrude honing, surface infiltration, and hand polishing, are also effective. Tumble polishing can produce an average surface roughness of 1.25 µm, however bead blasting can only decrease it to a maximum of 7.4 µm.

The BJ technique also makes extensive use of ceramic particles in addition to metal powders. Similar steps are taken to remove the polymer binder from ceramics using a thermal decomposition. Additionally, after sintering, a ceramic-metal composite part can be produced with metal powders. With regard to the vast majority of polymer powders, the “green body” is typically ready for use without requiring any additional post-processing. However, depending on the final product, some green bodies made from polymer powders may require post-processing processes [28].

BJ has recently been used for waveguide circuits, antennas, solid oxide fuel cells, electronic devices, culinary technology, concrete construction, renewable biobased materials, ceramic scaffolds, biopolymers and biomedical applications including drug delivery [46]. Combining PBF with MJ, BJ involves depositing a single layer of powdered material on the printing bed and afterward depositing a liquid binder at the curing locations. Typically, this technique is applied to metals, ceramics, and sands [47,48]. However, once the binder is removed, the manufactured item is frequently heated and sintered to improve its mechanical characteristics, requiring post-processing, which prolongs and increases the cost of the entire process [49]. The ability to print complicated designs in several materials, as well as the low cost and comfortable operating conditions, make this AM technology attractive for medical uses, including bone tissue engineering [50]. Thus, BJ is a reasonably inexpensive, high-speed process that can be utilized in mass production.

BJ is similar to the MJ technique, as was already stated. As a result, it has additional advantages in addition to the multiple upsides of MJ [39]. It is a faster process than MJ since only a tiny volume fraction of the whole amount (binder) needs to be deposited [31,39]. On the other hand, the BJ mechanism makes it easier to produce composite components by mixing powder materials and additives with a binder liquid [38]. Some material compositions that are difficult to be fabricated through traditional procedures might be achieved through this process. Additionally, larger solid-volume fraction binder slurries can be used in BJ [39]. Besides, BJ is an effective procedure for building multicolor parts, as it allows the addition of different colors while printing [31,51].

BJ has the following extra advantages [44,52–54]:

- Almost all powdered materials are compatible with it. The suitability of a material for its use on BJ depends on a number of parameters, including the extent to which it can be powdered and the way in which it interacts with the binder.
- Concerns with oxidation, residual stress, elemental segregation, and phase shifts are eliminated since the shaping process occurs at ambient temperature in a normal atmosphere. Due to this, the powder surrounding the components in the build box is quite recyclable.
- Due to the fact that BJ devices do not employ costly sealed chambers for vacuum or inerting, they can also produce some of the biggest build volumes of any AM technologies (up to 2200·1200·600 mm) while maintaining the exceptional inkjet resolution.
- The job box includes loose powder to support the part (no need for support material). Each part design produced during printing with BJ will not really require a support structure.
- To partially cure the binder during construction, a minimal amount of heating is used. Because no significant heating or melting occurs during BJ, thermally produced stresses and distortions in BJ components are therefore avoided.

- It can be used to make huge amounts of parts more quickly and cheaply. BJ is additionally more suitable than other AM methods for particular geometries and fine details.
- Depending on the sintering temperature and time, various densities with controllable porosity with respect to size and shape are possible.
- Since this technology is based on deposition, by varying the deposition material, especially in the case of natural-structure imitation, matrix, and reinforcement phase, it is easy to produce multi-material and multicolored parts.

However, the major drawback of BJ state as follows:

- Densification and curing are required as post-processing procedures in the multistep BJ [55].
- Given that printed parts have a lower relative density (50%) than other parts, densification after this point usually results in significant geometric deformation [56].
- Lower resolution and higher surface roughness are typical of the part produced (0.5–50 m) [57].
- Improvement of a post-processing procedure is still necessary for the majority of materials.

The primary downside of the BJ process at present is its incapacity of predicting the sizeable quantity of distortion that takes place when sintering single alloys at their full density. This further reduces the process' overall accuracy when manufacturing single-alloy parts, that are substantially larger compared to metal injection molding (MIM) size. The surface smoothness generated by this process is inferior to that of MJ or VP, and the strength of the components manufactured by this method is inferior to that of DED [58]. Additionally, the powder must be partially melted in the post-processing stage of the sintering process to generate dense pieces with reliable mechanical characteristics [31].

2.3. Vat polymerization (VP)

The fundamental concept of VP is to expose liquid polymeric precursors to UV-Vis light that promotes their polymerization and, therefore, solidification, and then repeat this operation layer-by-layer [59]. VP as seen in Fig. 8, is based on the selective curing of photopolymer resins, typically with UV-Vis light [59]. In comparison to other AM methods, dimensional precision and surface finish are the two main advantages associated with VP techniques. However, VP has limitations for use in medicine due to its expensive price tag, the requirement of manually removing support structures and postprocessing, and the limited choice of materials available (only photocurable polymers can be used) [60]. In an effort to expand the application of this strategy, several materials have been produced, such as investigating nanocomposites by adding nanoscale reinforcements to resin [61].

There are two primary forms for the photopolymerization process, which are as follows:

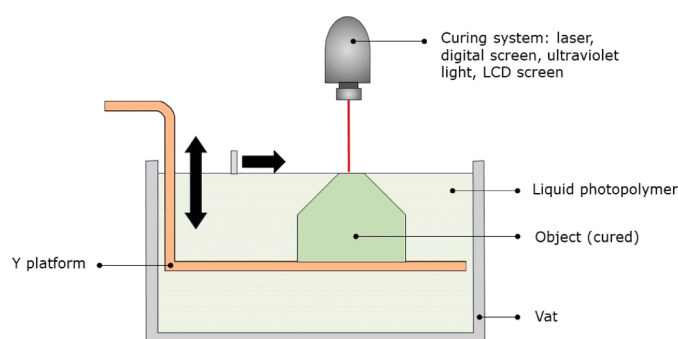


Fig. 8. Schematic diagram of Vat photopolymerization (VP).

2.3.1. Stereolithography (SLA)

The most popular VP-AM method, stereolithography (SLA, Fig. 9a), employs CAD/CAM software with a pre-programmed design or shape to concentrate a UV laser in a vat of photopolymer liquid resin [62]. The UV laser causes the resin to photochemically polymerize, forming a layer of the desired object. This procedure is performed for each layer of the design until the 3D item is complete [62]. This process is shown in Fig. 9b. SLA has excellent resolution and speed, yet it has numerous drawbacks: (i) it requires supporting structures to avoid deflection caused by gravity or to maintain newly produced sections that must be manually removed after printing [63]; (ii) despite having a rapid printing speed relative to other AM approaches, each layer is generated by a line-by-line path of the UV laser, resulting in a time-consuming procedure [64]; (iii) UV radiation can harm cells and tissues, and therefore has limited biomedical utility [64].

2.3.2. Digital Light Processing (DLP) and Continuous Liquid Interface Nature (CLIP)

To be able to overcome the obstacles brought about by the SLA technique, Digital Light Processing (DLP, Fig. 10a) projects a photomask that quickly cures each layer separately using digital microscopy capabilities, as illustrated in Fig. 10b [65]. As the aforementioned processes are discrete in nature, Continuous Liquid Interface Production (CLIP) allows the curing of the photopolymer layers in continuum, thanks to a dead zone of uncured resin between the cured resin and an oxygen-permeable membrane [66]. Oxygen works as a photopolymerization inhibitor, preventing the resin from adhering to the printing substrate and allowing for continuous printing of 3D objects between 25 and 100 times faster than DLP [60]. Furthermore, the mechanical properties of the printed item are isotropic because the CLIP procedure is continuous and does not entail the formation of stacked layers.

2.4. Powder Bed Fusion (PBF)

The Powder Bed Fusion technique (PBF) illustrated in Fig. 11 is a form of AM that melts powdered polymer, metal or ceramic materials using thermal energy (laser or electron beam) [67,68].

After the first layer has been sintered, the subsequent layer of powder is added to the powder bed. The thickness of each layer is determined by the distance from the completed layer's surface to the bottom edge [67]. Depending on the substance, its thickness can vary; for example, for metal powders, it can vary from a few tens of microns to 100 µm, whereas polymer systems have been found to have a thickness in the 50–150 µm range [68]. Once the layer has been placed on the plate, an energy beam is directed to the powder bed to create a slice of the object based on three-dimensional data. The instrument performs similar procedures for subsequent layers to complete the object after the first layer is completed. This process is shown in Fig. 12. PBF has attributes that include outstanding dimensional accuracy of the final item, high printing quality, and high resolution [68]. These attributes enable PBF technology to fabricate a wide variety of objects with intricate structural details. In many diverse fields, including aerospace, electronics, lattices, tissue engineering scaffolds, etc., this technique is frequently used for cutting-edge applications. Furthermore, PBF allows the printing of a wide range of materials, including composites, metals, ceramics, and polymers [67]. PBF, in comparison, has a slow processing time and significant expenses, which restricts its use. The high porosity in the finished products, in the case of powders fused with a binder, is another disadvantage of this method. Additional limiting parameters that must be selected with care include particle shape, size distribution, and size, with spherical particles of a particular size being employed to achieve the best results [69].

The PBF category can be subcategorized into four main technological subcategories [70]. (i) Selective laser sintering (SLS), which is utilized for plastics; (ii) direct metal laser sintering (DMLS), which is used for

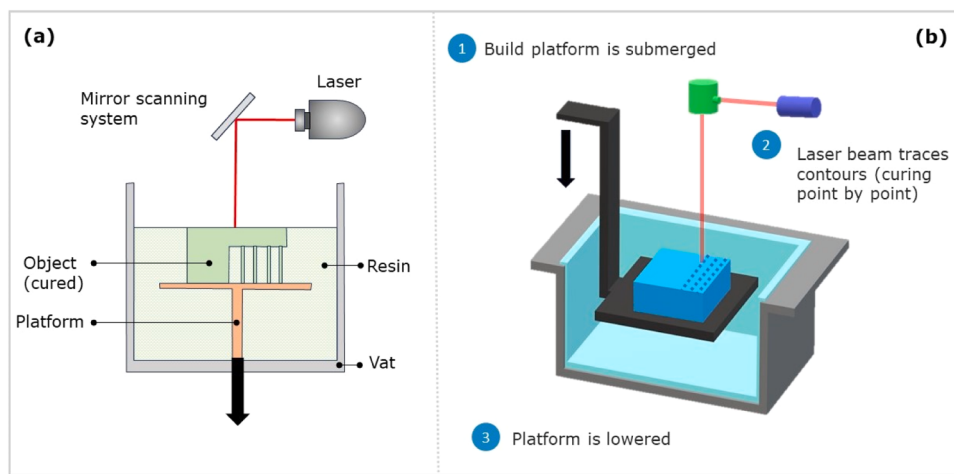


Fig. 9. Diagrammatic representation of stereolithography (SLA).

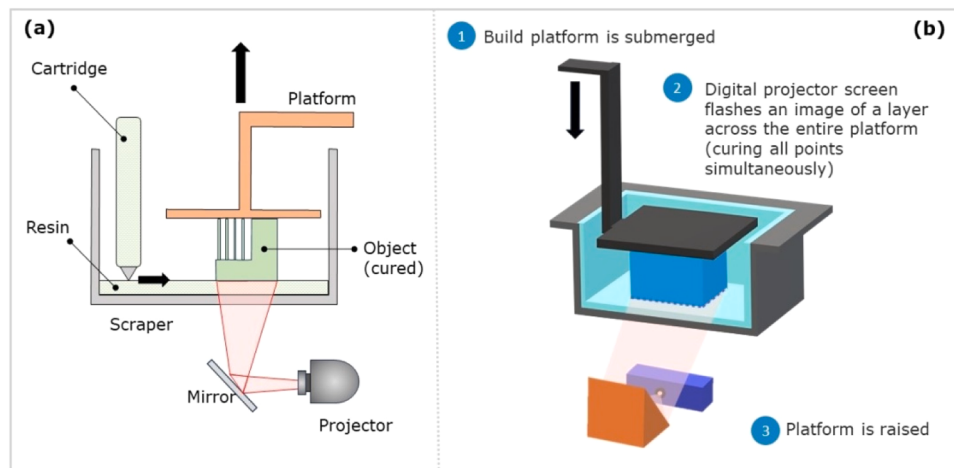


Fig. 10. Schematic diagram of digital light processing (DLP).

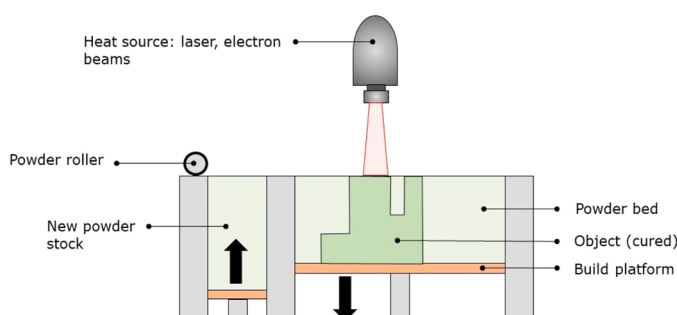


Fig. 11. Schematic diagram of Powder-Bed Fusion (PBF).

metals, including alloys; (iii) selective laser sintering (SLM), also used for metals; and (iv) electron beam melting (EBM), which operates similarly to SLM, with the exception that instead of using a laser, a high-energy electron beam is employed to melt the metal powder particles [71].

2.4.1. Selective Laser Sintering (SLS)

This SLS-AM technique illustrated in Fig. 13 involves heating microscopic particles with a powerful laser to temperatures where molecules can fuse together without completely melting them. As a

result, the energy beam employed for this operation must be carefully adjusted. For instance, SLS systems employ a CO₂ chamber controller and laser outputs in the range of 30–200 W. SLS is used to sinter any powdered material that does not decompose under a laser beam, such as polymers (polyether ketone, PEEK) or ceramics (hydroxyapatite, HA) [72]. A range of powder materials, including polyamide, steel, titanium, metallic alloys, ceramic powders, etc., has also previously been sintered by SLS. However, nowadays this technique is no longer employed to produce metal components [27].

2.4.2. Direct Metal Laser Sintering (DMLS)

DMLS is a well-known method for producing metal alloys utilized in a variety of fields, including aerospace, medicine, dentistry, etc. Since a liquid phase forms throughout the process, the powder cannot serve as a support; therefore, it is required to use an external support [27]. The mixed powder made of structural components and the binder can be produced using four different methods [17].

- Separate particles: the final powder contains both structural and binder particles that have been thoroughly mixed. Smaller binder particles may result in less shrinkage and reduced porosity in finished parts, according to the literature [27].
- Composite particles, which contain both structural and binding elements in each particle. Mechanical alloying is often used to create

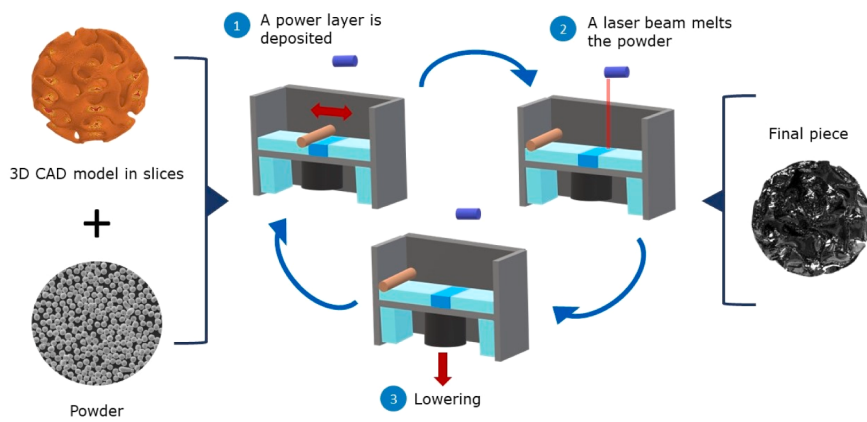


Fig. 12. Powder Bed Fusion (PBF) process.

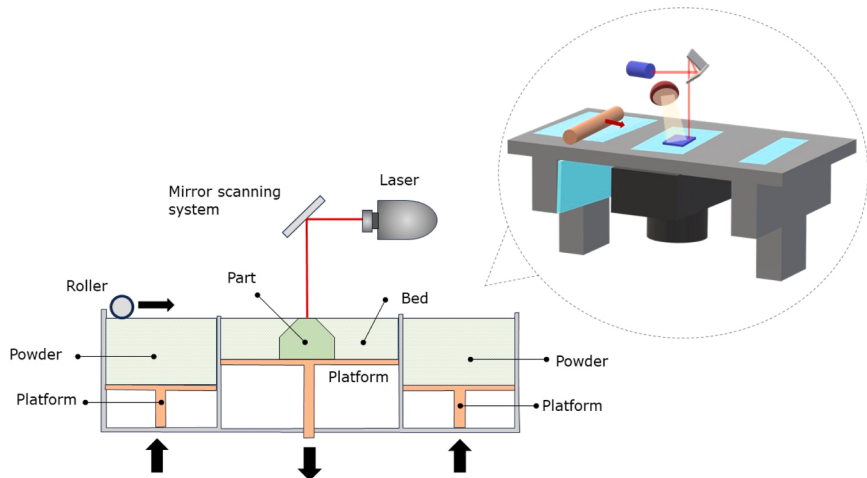


Fig. 13. Schematic diagram of SLS/SLM processes.

- composite particles. Having improved surface quality after the process is an advantage of these particles over separate particles [27].
- c) Coated particles: Such particles allow for the coating of structural material with a binder, improving flow characteristics, laser energy absorption, and structural particle binding [26].
- d) Pre-alloyed Particles: Each particle is an alloy made up of a combination of structural and binder components [17]. This type of particle cannot be divided into separate portions, which differentiates it from composite particles. In this scenario, only a portion of the particle melts, and the newly produced liquid phase breaks the particle into smaller pieces.

2.4.3. Selective laser melting (SLM)

Similarity to SLS, the SLM technique employs a potent laser energy to fuse the powder (316 L stainless steel, cobalt-chromium alloys, and titanium alloys) in a layer-by-layer manner as determined by the points specified by CAD file data, melting and consolidating each layer as it goes to create the final 3D product. Thermal energy itself is enough to melt the thin powder layer and fuse it to the previously formed layers. Consequently, the final products have compact architectures, excellent dimensional precision, and exceptional mechanical properties [73]. The ability to print layers with a thickness of 75–150 µm has recently been made possible by the introduction of a few contemporary machines with multi-laser technology [27].

Metallic alloys and semicrystalline polymers are the materials that are the most frequently used in SLM. For the highest strength to be achieved, nylon polymer, a common semicrystalline polymer, must be

completely melted. The materials employed in this technique for metal parts include cobalt chrome, steel, stainless steel, aluminum, and titanium alloys. When these metallic alloys are processed using SLM, their high melting and solidification produce a number of desirable features that conventional casting techniques would not be able to achieve [31].

The main issue that arises during the melting of metallic particles is oxidation. For example, metal particles that have grown oxide on their surface have less wettability. An additional issue with oxides in SLM processing is the possibility that they become trapped within the molten metal and create weak points within the component, lowering mechanical properties. Additionally, some metals with high reflectivity, such as aluminum, require higher laser strengths in SLM than in SLS. Additionally, increased laser power requirements caused by high thermal conductivity of metals may lead to higher energy and material costs [74].

2.4.4. Electron beam melting (EBM)

Fig. 14a illustrates electron beam melting (EBM), which works similarly to selective laser melting (SLM) but melts metal powder particles using a high-energy electron beam as opposed to a laser [71]. In reality, two magnetic fields focus the electrons to the required spot with the desired diameter of 0.1 mm after they have been expelled from a hot tungsten filament. When the beam strikes the powder bed, the quick electrons' kinetic energy is converted to thermal energy, which causes the powder to melt [75]. The EBM unit consists of a powder distribution system, vacuum chamber (10–4 torr), build tank, and electron beam guns [76,77]. The powder is fed into the bed through a rake framework,

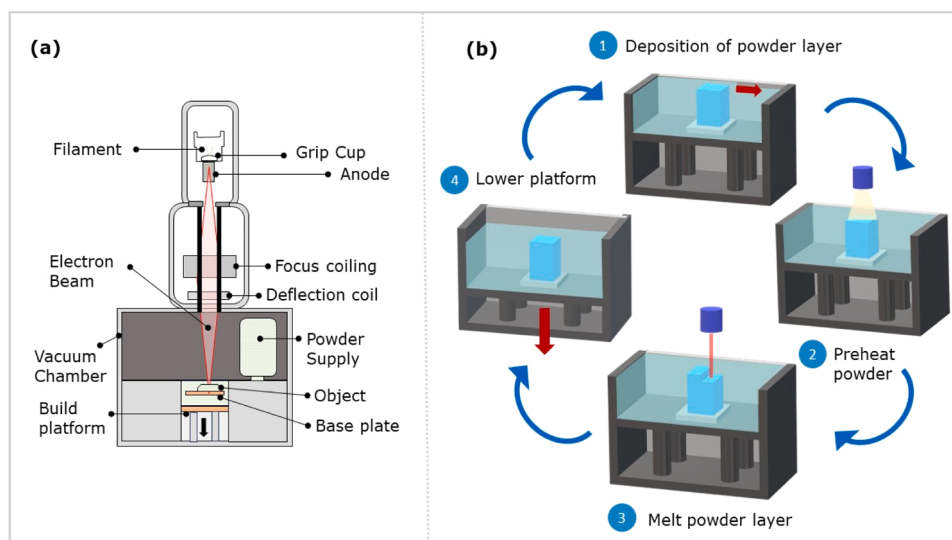


Fig. 14. Schematic diagram and process of the EBM system.

which is heated by an electron beam at the initial stage [76]. This causes the layer thickness to be 2–3 times higher than it has to be since the particles are randomly arranged next to one another with gaps. The thickness is decreased to the appropriate level with the melting of the powder layer [77]. Once the layer printing is completed, the platform is lowered to a layer thickness of (0.05–0.2 mm). Then another layer of powder is introduced, and the procedure is repeated until the whole thing is created, as illustrated in Fig. 14b. With the use of helium, cooling could last up to 6 h, depending on the size and nature of the object [77]. Various devices have been made in several industries, including the medical and aerospace sectors, using EBM. EBM is a technique used to manufacture metal parts made of Inconel 718 superalloy, titanium, and cobalt alloys [28,77].

Among the many advantages of EBM over laser processing is that, for the identical input energy, producing a beam energy from an electron beam is substantially more affordable. The quick beam movability of the EBM is another benefit that significantly accelerates manufacturing. Due to the greater bed temperature of EBM processing as opposed to laser manufacturing, minimal residual stress is arguably the most intriguing advantage [77]. However, the selection of materials is the major limitation of this technique. Only metal powders are used with EBM since the conductivity of the powder bed is crucial [31]. An additional issue with EBM is that electrical conduction from the plate to the powder is necessary for avoiding electron charging [31,77].

2.5. Directed Energy Deposition (DED)

Directed Energy Deposition (DED), illustrated in Fig. 15, commonly referred to as Direct Metal Deposition (DMD), functions similarly to

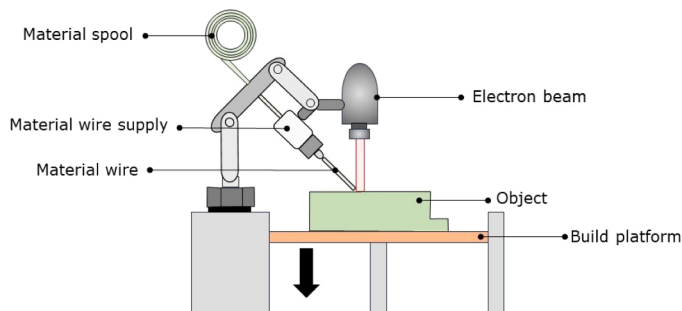


Fig. 15. Schematic diagram of Direct Energy Deposition (DED).

FDM, DED can be used with a variety of materials, such as metal matrix composites, polymers, and ceramics; however, it is most often used with metal parts [78]. The printing head melts metal in the form of powder or wire through the use of an electron or laser beam, which is then extruded and cooled [47,79]. The process is conceptually similar to material extrusion (ME), however with DED, a nozzle can travel in many directions along up to five separate axes, as opposed to only three for typical ME machines. The nozzle's varied degrees of flexibility making it perfect for maintenance and generating higher-quality products. The only limitation of this technique is that a balance between production speed and surface quality must be kept [58].

DED can refer to a variety of technologies [80]. Each is designed to perform a unique and distinct function, varying in how the material is fused. The following are the most common.

- Optomec LENS technology. In LENS 3D systems, lasers are employed to produce products in a layer-by-layer method using powdered metals, alloys, ceramics, or composites [81]. The LENS process must occur in a sealed room that contains argon to maintain extremely low levels of oxygen and moisture to avoid oxidation and preserve the cleaned part. The metal powder is provided directly to the deposition head and advances to the next layer after one layer has been deposited. Several layers are stacked on top of one another to create the full part. The completed item is removed and can then be heated, heated, isostatically pressed, machined, or polished. [81].
- Optomec Aerosol Jet Technology. Operational antennas for LTE, NFC, GPS, Wi-Fi, WLAN, and BT may be printed for a reasonable price using Optomec Aerosol Jet 3D printing technology [82]. This technology is comparable to straightforward deposition techniques; however, it works better for complex compound curved surfaces. Aerosol Jet systems are ideal for creating, enhancing, and maintaining high-performing electrical and biological devices for consumer electronics, semiconductor packaging, displays, aerospace/defense, automotive, and life sciences uses. The aerosol jet approach can be used employing a wide range of substances, comprising semiconductors, dielectric pastes, conductive nanoparticle metal inks, and other functional materials [83].
- An approximately ten times quicker powder nozzle than PBF technology is used in Laser Deposition Welding (LDW) and hybrid manufacturing by DMG MORI, as shown in Fig. 16a [84]. A 5-axis milling machine manufactured by DMG MORI also incorporates LDW-AM technology. The adaptability of the laser metal deposition process and the accuracy of cutting procedures are combined in this

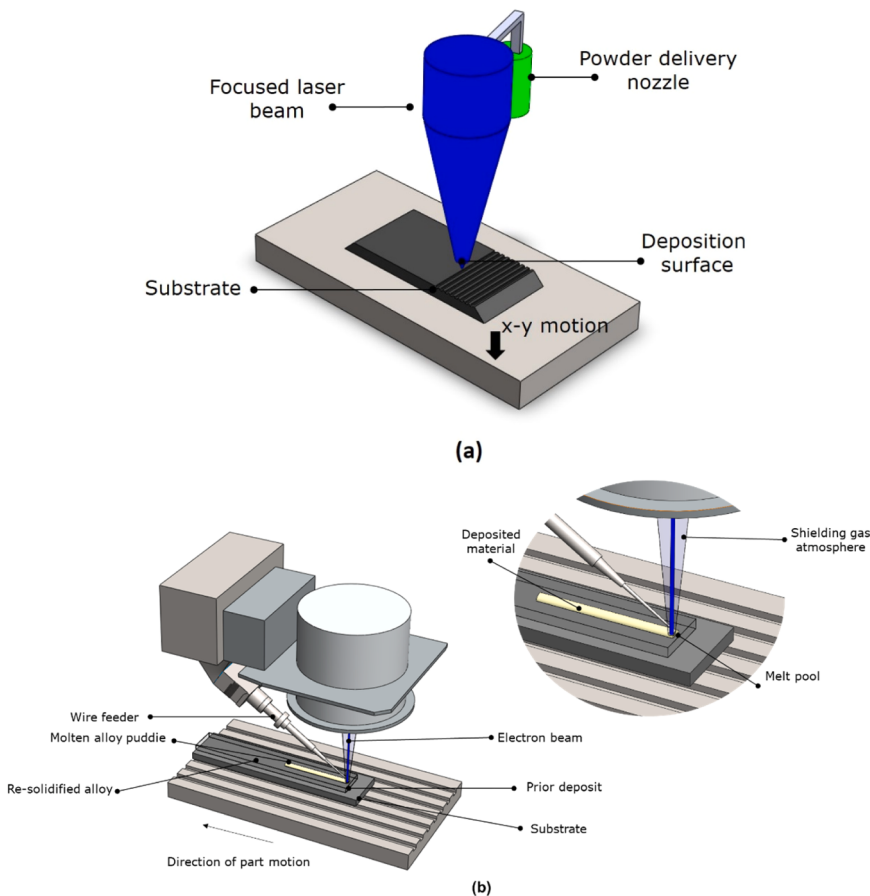


Fig. 16. Schematic diagram of (a) laser powder feed system and (b) electron beam wire feed system.

cutting-edge hybrid system to enable production [85]. Due to this combination, high-precision metal components in a range of sizes can be produced [85].

- Electron Beam Additive Manufacturing (EBAM) 3D printing technique illustrated in Fig. 16b, is an AM process used to create massive metal components. Metal deposition rates range from 3 to 9 kg per hour [86,87]. Metals that can be combined include titanium, tantalum, and nickel. The DED technique can also be used to repair damaged parts.

2.6. Sheet Lamination (SL)

With this AM technique, as shown in Fig. 17, sheets of material are sliced and bonded together to create a part. Originally designed for architectural paper models, it is now applicable to a wide range of

materials, including metals [47]. Sheet Lamination (SL), also called Laminated Object Manufacturing (LOM), is a process that connects and stacks sheet materials such as metals, ceramics, or composite fibers layer by layer to create 3D items [88]. These sheets are stacked on top of each other, and each layer is bonded to the one below it by using an adhesive. This bonding ensures that the layers adhere securely to create a cohesive structure. As shown in Fig. 17, once a layer is bonded, it is cut or shaped according to the object's design using techniques like laser cutting or knife cutting.

This procedure employs a limited number of polymers, metals, and ceramics [89]. It is less expensive than other processes and can be used to quickly produce enormous pieces, while the excess material left can be recycled [90]. However, there are difficulties in manufacturing its interior structure during the cutting phase of waste materials; hence, this technology has not been widely used [91]. SL uses metal laminates that

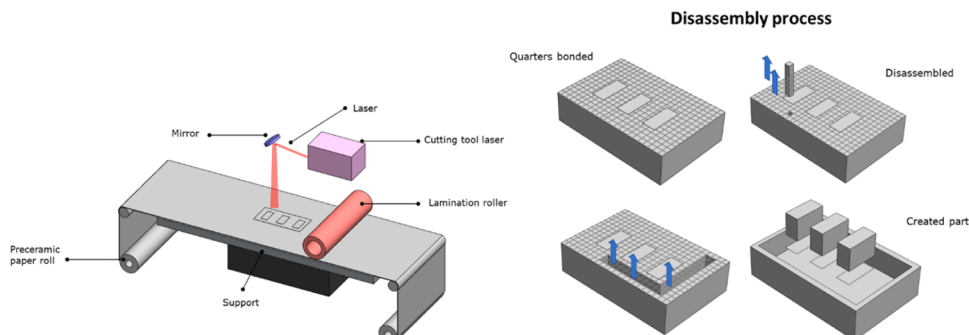


Fig. 17. Schematic diagram of LOM system.

can be several millimeters thick [91,92]. This increases productivity, lowering the cost of printed components, while making the process more cost effective than other AM methods [92]. However, SL does not meet expectations when it comes to producing items with complicated shapes and high surface precision. The increase in laminate thickness to expand production frequently results in a noticeable staircase effect [92,93]. SL is classified into two categories: "bond then form" (sheets are bonded prior to being cut to shape) and "form then bond" (sheets cut to shape initially and subsequently bonded) [89].

2.6.1. Ultrasonic Additive Manufacturing (UAM)

Ultrasonic Additive Manufacturing (UAM), also referred to as Ultrasonic Consolidation (UC), combines subtractive pattern milling and ultrasonic metal junction welding [94]. The sheet materials are bonded together, and the item is constructed onto a heated plate by rotating a sonotrode at a low-energy ultrasonic frequency [94,95]. The UAM shown in Fig. 18 is one of the most efficient methods for creating metal parts with the fewest changes in characteristics since objects can be produced from bottom to top at relatively mild temperatures between room temperature and 200 °C [95]. The piece is ultimately milled to achieve the appropriate shape.

UAM, on the other hand, can be thought of as a bond-then-form procedure, where the object is created after ultrasonic bonding. The most important factors that affect bonding quality in UAM include oscillation amplitude, average force, travel rate, and temperature [96]. The amount of ultrasonic energy is measured by the oscillation amplitude, with a larger amplitude indicating more energy [96]. According to published research, increasing the input of ultrasonic energy results in improved welding (bonding) quality [31]. However, depending on thickness, material and shape, there may be an ideal degree of input energy that must be used in harmony with the welding moving speed. Layers must have a sufficient load exerted on them by the sonotrode to achieve the optimal metallurgical bonding. Metals can form bonds more easily when heated, but too much heat will have negative effects [31, 96].

2.7. Material Extrusion (ME)

Material Extrusion (ME), depicted in Fig. 19, is one of the most widely used 3DP technologies due to its low cost and ability to be used with little or no additional equipment [97]. In the literature, it is alternately referred to as Fused Deposition Modeling (FDM), Fused Filament Fabrication (FFF), or Direct Ink Writing (DIW, which is typically utilized when the extruded material is a highly viscous and concentrated polymer) [97]. This process involves melting the materials and forcing them through a number of nozzles (extruders) to build up the 3D item layer-by-layer [98]. Printing with multiple materials at once can be achieved with various nozzles. Once a layer is printed, the build platform descends and the subsequent layer is deposited and adhered to the top of the preceding layer [98].

The diameter of the nozzle is a key factor in the extrusion process, as it determines the size and form of the material that is extruded. More material is deposited on the construction platform as a result of the

larger diameter, which also lowers the accuracy of the manufacturing [98]. The thermoplastic polymers most frequently used are polylactide (PLA) and acrylonitrile butadiene styrene (ABS) [17]. It is also common to find composite materials that combine various polymers with additional materials such as carbon fiber, para-aramid fibers (Kevlar fiber, KF), wood, etc. [17]. The three types of extruders utilized in this technique are plunger-based, filament-based, and screw-based, with filament extrusion being the most commonly used than the others [98]. These 3D printers are commercially affordable and are a well-liked option for homes or small businesses.

- Filament-based extruder (Fig. 20a). In this method, an already-formed polymer filament is remelted and extruded into the desired shape, where it quickly hardens [99]. The technical term for filament-based AM is FDM, also known as FFF [99]. To ensure continuous printing, the filament must simultaneously meet two opposing requirements in terms of quality, in addition to strict dimensional limits on the diameter of the filament (usually $\varnothing \pm 20 \mu\text{m}$) [100,101]. These properties, which have to do with stiffness and flexibility, assure that the filament cannot bend in the feeding system while still enabling it to be spooled in the winding machine [100].
- Screw-based extruder (Fig. 20b). A heated extrusion vessel is used to soften or liquefy a solid pelletized feedstock before it is advanced through the nozzle aperture by rotating the helical screw [102]. There is consensus that the use of pellets rather than filaments allows higher extrusion speeds and solid loading [103].
- Plunger-based extruder (Fig. 20c). This technique uses a plunger and a liquid-state material with a high solid content. Compared to their screw-based counterparts, plunger-based extruders are typically less precise in the start/stop phases; however, they do not need solid subproducts for feeding, such as filaments or pellets [104].

Table 2 sums up the fundamental ideas, advantages and disadvantages, and materials for various 3D printing processes.

3. Materials for 3D printing

3DP is thought to be one of the most inventive ways to fabricate different components from a variety of materials. An extensive variety of industries, including automotive, aerospace, medical, construction, electronics, and food industries, can use a variety of materials from many categories, such as metals, ceramics, polymers, composites, and hybrids. High-quality materials must meet rigorous standards in order for 3DP to reliably generate products of outstanding quality. To do this, the producers, consumers, and end users of the material agree to certain procedures, requirements, and material control obligations. Materials that can be used to create fully functional objects using 3DP technology include ceramics, metals, polymers, and their combinations in the form of hybrid, composite, or functionally graded materials.

Regarding 3DP materials used for biomedical applications, these biomaterials are categorized in four generations to the clinical needs of each generation. Since 1950, first-generation inert biomaterials have been manufactured and adopted to assist in the substitution of host tissue or healing processes while generating no negative effects on the biological system. Cobalt alloys, alumina, and stable polyurethane were among them, and they were crucial for use in orthopedic and dental applications. Ceramics such as alumina (Al_2O_3) and zirconia (ZrO_2) are examples of these materials. Since 1960, these materials have been used in total knee replacements, hip balls, and 120 femoral head implants [121]. The second generation of biomaterials emerged as a result of poor adhesion and implant loosening and the demand for materials with bioactive surfaces that are capable of building intricate interactions with the tissue. Therefore, since 1970, when the application of biodegradable materials was explored, materials with bioactive or biodegradable characteristics have been investigated [122]. Second-generation

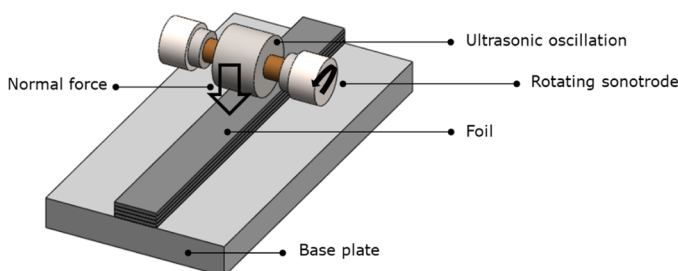


Fig. 18. Schematic diagram of the UAM system.

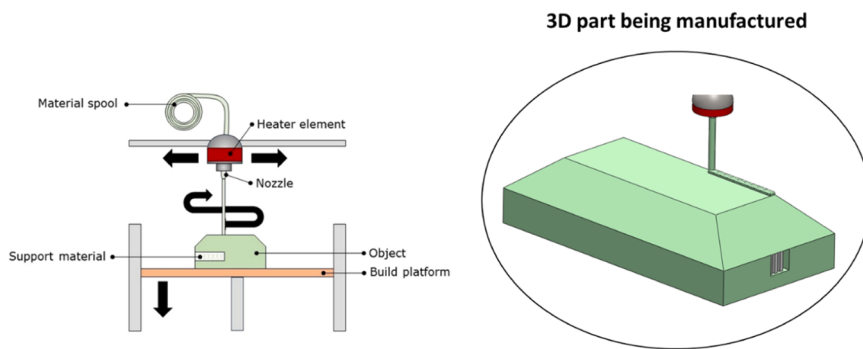


Fig. 19. Schematic diagram of Material Extrusion (ME).

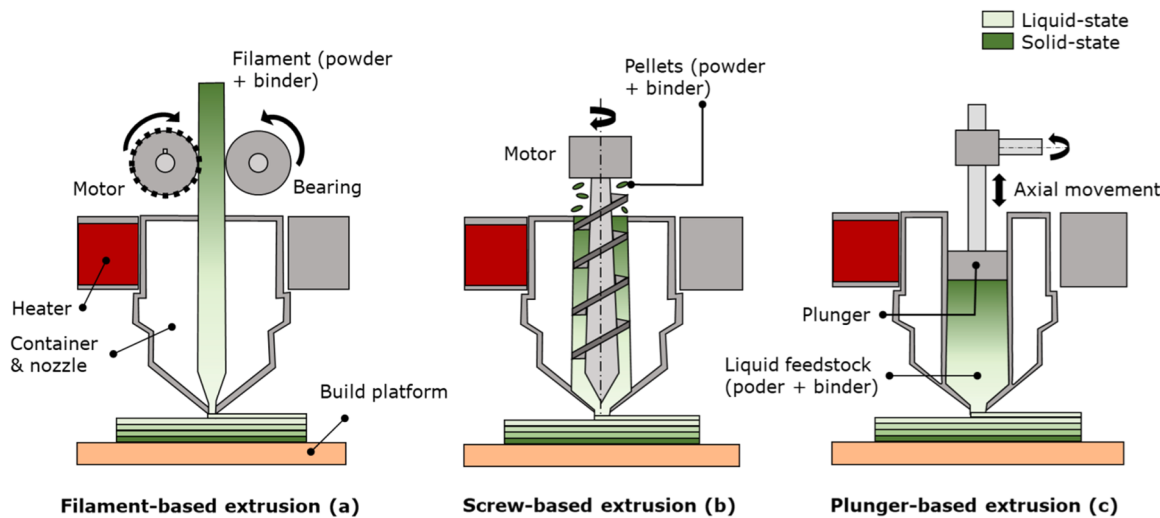


Fig. 20. Shows an overview of each of the three Material Extrusion systems: (a) filament-based, (b) screw-based, and (c) plunger-based.

biomaterials include, for instance, titanium and calcium phosphates, particularly hydroxyapatite [123,124]. The next phase of the study focused on finding temporary materials that can slowly degrade in a controlled manner to ensure natural integration of the implant with the living tissue that is intended to replace. Researchers are actively examining the bioactivity and biodegradation characteristics of third-generation materials such as magnesium and its alloys for cardiovascular stents and tissue regeneration [125]. Around 2010, scientists started investigating a new set of biomaterials. For its use in tissue engineering, this most recent generation of biomaterials includes biomimetic nanocomposites [126]. The four generations of biomaterials are depicted in Fig. 21.

3.1. Metals

A range of intricate manufacturing processes, including the 3DP of human organs and aircraft parts, can benefit from the usage of metallic materials due to their exceptional physical attributes [127–129]. Aluminum alloys [127], cobalt-based alloys [130], nickel-based alloys [131], stainless steels [132], and titanium alloys [133] represent just few of the instances of these materials. Due to its high specific stiffness and toughness, a cobalt-based alloy is suitable for dental applications in 3DP [130]. Furthermore, 3DP can be used to manufacture aircraft components using nickel base alloys [131]. 3DP objects produced of nickel base alloys can be utilized in dangerous environments owing to their exceptional resistance to corrosion and heat of up to 1200 °C [134]. Lastly, items made with 3DP technology may also be made from titanium alloys. The flexibility, excellent resistance to corrosion as well

as oxidation, and low density of titanium alloys are their distinguishing characteristics. It is employed, for instance, in biomedical devices [3, 135–137] and aircraft parts where there are high stresses, severe operating temperatures, and significant stresses [133].

3.1.1. 3DP metallic-based implants

Metal implants are required to restore function in many anatomical areas with typical orthopedic disorders. Adequateness is primarily determined by two factors: (1) biological reaction to the host bone, which is frequently attained by bulk or surface modification of such implants, and (2) mechanical stability, which can be further accomplished by using 3DP of tailored component based on the CT scan or MRI of the patient's defect site. According to the same principles as other 3DP operations, 3DP of metals generally involves the melting of metal powder feedstock employing either an electron beam or laser source. Consequently, PBF, DED (laser or electron beam) and MJ are common 3DP techniques for metallic-based implants. Metal implants have historically been used to assist bone regeneration mechanically [129,138, 139]. However, recent advances in AM have enabled the production of composite scaffolds with additional capabilities.

3.1.1.1. Titanium (Ti) and Ti alloys.

Cobalt-chromium-molybdenum (Co-Cr-Mo) and Ti-6Al-4 V alloys remain the metals most frequently used for AM in orthopedic implants. Wrought titanium Ti-6Al-4 V (ISO 5832-2) is the most widely used Ti alloy [3,140]. Compared to stainless steel and the Co-Cr-Mo alloy, it has a higher mechanical strength-weight ratio and better corrosion resistance, making it one of the most significant biomedical materials for the production of orthopedic implants [3].

Table 2

Key concepts, advantages and cons, and materials for various 3D printing techniques.

AM	Mechanism	Materials	Positive aspects	Negative aspects
BJ	A thin film of binding liquid is applied by spraying onto a layer of powder, and this process is repeated until the final item is obtained [13].	Metals [38] Polymers [36] Ceramics [37] Composites [39]	1. No need for support, 2. low cost, 3. rapid delivery, 4. large construct volume	1. Poor surface finish 2. Delicate pieces manufactured.
ME	The material undergoes heating until it is semi-solid, and it is then pushed along the designated path. Filler material is employed as required and is then easily removed [105].	Polymers [105] Composite [106]	1. Printing on a variety of materials, Color printing, 2. parts that are completely functional, 3. Cost-effective	1. Structured Step Surface 2. Vertical Anisotropy
DED	Same as ME. However, the nozzle has numerous degrees of freedom [107].	Metals [108] Hybrids [109]	1. Nozzle with many degrees of flexibility 2. used for repair parts of superior quality	1. Speed and finish must be balanced.
MJ	The material is released in droplets that solidify once exposed to UV radiation [110].	Polymers [111] Ceramics [112] Composites [110] Hybrid [112]	1. printing on multiple materials, 2. Surface finish that is smooth, 3. Exceptional dimensional precision	1. Support is needed. 2. Use of a limited variety of materials
PBF	Powder is melted and bonded using either an electron beam or a laser [113].	Metals [114] Polymers [115] Ceramics [116] Composites [117] Hybrids [118]	1. High Velocity, 2. There is no need for support, 3. high precision, 4. Quite affordable	1. Minimal build size, 2. high energy consumption, 3. Poor surface finish
SL	Layered object manufacturing and ultrasound AM, strips of material are bonded to make the desired part [119].	Metals [119] Polymers [119] Ceramics [119]	1. Full-color reproductions, 2. reasonably priced, 3. Material handling is made simple, 4. The excess material can be reused.	1. restricted variety of materials, 2. The surface finish is poor. 3. Strength is determined by the adhesive applied.
VP	Light is shone on a solidifying liquid polymer and this process is repeated layer-by-layer [120].	Polymers [114] Ceramics [114]	1. high precision, 2. Superior Surface Finish	1. Use of a limited number of materials, Poor mechanical aspects

Ti-6Al-4 V has good biocompatibility, particularly when direct contact with bone or tissue is required. The Ti alloy has been shown to offer a favorable surface for osteoblast attachment and osteogenic differentiation [3,141]. The development of a surface oxide layer that encourages osteoblast adherence can be achieved by binding adsorbed fibronectin to surface-expressed integrins [141,142]. An additional investigation found that growing osteoblast-like cells on a Ti-6Al-4 V alloy surface

could promote osteoblastic maturation by creating an osteogenic environment full of bone morphogenetic proteins and encouraging bone formation [141]. The findings indicated that altering the surface of Ti implants can improve osseointegration at the bone-implant contact for improved implant fixation [142]. Table 3 shows a comparison between orthopedic implants produced using AM and those produced using conventional methods.

Even before the invention of AM, Ti and its alloys were the preferred material for load-bearing biomedical implants [140,142]. Ti has excellent biocompatibility, excellent corrosion resistance, exceptional fatigue strength, and an adequate strength-to-weight ratio, making it the ideal material for orthopedic applications [3,140,141]. Unlike stainless steel and Co-Cr alloys, Ti has an elastic modulus that is similar to the one of bone [140]. In addition, Ti has excellent laser absorption and low thermal conductivity, making it a perfect material for metal AM [143]. By adding porosity to most Ti implants that have undergone AM processing, the elastic modulus can be brought even closer to the bone, reducing stress shielding and subsequently osteoporosis [140]. Most of the load-bearing implants developed today in the biomedical industry are additively made of Ti using AM technology [144]. Given their superior biocompatibility, initial stability resulting from a lower modulus, and a relatively inexpensive cost of production, 3DP Ti alloys have been widely used in biomedical devices for total knee and hip arthroplasty. Fig. 22 shows a brief timeline of Ti implant development for use in biomedical devices.

To achieve mechanical stability at the implantation site, Dumas et al. constructed a unique pore structure-graded diamond-type lattice design using the PBF-AM technique. They assessed the stiffness and yield strength of Ti64 structures with various porosities (80%, 58%, and 40%) [145]. Compared to those of trabecular and cortical bone, moduli of the porous structures, which ranged from 1.6 to 20.3 GPa, were found.

However, Ti and its alloys have some limitations, including poor tribological performance and a potential risk of metal ion leakage from wear debris close to the articulating surfaces [144]. Furthermore, despite the fact that Ti is biocompatible, it does not efficiently interact with adjacent bone and tissue for remodeling [144]. The improvement of osseointegration in vivo through Ti alloying with other elements such as tantalum or modifying the surface by the development of TiO₂ nanotubes has been verified [146].

Commercially pure Ti (CP-Ti) has better biological results under physiological conditions compared to other frequently used Ti alloys, as a thin TiO₂ coating forms on its surface [147]. However, it is weak and has poor fatigue resistance [148]. On the other hand, the Ti-6Al-4 V alloy is well known for its great strength and superior fatigue resistance. Since its development by aerospace firms, the Ti-6Al-4 V alloy has seen widespread use in orthopedic load-bearing applications [149]. In the early stages of Ti alloy production for medical purposes, vanadium (V) was not employed as an alloying element. Instead, nontoxic elements have been used as alloying elements in Ti, including Ta, Zr, Mo, Fe, Sn, and Nb. In the initial stages, alloys such as Ti-6Al-7 Nb, Ti-13 Nb-13Zr [150], and Ti-5Al-2.5Fe [151] were investigated in an effort to increase corrosion resistance against Ti-6Al-4 V by adding alloy elements [152].

CP-Ti is classified as Ti that has an hexagonal closest packed (hcp) unit cell [153]. Due to the poor strength and fatigue resistance of α -Ti, the dual-phase alloy Ti-6Al-4 V, classified as $\alpha + \beta$ phases with β -Ti as face centered cubic (fcc) was created [140]. Compared to α -Ti, the mechanical characteristics of the $\alpha + \beta$ Ti-6Al-4 V phase were superior [140]. However, the elastic modulus of Ti-6Al-4 V is around 110 GPa, which is significantly higher than that of cortical bone (about 30 GPa), leading to stress shielding in vivo [140]. The manufacture of β -Ti alloys with elastic moduli that are lower than those of dual-phase Ti alloys has long been a topic of research. Mo, Ta, Nb, and Zr, among other phase stabilizers, are present in higher concentrations in β -Ti alloys [154]. As a result of their improved intrinsic biocompatibility, these alloying elements also improve the biocompatibility of the Ti alloy. Furthermore, several β -Ti alloys have lower elastic moduli than Ti-6Al-4 V [140]. As

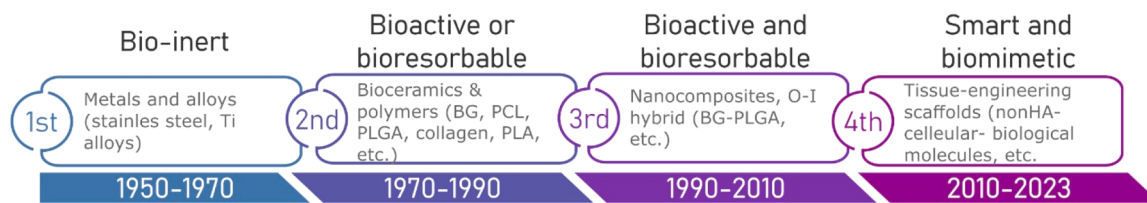


Fig. 21. Graphic representation of generations of biomaterials over time.

Ti-24 Nb-4Zr-8Sn was processed using SLM, the elastic modulus ranged between 46 and 55 GPa, which is considerably more similar to the native structure [155]. Consequently, using β -Ti alloys can enhance in vivo biocompatibility while reducing stress shielding.

Furthermore, Fischer et al. produced Ti-27.5 Nb using DLP, and concluded that the alloy has an elastic modulus of 70 GPa and a yield strength of between 750 and 800 MPa, along with good biocompatibility, demonstrating its non-toxicity [156]. Through AM, scientists have been manufacturing several β -Ti alloys and analyzing their mechanical, biocompatibility, corrosion, and wear characteristics. However, Ti-6Al-4 V is still widely used often in medical devices today due to its favorable mechanical characteristics, biocompatibility, and ease of availability.

The biocompatibility AM Ti and related alloys has been thoroughly investigated. On a DED machine, Xue et al. constructed porous CP-Ti alloys and discovered that samples with 27% porosity showed an elastic modulus of 24.3 GPa, which is similar to the cortical bone. Osseoprecursor cell line (OPC1) cells were used to compare the biocompatibility of the 27% porosity CP-Ti plate in vitro with a polished CP-Ti plate. As concluded, porous Ti demonstrated a higher optical density for the MTT assay at 3, 10, and 21-day time intervals, indicating increased cellular proliferation caused by porosity [157].

Sheydaei et al., on the other hand, used BJ multiscale 3DP to examine porosity variation in functionally CP-Ti using various layer thicknesses [158]. Except for a 5% variance in the porosity of the manufactured parts, there was no detectable change in the Young modulus (2.9 ± 0.5 – 3.5 ± 0.4 GPa) or the yield stress (158 ± 10 – 175 ± 27 MPa).

To better understand how porosity affects elastic modulus and in vivo biological performance, Bandyopadhyay et al. created porous Ti-6Al-4 V using DED. The elastic modulus of the Ti-6Al-4 V structures with a porosity of 23–32% (v%), determined by the uniaxial compression test, was found to be closer to that of natural bone. Male Sprague-Dawley rats were used to test samples with densities of 97.2%, 89.3%, and 75%, and calcium ion concentrations were used to track the formation of new bone. Ca^{2+} ions were found at the highest concentrations in samples with a density of 75%, showing the benefits of porosity for improved tissue integration and regeneration [159].

The exceptional fatigue response of Ti-6Al-4 V is well recognized. Bandyopadhyay et al. examined the impact of Ti-6Al-4 V produced through the orientation of DED deposition on their fatigue response at stress intensities of 50%, 75%, and 90% of compressive yield strength. The samples produced using a horizontal hatching angle of 90°, a residual porosity and more than 2.7 million cycles to failure at 50% stress amplitude demonstrated the highest fatigue resistance [160].

Yavari et al. studied the impact of porosity on the fatigue response of porous Ti-6Al-4 V structures produced by SLM. These structures had high porosities ranging from 63% to 89% and were designed as diamond, truncated cuboctahedron, and cubic unit cell designs. They noticed that the design of the unit cells and porosity had a significant impact on the extent to which the samples responded. Even with greater loads equal to 80% of their yield strength, the structure of cubic unit cells remained stable [161].

Balla et al. used a DED machine to examine laser surface melting of wrought Ti-6Al-4 V for single and double-laser passes at 250 W of laser power. Due to the high hardness and grain refinement produced by the

laser surface melting, it was demonstrated that the wear rate decreased by a factor of 2 for single and double passes compared to untreated Ti-6Al-4 V. This was the case regardless of whether the material passed in a single or double pass [162].

Avila et al. examined the impact of a Ti-6Al-4 V with the addition of Si that has undergone DED processing. Compared to Ti-6Al-4 V, Ti and V silicides increased hardness by 114% and reduced wear rate by 45.1% when 10% Si was added. Additionally, the incorporation of Si caused the formation of a protective tribofilm, increasing the resistance to corrosion [163].

Wang et al. produced a custom Ti-6Al-4 V bone plate with a yield strength of 900–950 MPa as well as a hardness of 360–390 HV1 for a complicated pelvic bone fracture. The implant was subjected to post-processing and surface treatment before being clinically inserted into the pelvic region. Using AM, the surgery took place in 2 h less time [164].

To increase the mechanical strength and add functionality to composite scaffolds, iron and strontium have been investigated. In recent years, Ti alloy implants produced using AM technology have demonstrated their ability to deliver drugs in addition to providing mechanical support. According to a reported study, these printed implants may deliver anticancer drugs and have good osseointegration capabilities [165]. Gu et al. [166] have developed micropatterns on the surface of Ti and glass with the ability to deliver rifampicin (RFP), while Yang et al. [167] have also developed a porous Ti dental implant for drug delivery.

3.1.1.2. Cobalt-Chromium Alloys (Co-Cr). Co-Cr alloys exhibit the highest wear resistance and good biocompatibility among existing metallic implants [184]. As a result, they are ideal for making biomedical implants with articulating surfaces which undergo constant wear and friction. The intermetallic phases that constitute up the Co-Cr alloys and precipitated forms of Cr-rich carbides are what gives them their remarkable wear resistance [185]. Due to the brittleness and potential for catastrophic failure of ceramic coatings, Co-Cr alloys have been used to replace them in orthopedic implants [186]. Co-Cr alloys can increase their wear resistance even more by implantation with oxygen, carbon, or nitrogen [187]. Among the most popular Co-Cr alloys, which also contain traces of carbon, are cobalt-chromium-tungsten (Co-Cr-W) and cobalt-chromium-molybdenum (Co-Cr-Mo). Strength is enhanced by the Mo and W alloying elements, while the Cr alloying element generates a passive oxide layer of Cr_2O_3 that prevents corrosion [188]. With these alloys, nickel is also included as an alloying element [189]. The elemental proportions of Cr and Mo in the Co-Cr-Mo alloy are 26–30 and 5–7%, respectively, with approximately 1% nickel (Ni), according to the generally accepted Co-Cr-Mo alloys as defined by ASTM F75. The most popular application of this alloy is in orthopedics. According to ASTM F90, the percentages of Cr, W and Ni in the Co-Cr-W-Ni alloy are 19–21, 14–16 and 9–11%, respectively [187]. Co-Cr alloys are often manufactured by AM. SLM and EBM have been used in the majority of the reported research on Co-Cr-based alloys. Certain researchers have employed the LENS system to investigate the wear characteristics of Co-Cr alloys [190].

Sahasrabudhe et al. manufactured a Co-Cr-Mo alloy that was reinforced with biocompatible calcium phosphate ceramic (CaP) using a LENS method and observed that the alloy wore down more slowly and had less leaching of Co^{2+} and Cr^{2+} ions. Therefore, CaP reinforcement in

Table 3

Comparison between orthopedic implants produced with AM and those produced using conventional methods.

	Conventionally manufactured implants	AM manufactured implants
Metal Fabrication Technique	Ti and cobalt-based alloys 1. Subtractive processing, including turning, milling, and drilling, involves gradually removing material from a solid piece until a specific form is obtained [168]. 2. Formative shaping: Using mechanical forces, such as bending, casting, forging, or pressing, the material is shaped to take on the needed form [169]. 3. Designing, creating and using a specialized tool is necessary [170]. 4. Good for mass manufacturing [171]. 5. Implants made with more sophisticated technologies than those produced additively [168].	Ti and cobalt-based alloys 1. Using metal components joined layer by layer, AM creates items using 3D model data until the finished implant is constructed [172]. 2. Flexible supply chains because no special equipment is required for this procedure [173]. 3. Excellent for low-volume patches (down to one if necessary) and prototyping [174].
Mechanical Attributes		1. Superior to cast implants and nearly as strong as forged implants [176].
Design Intricacy	1. At each stage of the design process, the manufacturing limitations associated with casting or machining must be considered. As a result, the implant should not have an excessively complicated or challenging manufacturing process.	1. The integration of a porous scaffold and solid components within a single implant is made possible by the design freedom of complicated geometries [177]. 2. To allow the removal of non-melted metal powder, the porous scaffolds must have open cells [178].
Porosity	1. Hard to implement in machining applications, since it depends on a laser that removes material from a solid item or applies a secondary substance [179]. 2. Stress shielding issue [179].	1. It is possible to precisely build and incorporate porosity in designs [180]. 2. Lower stiffness to align with the modulus of the adjacent bone structure and minimize stress shielding [180].
Osseointegration	1. More treatments to be applied to the implant surface, such as hydroxyapatite coating [181].	1. Porous network with optimal pore size and porosity that allows ingrowth of bone tissue [182].
Post-processing	1. Stages of labeling, cleaning, and sterilization [183].	1. Stages of labeling, cleaning, and sterilization [183].
Implant size	1. Approximately tailored to the geometry of the patients [183]. 2. However, implant placement requires necessary adjustments (bone reduction) during surgery [183].	1. Adapt to the area and type of bone defect [183]. 2. The surgical process involves minimal adjustments [183].
Medical uses	1. Common, commercially available implants in a range of sizes to accommodate the majority of patients [183].	1. Patients can only receive a "one-off" implant if an ordinary ready-made implant cannot satisfy surgical needs [183].

Table 3 (continued)

Conventionally manufactured implants	AM manufactured implants
2. More adaptability during operation [183]. 3. Safety and efficacy have been supported by long-term clinical evidence [183].	2. Limited flexibility during surgery [183]. 3. Only a few short-term case series are available to evaluate the clinical outcomes of implants [183].

Co-Cr-Mo can decrease the release of harmful metal ions, reduce cytotoxicity, and prolong the implant [191].

Bandyopadhyay et al. conducted more investigation on the biological function of CaP reinforced in the Co-Cr-Mo alloy. A 12-week in vivo rat study demonstrated that adding 3% CaP to the Co-Cr-Mo alloy increased osteoid formation by five times compared to the Co-Cr-Mo alloy without CaP addition, despite an in vitro test that found no signs of cytotoxicity. Contact between bone tissue and implant had good interfacial binding strength and the addition of CaP had no discernible effect on metal leakage [192].

Although they have great strength and good fatigue resistance, Co-Cr alloys experience stress shielding due to their extremely high elastic modulus (220 GPa). As a result, bulk orthopedic implants in load-bearing areas rarely use Co-Cr alloys. However, Co-Cr alloys are frequently utilized in dental use for crown and bridge structure restorations, because of their exceptional mechanical qualities and resistance to corrosion. Compared to traditionally cast alloys, the SLM produced Co-Cr alloy demonstrated better mechanical properties with increased porcelain bond strength for metal-ceramic restorations [193].

Although Co-Cr alloys are widely known in the biomedical sector, there is still concern about the toxicity and carcinogenicity of Co^{2+} and Cr^{3+} ions, which can lead to inflammation [194]. Cr ions injure the central nervous system and induce ulcers, whereas Co could harm the neural, endocrine and cardiovascular systems [195].

3.1.1.3. Stainless Steel 316 L (316 L SS). Among metals, stainless steel (SS) was the first to be employed as a biomaterial [196]. Especially SS 316 L, also referred to as 316 L SS, has been used for implant purposes. This alloy is often researched and used for medical uses owing to its strong biocompatibility, great corrosion resistance, good durability, and comparably affordable cost [197]. Considering its weak bone bonding capabilities, 316 L SS was first recommended for plates, screws, and nails as applications for fracture fixation devices. In addition, it is used in catheters, cardiovascular stents, and spinal fixation devices [196].

The main component of 316 L SS is Fe, with alloying elements including 10–14% Ni, 16–18% Cr, 2% Mn, 2–3% Mo, and 0.03% C. While C gives the alloy strength, Cr gives it resistance to corrosion. Additionally, Cr and Ni together offer improved ductility and yield strength. SS are recognized for their excellent corrosion resistance since they contain a lot of Cr. However, it has been shown that the chance of corrosion in 316 L SS is increased when exposed to high stress and low oxygen levels, making their use as a biomedical implant challenging [198].

The corrosion resistance of 316 L SS has improved substantially, and the antibacterial effectiveness in preventing implant-associated infections (IAI) has increased due to a zinc-incorporated niobium oxide coating [199]. Another concern with 316 L SS is the discharge of Cr ions from alloy wear debris, which, like Co-Cr alloys, can lead to ulcers and abnormalities of the nervous system. Ni is toxic, and studies have shown that its cytotoxicity can cause a skin ailment known as "dermatitis," which is another reason why the alloy's high Ni level is worrisome [200].

An additional problem with 316 L SS is its high elastic modulus, that has the potential to cause stress shielding in load-bearing regions, leading to osteolysis and implant loosening [200]. The appropriateness

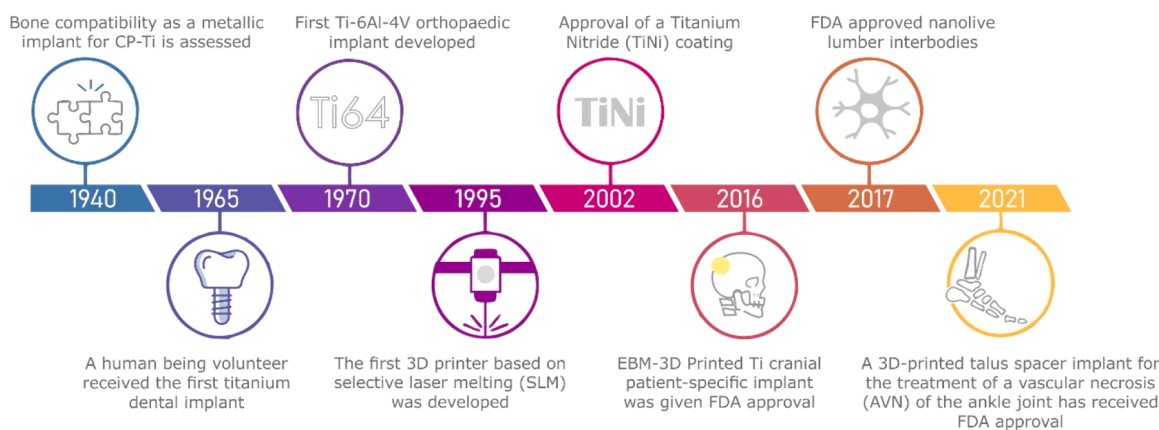


Fig. 22. Development timeline of titanium implants for use in biomedical devices.

of 316 L stainless steel as a biomaterial for long-term implants has been questioned despite its usage in permanent orthopedic implants [201].

An SLM-fabricated composite made of porous hydroxyapatite structures with 316 L SS displayed high biocompatibility. This alloy may be used as a load-bearing implant, since it has a Young modulus of 20 GPa, similar to the cortical bone [202]. Additionally, by adding ceramic to create a metal-ceramic composite, the wear resistance of 316 L SS can be increased. AlMangour et al. [203] discovered that 10% vol% of TiB₂ ceramic was the ideal quantity in 316 L SS manufactured using SLM technology. Because the tribofilm formed when TiB₂ was present, it was found that the wear resistance increased by a factor of 10 as a result. The metal-ceramic composite, which had enhanced grain boundaries and refined grains, had greater microhardness and yield strength as well as a lower friction coefficient than 316 L SS without reinforcement.

Additionally, 316 L SS implants with varying porosity can be manufactured via SLM, with the dense component serving as a source of strength and the porous component acting as a catalyst for improved tissue integration [196]. Shang et al. investigated how the scanning rate affected the biocompatibility of 316 L SS parts produced using the SLM-based AM technique. The MTT proliferation test for 24 h of in-vitro cell culture with L929 cells revealed considerable cell proliferation for SLM-made 316 L SS constructs, with the maximum proliferation for samples created with 900 mm/s. The exceedingly low hemolytic rate did not, however, lead to any modifications in scanning rate [204].

Although Ti is more expensive than 316 L SS, Ti implants have been shown to have fewer failure rates and greater biological performance in load-bearing locations. 316 L SS, on the other hand, was more effective for fracture fixation devices. Currently, 316 L SS is used primarily for dental and fracture fixation [205].

3.1.1.4. Other metals and metal alloys: Nickel (Ni), Tantalum (Ta), and Magnesium (Mg). The load bearing implants are typically made of Ti alloys, Co-Cr alloys, and 316 L SS. In addition to these, tantalum (Ta) and nitinol (NiTi) also exhibit good biocompatibility [206]. The primary objective of several investigations using metal-AM methods has shifted to research on these elements [207,208]. Shape memory alloys made of 49% nickel and 51% titanium, also known as NiTi, are essential for medical devices including vascular stents, orthodontic wires, and bone implants. The importance of these alloys in the medical sector is due to their shape memory characteristics, low stiffness (59 GPa) [209], biocompatibility, enormous elasticity and durability against corrosion [210]. NiTi has distinct stress-strain properties with up to 8% recoverable strain that are comparable to those of live tissues [211]. However, conventional production of NiTi is difficult due to machining issues, hardening properties, and martensitic transformation. To overcome the challenges of conventional production while making it easy to fabricate complicated geometries and porous materials, 3DP procedures for NiTi

structures have been developed. SLM and DED are the AM fabrication methods that are most frequently used to produce NiTi [212,213]. NiTi that had undergone LENS processing had outstanding compression fatigue behavior and could withstand approximately 10^6 cycles at 1.4 times their yield strength before failing [214]. As a prospective biological implant with such unusual features, NiTi has attracted a great deal of interest. Although NiTi exhibits good biomechanical qualities, AM research is not frequently pursued. Compared to Ti, Co-Cr, or 316 L SS, it is more difficult to adjust the process parameters for AM made of NiTi. Poor surface quality and fault porosities in AM-fabricated NiTi have a noticeable impact on their fatigue performance [215]. NiTi also contains a lot of Ni, and the discharge of Ni ions can be hazardous to cells [216]. Despite the fact that 3DP has allowed us to properly build these structures, porosity increased the surface area, which in turn increased the rate of corrosion and the release of Ni ions [217]. As a result, 3DP coating methods are recommended for the efficient use of NiTi in biomedical applications. Similar to this, several researches recommend bio-functionalizing NiTi surfaces, using biologics to lessen Ni ion release and improve interactions between cells and materials [218].

Taking into account its good biocompatibility in vivo, tantalum (Ta) is a newly developed biomedical implant material [219]. Ta additionally has properties similar to those of human bones, including toughness, chemical resistance, and hardness [220]. Ta is heavier than Ti for use in implants, as its density is approximately four times higher. Due to its high melting point of about 3200 K, Ta presents a challenge for AM. Ta is also a costly metal. Therefore, Ta is not utilized as an independent load-bearing device. For orthopedic purposes, Ta is frequently alloyed with Ti [221]. Compared to a Ta implant, a DED alloy containing Ti and 10–25% Ta with TiO₂ nanotubes formed on the surface exhibits higher biocompatibility [221]. Future generations of biomedical implant materials may include Ti-Ta alloys.

Ta alloyed with Ti has also been investigated for the structural dependence of mechanical properties based on 3DP fabrication. As a case study, Soro et al. produced solid and porous lattice structures of Ti-25Ta alloys using SLM, and it was observed that these alloys showed mechanical compatibility similar to Ti64 but with a lower elastic modulus and higher strength [222]. As a lower elastic modulus of the material or design indicates, the likelihood of stress shielding owing to a modulus mismatch is reduced; this is especially helpful in applications involving bone healing.

With the use of LENS, Bandyopadhyay et al. demonstrated the viability of processing porous Ta structures while maintaining manufacturing conditions similar to those of Ti64. Similar in vivo biological performance was demonstrated by 30% porous Ta structures, as well as 30% porous Ti64 with nanotube surface modification [223]. The capacity of these implants to osseointegrate in the early stages was determined by in vivo investigations conducted over durations of 5 and

12 weeks in a rat distal femur model using 3D designed volume fraction porosity. This was due to increased bone ingrowth due to bulk porosity. Additionally, as a result of surface chemistry (titania nanotubes), greater and continuous osteoid or new bone production was observed for extended periods of time at the interface of these implants and host bone. The capacity of these 3DP implants for bone regeneration raises the possibility that they could serve as successful biomedical devices for bone replacement.

The biodegradation form of metallic implants for orthopedics has recently gained prominence. Therefore, soft metals that occur naturally in the human body, such as magnesium (Mg) or iron (Fe), are used to make biodegradable metallic bone implants. Considering Mg is a vital mineral for human nutrition, Mg implants have been suggested, as they possess mechanical qualities similar to those of bone and can encourage the growth of new bone [224]. Nevertheless, since Mg is a soft metal and corrodes more quickly compared to other inert metals like Ti or Co-Cr alloys, it degrades quickly [225–229]. However, Fe degrades more slowly, which may be a drawback when used in orthopedic applications. By addressing all these issues, 3DP techniques enable the effective fabrication of implantable parts with modest degradation rates and mechanical qualities similar to those of human bone. The role of additively manufactured Mg and Fe implant designs in achieving optimal effective performance has been thoroughly investigated by Li et al. [230]. SLM was used to manufacture porous iron lattice structures, while DMD was used to create Mg scaffolds. The structural or design dependencies on both mechanical and biological characteristics were evident in both implants. *In vitro* testing of Mg constructs exhibited less than 25% cytotoxicity and retained mechanical stability as trabecular bone after 4 weeks of biodegradation. However, after being subjected to biodegradation for 28 days, porous Fe structures also demonstrated mechanical durability. An essential role for topology or design in additively constructed porous iron is suggested by the biodegradation behavior of Fe scaffolds, which was shown to be more rapid in the periphery than in the center.

The use of 3DP in metals facilitates the manufacture of intricately shaped parts with non-expensive or difficult-to-work-with materials. The use of metals is expanding rapidly due to several developments in new techniques, alloys, and part enhancement. In addition to one-step component consolidation, metal 3DP benefits us with lower tooling costs, design flexibility, and complicated shape fabrication.

3.2. Polymers

Polymer items, including functional components with intricate geometry and prototypes, are frequently produced using 3DP technology [231]. Extruded thermoplastic filament, such as polylactic acid (PLA), acrylonitrile butadiene styrene (ABS), polypropylene (PP), or polyethylene (PE), can be stacked in successive layers to create 3DP things using FDM [231]. As 3DP materials, thermoplastic filaments that have higher melting points, such polyetheretherketone (PEEK) and polymethyl methacrylate (PMMA), have recently been employed [232].

Given their affordable price, lightweight, and manufacturing flexibility, 3DP polymer materials in liquid form or having a low melting point have become popular in the industry [233]. As inert materials, polymer-based materials perform a significant role in biomaterials and medical device items, supporting the mechanical function of various orthopedic implants and ensuring efficient operation [130].

3.2.1. 3DP polymeric-based scaffolds

Polymer implants for bone regeneration have become increasingly popular in the past few years due to the use of biodegradable polymers, including PCL, PLGA, and PLA [19]. Polymers were recently combined with bioactive mesoporous glass, calcium phosphates, and various additional materials to create composite scaffolds that possess higher mechanical strength [234]. AM technologies have made it easier to produce composite scaffolds that are packed with proteins and

antibiotics for faster bone healing [235]. However, there may be questions about the stability and integrity of bioactive proteins delivered by such devices. Controlled release is preferred for treating infections without adverse effects, as several variables of the AM process can decrease the efficiency of drugs [236].

Huang et al. [237] and Wu et al. [238] developed polymeric implants employing AM techniques that contained pharmaceuticals such as levofloxacin, anti-tubercular medications and anticancer drugs. Implants were constructed from PLLA and PDLA, respectively. Both investigations showed that it was possible to achieve regulated drug release over a number of weeks under both in vitro and in-vivo conditions. Wu et al. also showed the potential to combine pharmacotherapy with anticancer chemotherapy in the treatment of chronic osteomyelitis [238].

Shim et al. [239,240] manufactured scaffolds using a multi-head printer. The primary head served to print the PCL/PLGA/TCP construct, while the second head was employed to add rhBMP-2 by filling in the spaces left by the printed layer. In rabbits, the research group demonstrated improved and directed bone healing. Using a low temperature 3D printer, Yu et al. [241] constructed an rhBMP-2 loaded composite scaffold that revealed excellent osteogenesis in goats.

3.3. Ceramics

Modern 3DP technology allows for 3DP products using ceramic and concrete that lack many pores or cracks by adjusting conditions and setting up appropriate mechanical characteristics [242]. Ceramics are solid, long-lasting, and fire-resistant materials. In their fluid state prior to construction, they can be used to create nearly any geometry and shape, making them ideal for the design of the next buildings and structures [242]. A recent study [243] came to the conclusion that ceramic materials are useful for use in dental and aerospace applications. Alumina [244], bioactive glasses [245], and zirconia [246,247] are some examples of these materials. For instance, 3DP technology could be used to treat alumina powder. Alumina is a delightful ceramic oxide that serves a variety of purposes in high-tech industries like microelectronics, adsorbents, chemicals, and aerospace manufacturing [248]. Alumina has a complicated curing process [243]. Complexly shaped alumina pieces that have substantial green and after sintering densities could be manufactured utilizing 3DP technology [244]. In a subsequent experiment, glass-ceramic and bioactive glass were processed into 3D parts using SLA. The bending strength of these materials improved significantly. The possibility of using bioactive glass in clinically relevant constructs such as scaffolds and bone could be made possible by the increase in mechanical strength [245].

3.3.1. 3DP ceramic-based scaffolds

AM has evolved into a flexible and varied technology that has significantly changed the way objects are produced. Bone defects are extremely challenging to treat since they do not self-heal within individuals [249]. Therefore, implants are required to aid in bone reconstruction. Currently emerging as viable treatment alternatives for bone engineering repair are bioceramic implants based on AM. On the one hand, bioceramic implants made using AM are ideal for bone regeneration because of their high mechanical and biocompatibility characteristics. On the other hand, bioceramic implants made by AM are capable of promoting the appropriate degree of cell growth and tissue development due to their designable structure and adjustable porosity [250]. Research and development of ceramic materials for AM methods have made significant progress. Porous ceramics produced by 3DP function more effectively compared to those developed using more traditional techniques, as they offer a number of positive aspects for the production of lightweight, multipurpose materials that meet or surpass patient demands [251]. Both biodegradable ceramics, such as calcium phosphate (CaP) and calcium silicates, as well as non-biodegradable ceramics, such as alumina and zirconia, are employed in 3DP operations. Ceramics mentioned above are usually structurally adjusted to

carry out a particular function or may be functionalized by drugs, dopants, and growth factors depending on their purpose and application. Among the most popular ceramics used for bone regeneration are calcium phosphates [252]. CaPs are typically made using powder bed 3DP processes, such as BJ, which can produce exceptionally high structural resolution. According to processing conditions, there are two primary types of 3DP CaP scaffolds for medical uses: (1) high-temperature 3DP CaP substrates for healing bones, and (2) scaffolds for delivering drugs and growth factors that are 3DP at low temperatures. In the first case, high-temperature post-processing, such as sintering, is done after using thermal ME or PBF processes. Integration of pharmaceuticals or biologics during construction is not possible with these scaffolds, despite their considerable mechanical durability.

Calcium-based materials, including calcium sulfates and phosphates, are frequently used in bioceramics, which are a popular choice for bone repair. To achieve a modified release of bioactives, Vorndran et al. [253] showed how to fabricate bioceramics that are preloaded with proteins and antibiotics. Both Gbureck et al. [254] and Inzana et al. [255] produced bioceramics with antibiotics embedded in various calcium phosphates for bioceramics intended for prolonged antibiotic delivery.

The biological efficacy of 3D printed CaP scaffolds with dopant systems such as strontium (Sr), magnesium (Mg), iron (Fe) and silicon (Si) demonstrated the higher bone formation capacity of such scaffolds as a joint consequence of the dopant chemistry and structural design through 3DP [256].

Since dopants such as Fe and Si are naturally present in human physiological systems, they are considered harmless. When these components are included in ceramic scaffolds, the osteogenesis potential is increased and full bone regeneration eventually occurs, however scaffolding materials degrade in vivo. The combined osteogenic impact of CaP and Fe, Si, Sr, or Mg shows that these mixtures are not only practical for manufacturing, but also have the potential to be an efficient means of creating an all-encompassing bone regeneration scaffolding device [257].

In recognition of its durability and great mechanical strength, alumina and zirconia are used to repair bone in the mouth and musculoskeletal system [258]. Studies have been done on alumina parts made using SLA and the addition of liquid phase zirconium by in situ precipitation [259]. When portions were taken with and without liquid infiltration, an increased strength was observed. Nevertheless, these constructions have a lower fracture toughness.

Dehurtevent et al. [260] investigated the relationship between particle size and contraction of printed alumina dental crowns to demonstrate that the flexural strength is independent of the particle size. Furthermore, studies have demonstrated that bimodally distributed alumina particle sizes (micro- and nanosized) might lead to larger component densities when compared to alumina particles of a single uniform size [261]. Direct ceramic SLA is expensive and there are now just a few materials suitable for this method [262].

3.4. Composites

Composite materials have profoundly influenced high-performance industries because of their exceptional adaptability, light weight, and tailored features. Examples of composite materials include glass fiber and carbon-fiber reinforced polymer composites [263]. A significant percentage of the aerospace industry employs polymer-carbon fiber composite components due to their extraordinarily high specific stiffness, strength, improved durability against corrosion, and good resilience to fatigue [263]. Furthermore, a variety of 3DP applications utilize fiberglass polymer composites, which have several uses owing to their excellent performance and affordability as well as high thermal conductivity and a modest coefficient of thermal expansion [264]. Due to its non-combustibility and resistance to the production process's high curing temperatures, fibreglass is the appropriate material for use in 3DP [264].

3.4.1. 3DP polymer-ceramic composite

In the medical field, 3DP of polymeric composites has received a great deal of attention, particularly for non-load bearing uses such as dentistry and craniomaxillofacial surgery [265]. With the aid of the polymer-ceramic composite 3DP, numerous soft tissue and bone mimic models have been created [266]. Due to its greater mechanical strength relative to other polymers including polylactic acid (PLA) or polylactide glycolic acid (PLGA), in addition to its slower biodegradation rate, Poly ϵ -caprolactone (PCL) has broad use in these sectors. For these 3DP scaffolds used in non-load bearing applications, a remarkable bone regeneration response has been observed [267]. With the use of FDM, porous structures with extremely high resolution and patient-specific designs can be created, triggering efficient bone regeneration and ingrowth. These scaffolds slowly break down in the physiological conditions. Simulated bone has been made using PCL and the decellularized extracellular matrix (ECM) [268].

Starch-based constructs have just been 3DP as bone regeneration scaffolds with the added benefit of drug release from pores. Koski et al. used calcium phosphate (CaP) and starch-based composites to create bone scaffolds through SFF. The addition of CaP, PCL, and starch enhanced both the mechanical and biological performance. Subsequently, these scaffolds were investigated as drug-eluting carriers for chemopreventive practices [269].

Despite the fact that polymers have been found to greatly improve the mechanical properties of ceramic scaffolds, they are also often used as coatings on ceramic drug delivery systems. To help keep a drug's therapeutic efficacy, polymeric coatings (PCL, PLGA) have the ability to control how quickly pharmaceuticals are released from scaffolds based on the pH of the environment. The CaP scaffold has been coated with polymer in experiments that aim to distribute natural pharmaceuticals for a long time [270].

3.5. Smart materials

Smart materials are those with the capacity to alter its geometry and shape in response to environmental factors including moisture, heat, and pH [112]. Examples of 3DP objects built with intelligent substrates include self-evolving structures and soft robotic systems. Smart materials can also be considered as 4D printing (4DP) materials, such as shape memory alloys and shape memory polymers [271]. Certain memory-forming alloys, such as NiTi, can be applied to microelectromechanical devices and biomedical implants [272]. Shape-memory polymer (SMP) is a form of smart material that reacts to stimuli including light, electricity, heat, some types of chemicals, etc. [271]. The complex form of the SMP can be produced easily and quickly by employing 3DP techniques. When manufacturing using 3DP, the accuracy of dimensions, surface roughness, and piece density are used to evaluate the quality of the material [271]. Fig. 23 shows a schematic

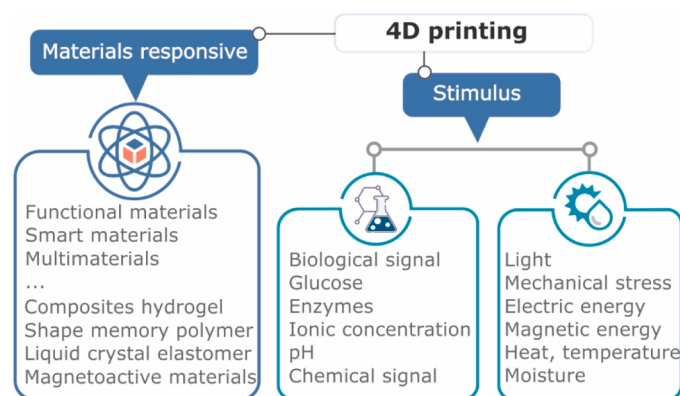


Fig. 23. Schematic illustration of the 4D-printing technology that considers materials and stimulus type.

representation of 4DP, which considers materials and stimulus type.

4. Applications of 3D printing in manufacturing

By integrating innovative 3DP techniques around the world, 3DP is proving its strength and potential in a variety of fields [273]. AM technology has proven enormous potential and advantages in several industrial fields by providing a practical method for producing high-performance parts. Its unique capacity to lower capital expenditures, improve shape complexity and increase design for production are the key contributing reasons [273]. The aerospace, automotive, maritime, energy, biomedical, and other industries have all made substantial use of this technology. By scanning or developing specific components using designing software, existing and nonexistent components can be manufactured in numerous fields. Rapid printing of more durable and lightweight components is possible with additive manufacturing [273]. Components can also be made from other types of plastic and metal. Rapid prototyping is one of the timesaving 3DP processes used in the aerospace and automotive industries.

4.1. Aerospace industry

Using 3DP technology allows flexibility in both manufacturing and component choice. The aerospace industry can make parts with improved and complex geometries that are lightweight while consuming less resources and less energy due to the use of 3DP [274]. Aerospace parts frequently feature complex structures and are manufactured using advanced materials, such as titanium, nickel, super steel, or ceramics that can withstand extremely high temperatures. Nickel-based alloys are increasingly desired in the aerospace industry due to their tensile characteristics, resistance to oxidation and corrosion, and tolerance to damage [275].

The process requires a lot of effort, money and time to manufacture these novel materials [276]. Through the use of AM, functional items in nearly net shape can be produced quickly, wasting less material, and spending less money. The fabrication of complex cross-sectional regions, such as the honeycomb cell or other material sections with cavities and cutouts, has additionally been made possible by printing technologies, which reduce weight and increases flue efficiency [277]. Using 3DP technology can also result in fuel savings, since less material is needed to fabricate aircraft parts. Furthermore, 3DP technology has been extensively used in the production of replacement parts for specific aeronautical components, such as engines. Engine components are easily damaged and often need to be replaced. To obtain such spare components, the use of 3DP is an excellent option [278]. With the AM technique, it is also possible to repair complicated parts like combustion chambers, engine blades/vanes, and so forth. Other significant elements that motivate the aerospace sector to employ AM technology include complex geometries, thin-walled aircraft engine parts and structures, and the difficulties of machining materials [279].

4.2. Automobile industry

Modern 3DP technology is rapidly changing our industry by enabling us to innovate, develop, and produce novel items. One of the business sectors with the highest levels of global competition is the automotive sector. Continuous technological advancement and new design trends require the invention of new manufacturing techniques to keep up with the automotive industry [280]. Since AM can produce parts with complex lightweight structures and good rigidity, it has a significant impact on gaining competition among automakers. The ability of the AM process to create parts with complicated shapes while preserving relative strength can drastically reduce the weight of automobile parts [281]. Additionally, the concept of mass customization was made possible by a dramatic reduction in the time to market for AM parts. These days, automobile producers are using it for more and more practical purposes.

Technology at AM has significantly changed the way we develop, design, and produce new products. For example, URBEE-2 was designed by American engineers using AM-fabricated components. However, low-volume production and the production of massive AM-based components are two issues that prevent AM from being widely used in the automobile sector [277].

The 3DP revolution has changed the automotive industry by enabling the faster production of lighter and more sophisticated structures [282]. For example, in 2014, Local Motor produced the first electric car using 3DP technology. The OLLI, a 3DP bus developed by Local Motors, broadened the range of applications for 3DP technology beyond the automobile industry [283]. OLLI is a driverless, electric, 3DP bus that is also exceptionally smart. Ford is also a leader in the application of 3DP innovation and utilizes it to produce prototypes and engine components [282]. Additionally, BMW uses 3DP technologies to make hand tools for testing and assembling autos. In 2017, AUDI collaborated with SLM Solution Group AG to produce prototypes and spare parts [284]. Due to this, using 3DP in the automotive sector enables companies to produce fresh concepts and areas of focus early on in the development process, leading to the construction of perfect and efficient car models. Technology for 3DP also reduces waste and resource use. Furthermore, 3DP technology can save both time and money, allowing quick experimentation with novel concepts [285].

4.3. Electric and electronic industries

Multi-material Smart devices including 3D structural electronics, sensors, batteries, and other parts have been made possible by 3DP with electrically useful materials, such as conducting, sensing, insulating, and semiconducting materials. Electronically smart devices are a contentious topic in 3DP, as they may unquestionably profit from technology, offering considerable design flexibility and specialized functionalities. Modern 3DP techniques, such as FDM, have allowed the customization and creation of complicated material structures. The potential of 3DP continues to be realized in several of intriguing ways as it becomes increasingly readily accessible to the sciences, technology, and manufacturing sectors. Regarding structural electronic devices, many 3DP techniques are now often employed. These techniques include electrodes, active electronic materials, and devices with mass customization and adaptable layout [286]. The application spectrum of 3DP has been increased by the incorporation of thermoplastic polymers like polylactic acid (PLA) and acrylonitrile-butadiene-styrene (ABS), which can be utilized to produce affordable 3D parts for an array of uses [287]. Due to their quick production process and high level of precision when building a complicated structure, 3DP components have lately been the subject of research with the aim of generating a working electrochemical system [288].

With the emergence of novel technologies like wearable electronics, human-machine interfaces, soft robotics, etc., structural, stretchy, and/or flexible electronics have recently attracted attention. These novel technological devices demand hybrid or novel fabrication processes using 3DP technology [289]. Electrically functioning materials need to be modified for the printing process so as to fully use 3DP to electronic devices [290]. In this section, electronics, sensors and batteries are introduced in 3DP devices.

4.4. Functional energy devices

Currently, clean (hydrogen) and renewable (solar and wind) energy offer attractive options to reduce pollution and the release of greenhouse gases, as well as to decrease our dependence on fossil fuels [276]. Through improved material properties and energy efficiency, AM technologies have demonstrated their potential for use in a number of energy-related industries. AM has been regarded as one of the energy generation, conversion, and storage technologies of the future [291]. The application of printing technologies in functional parts or devices is

of special interest since they typically require expensive advanced materials, like ceramics or composites, which have significant shape and functionality constraints when handled with conventional manufacturing processes. Given the advent of printing technologies, the design for production and fabrication processes have become considerably easier, which represents a significant improvement in shape complexity [292]. The use of AM in the areas of nuclear energy, batteries, fuel cells, oil, and gas is shown in Fig. 24 [291]. To address the main technical obstacles, further research and development is needed.

4.5. Architecture, Construction, and related industries

The rise of AM is turning the construction market into one flexible and innovative one. Automation of the manufacturing process, the great freedom of design, and the consequent opportunity for optimization are key advantages of AM. This method has been used to build architectural models for more than ten years [293]. Architectures and designers are now able to manufacture complex interior and exterior geometries that would be difficult and expensive to manufacture using traditional techniques [294]. By reducing the amount of time that on-site personnel are exposed to dangerous conditions and automating some building operations, AM could offer services to the construction sector. Reduced supply chain length and waste are two additional advantages of AM. Currently, full-scale architectural components and building features, such as walls and facades, are delivered using AM in the construction industry rather than only as a tool for architects to model their designs [295]. Success in printing houses has already been documented in some cases. For example, in 2016, WinSun produced the first 3DP office in the world. By comparing traditional buildings of the same size, the labor cost was reduced by more than 50% [296].

The use of 3DP offers countless opportunities for the achievement of complicated geometry and can be seen as an environmentally friendly derivative. The complete structure of a building or specific construction components might be printed using 3DP technology in the construction sector. The more efficient use of 3DP technology could be made possible by implementing Building Information Modeling (BIM) [297]. Building information modeling is a digital representation of both functional and physical features that allows for the sharing of information and expertise about 3D structures [297]. When making decisions about how to build or design a structure, it can serve as a reliable source from the beginning

of the process through demolition [297]. This cutting-edge collaborative technology will support a more effective approach to designing, producing, and maintaining the built environment. Companies can rapidly and economically create and manufacture the building's design, in addition to avoid delays and assist in locating areas of concern with the aid of 3DP technology. Due to 3DP technology, communication between construction engineers and their clients is more efficient and straightforward. In contrast to the antiquated practice of using pencil and paper, 3DP makes it easy to fulfill a customer's vision [298].

4.5.1. Office of the future in Dubai

The United Arab Emirates constructed the 3DP building to serve as the headquarters of the Dubai Futures Foundation [299]. The futuristic "Office of the Future" serves primarily as a gathering place for visitors from all over the world. The 3DP office is an entirely functional structure with plumbing, electrical, and climate control systems [299]. China is where the 3DP house was made. The printed parts were delivered to Dubai after printing. In the end, the initiative reduced construction waste by 30–60% and labor costs by 50–80%. It is believed to have ignited the 3DP revolution for construction that is currently taking place in Dubai [299].

4.5.2. Apis Cor printed house in Russia

A Russian company was able to construct a 400 square foot residence in Moscow from scratch in less than twenty-four hours [300]. The building itself only cost \$10,000, showcasing the incredible potential of 3DP technology. The results are astonishing because the entire house was constructed on site using only a portable 3D printer [300]. There is not much space in the house, but it is undoubtedly livable. Its rapid 24-hour production at such an affordable cost. All walls and substructure were created with a cement mixture, and later components such as windows, fixtures, and furniture were installed. The final cost of the entire renovation was modest (\$10,134) and the house received an all-new coat of paint [301].

4.6. Healthcare and medical industry

It is a potential strategy to provide high-quality and cost-effective healthcare by offering personalized treatment based on the unique needs of individuals. With the use of "on-demand" (patient-by-patient)

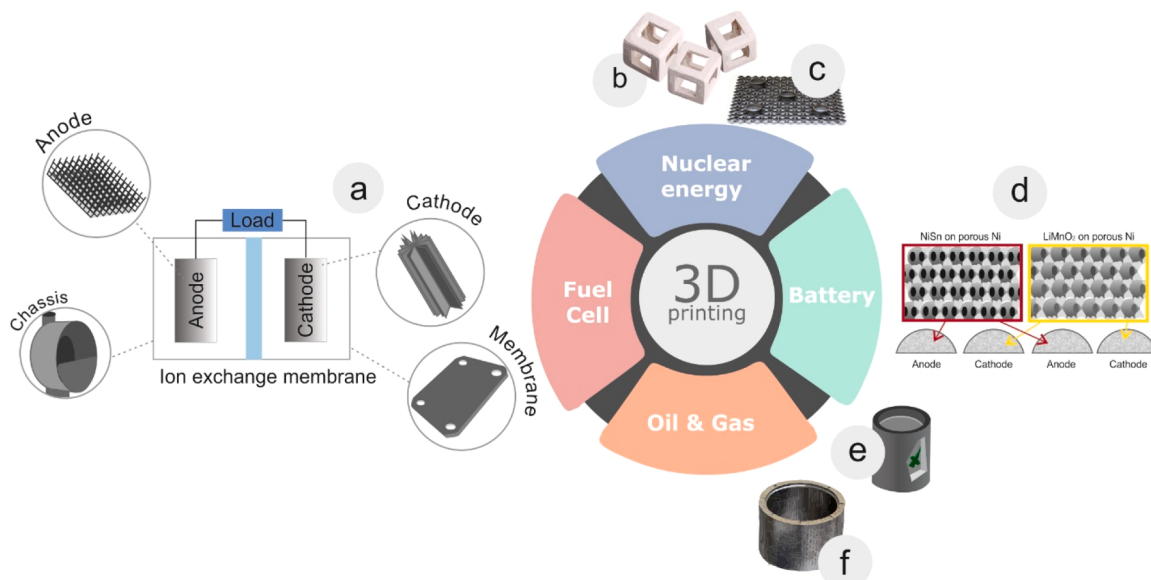


Fig. 24. AM-fabricated parts, items, and products in the four primary energy sectors [291]: (a) nuclear fuel; (b) thorium dioxide fuel; (c) interdigitated electrodes of a micro-battery; (d) membrane and anode elements in a microbial fuel cell; (e) nozzle component used metal AM to include down-hole oil and gas wellbore cleanouts; and (f) special configurations for Masoneilan control valve parts.

AM, it is possible to fabricate specialized biomedical implants using a wide range of metallic, plastic or ceramic materials [302]. Many scientists and companies have recently found the use of the AM method in medical applications attractive. Fig. 25 illustrates the uses of AM in the medical industry [303]. Despite the fact that these techniques are quick, scalable and affordable, they have limitations when it comes to the production of improved tissue architecture, biomaterials free from imperfections, and necessary properties such as printability, biocompatibility, mechanical properties, and biodegradation [302]. Therefore, to overcome these challenges regarding building 3D structures for medical demands, more research is necessary.

The application of 3DP technology has been documented for the production of 3D skin [304], bones and cartilage [305], tissue replacement [306], and organs [288]. The 3D printing technique is useful for biomedical items since it has a variety of upsides, including the following:

1. The manufacturing of implants and prosthetics, which the FDA recently approved, was among the first medical applications of 3DP [12].
2. At a reduced cost, 3DP technologies can duplicate the natural structure. Drug, cosmetic and chemical-based product testing can be done on 3D manufactured skin. Therefore, the use of animal skin in product testing is not needed. As a result, employing an exact replica of the skin will assist the researcher in obtaining an accurate conclusion [307].
3. Efficiency can be improved by using 3DP technology to print medications. It is achievable to build dosage forms with sophisticated drug release characteristics, and the dropped size and dose can be precisely controlled [288].
4. The use of 3DP technology allows for the filling of bony deficiencies in cartilage or bone brought on by diseases or traumas [51]. This treatment is distinct from the use of autografts and allografts, as it emphasizes bone genesis, bone maintenance, or improving bone function *in vivo* [51].
5. The functionality of tissues might be improved, replaced, maintained, or restored using 3DP technology. Replacement tissues produced using the method of 3DP feature a network of



Fig. 25. Uses of AM in the healthcare and medical industry: (a) medical models; (b) implants; (c) tools, instruments, and parts for medical devices; (d) medical aids, supportive guides, splints, and prostheses; (e) bio-manufacturing [303].

interconnected pores, are biocompatible, possess an appropriate surface chemistry and excellent mechanical characteristics [306].

6. Comparable organ dysfunction caused by serious conditions such as disease, accidents, and birth defects can be printed using 3DP technology [308].
7. Technologies like 3DP possess the potential to accelerate the investigation of cancer since they may produce highly controlled models of diseased tissues. The 3DP technology allows patients to get more precise and trustworthy information [309].
8. Neurosurgeons can practice surgery procedures with the help of 3DP models as they learn [310].
9. Considering a 3D model provides a representation of a real patient's pathological condition, this might improve accuracy, allow the trainer to carry out clinical operations more rapidly, and provide possibilities for hands-on training for surgeons [310].
10. Anatomical models: 3DP can produce incredibly accurate and thorough anatomical models to help surgeons train for challenging procedures, leading to better outcomes and at a reduced cost. The use of 3D technology also reduces surgery time [311].
11. Medical supplies. The employing of 3DP to produce medical tools including scalpels, forceps, needle drivers, handles, and clamps is essential in addressing the growing demand for quick development of medical equipment and alleviate supply chain challenges [312].

Fig. 26 illustrates the main uses of 3DP in healthcare.

The use of 3DP in medicine is growing rapidly and is predicted to completely change the way healthcare is provided [313]. The manufacture of tissues and organs, the design of specialized prosthetics, implants, and the anatomical models, and the investigation of medication dosage forms, delivery, and discovery are all examples of current and possible medical applications for 3DP [314]. Aside from affordability, greater efficiency, freedom of design and manufacturing, the use of 3DP in medicine can offer a number of advantages. These advantages include the ability to customize and personalize medical products, medications, and equipment [313].

According to predictions from Global-Data, spending on 3DP would increase to \$20 billion globally by 2025, almost double what it was in 2017 [315]. According to a posting on the website of the American Hospital Association [316,317], 113 hospitals had centralized 3D facilities for point of care manufacturing in 2019 as opposed to just three in 2010. Furthermore, according to Pew Trust, the market for 3DP in healthcare underwent a sharp increase during the COVID-19 epidemic, when many hospitals were relying on this technology for the distribution of personal protective equipment (PPE) and medical gadgets [315].

4.6.1. Advantages of 3DP for medical uses

3D printing technology can be employed to produce lab and medical devices. A 3D printer may produce plastic equipment parts. Once this is done, expenses and the amount of time spent holding out for fresh medical supplies from outside firms are greatly decreased. Further, the production procedure as well as subsequent applications are made simpler. As a result, 3DP medical equipment is easier to obtain and more accessible to low-income or difficult-to-reach places. The application of 3DP technology and its impacts are shown in Fig. 27.

i. Customization and Personalization

The freedom to manufacture specialized medical supplies and instruments is the most significant benefit that 3DP offer in the healthcare industries [318]. For example, using 3DP to manufacture personalized implants and prostheses can be very beneficial for patients and medical professionals [318]. Additionally, custom fixtures for surgical applications can be produced via 3DP [319]. The efficacy of the procedure or implant, as well as the timeframe of patient recovery, can all be improved with the use of

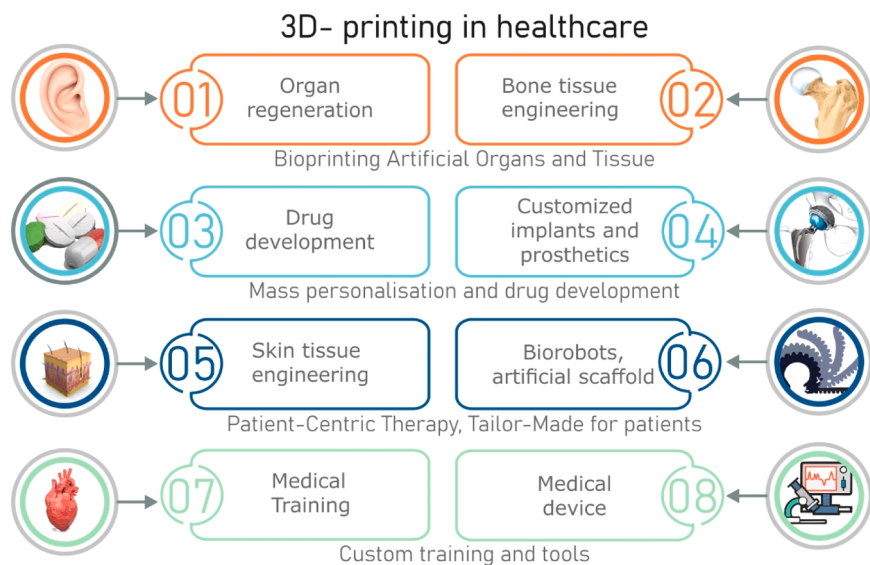


Fig. 26. Major Applications of 3D Printing in Healthcare.

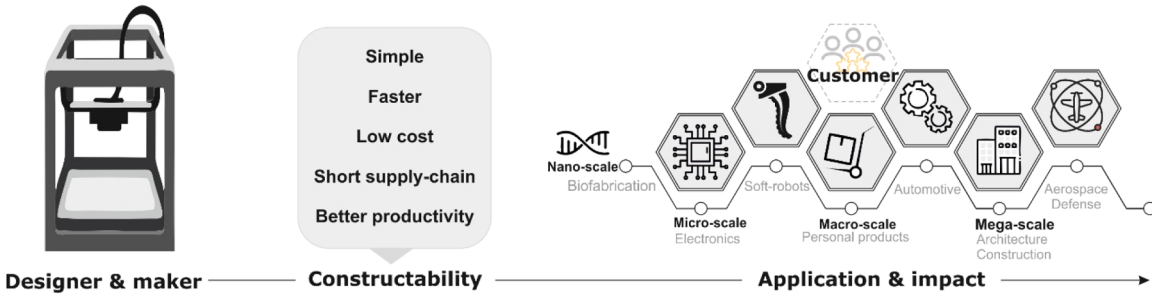


Fig. 27. Application and impact of 3D printing technology.

custom implants, fixtures, and surgical equipment [319]. Furthermore, 3DP technology is expected to individually tailor the dosage forms, release profiles, and distribution of drugs for each patient [320].

ii. Cost-effectiveness Improvement

A key advantage of 3DP is its ability to produce products at a reasonable cost [313]. For massive quantities, conventional methods of manufacture continue to be cheaper; but the price of 3DP is becoming more and more affordable for small-scale manufacturing. This is especially true for implants or prostheses smaller than usual, such as those for dental, craniofacial, or spinal diseases [318]. The cost of printing a custom 3D object is quite low, with the initial and last pieces equally reasonable, [313]. This is especially beneficial for companies with low manufacturing numbers, those that create intricate components or products, or those who frequently modify their products. [319].

Using less-unimportant materials, 3DP may also reduce manufacturing expenses. For example, a 10 mg pharmaceutical tablet could be ordered as a 1 mg tablet [320]. Furthermore, certain drugs could be printed in dose forms, facilitating and decreasing cost when they are provided to patients [320].

iii. Improved Productivity

Being capable of creating a product in a matter of hours is referred to as "fast" in the context of 3DP [319]. Due to the lack of grinding, machining, and long delivery times, 3DP technology is much quicker than conventional methods to produce products such as implants and prosthetics [318]. The resolution, precision, dependability, and

repeatability of 3DP technologies are some of the other features that are advancing along with speed [318].

4.7. 3D Bioprinting (3DBP) of tissues and organs

Several challenges in healthcare have been proposed to be addressed by 3D Bioprinting (3DBP), notably drug delivery, regenerative medicine, and functional organ substitution [321]. 3DBP is the use of 3DP techniques to combine cells, growth factors, and/or biomaterials to generate biomedical parts, often with the objective of mimicking the functions of genuine tissue [322]. Fig. 28 shows an overview of the development of 3DBP.

4.7.1. 3D bioprinting manufacturing procedures

Today, constructing tissue-like structures using bioprinting the methodology requires adhering to a manufacturing process that comprises pre-bioprinting (organ imaging, gathering data, and 3D modeling), cell and bioink selection, bioprinting, and post-bioprinting stages must be followed (Fig. 29) [324]. Normal tissue is imaged using CT scans and converted to digital patterns for bioprinting. The bioprinting stage involves selecting a suitable technique, selecting the type of cell, the scaffold, and the growth factors, and obtaining enough cells [325]. Before 3DBP, equipment and parameters must be configured and defined. Live cells and bioinks are placed in ink cartridges at physiological temperature and pH [326]. The bioprinter creates 3D tissue with better resolution, extending the useful life of the scaffold. Post-processing involves crosslinking 3DP scaffolds with cells using thermal, chemical or physical techniques [327].

Scaffold-based 3DBP involves extrusion, droplet-based, laser-

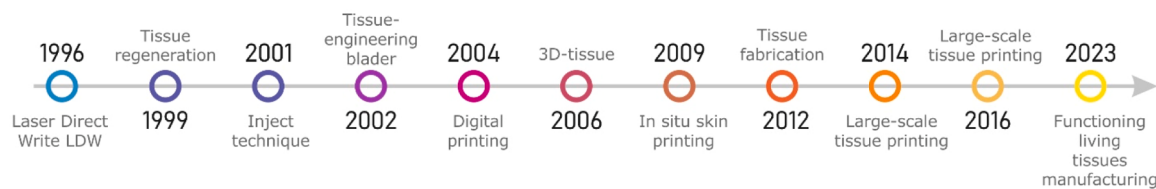


Fig. 28. A diagram illustrating the development of 3D bioprinting (3DBP) methods [323].

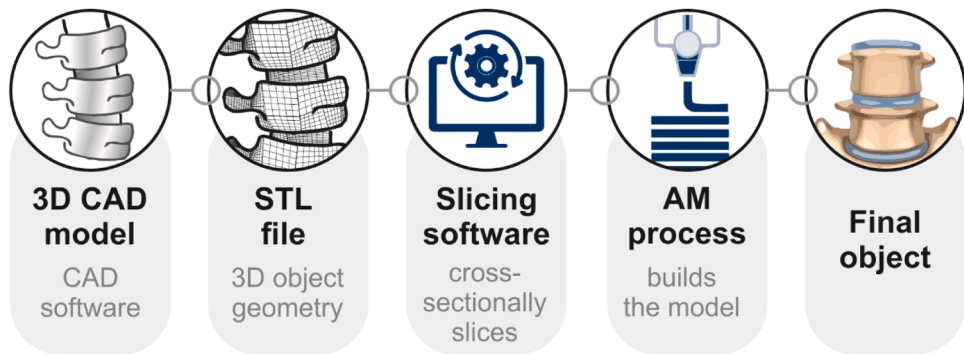


Fig. 29. Diagram illustrating the stages in the 3DBP process for building organs.

assisted, and vat-based polymerization bioprinting (Fig. 30). Extrusion processes deposit bio-inks, droplet-based processes gather bio-ink droplets, laser-assisted bioprinting uses laser energy, and vat polymerization-based bioprinting uses ultraviolet or infrared light [328]. Table 4 lists some examples of 3D bioprinters employed for tissue engineering and regenerative medicine.

4.7.1.1. Extrusion-based bioprinting. Extrusion bioprinters (Fig. 31a), developed in 2002 [348], are the most popular bioprinting technology due to their versatility, affordability, and capacity to produce massive 3D structures [349]. These printers have two or more printing heads that extrude bio-ink made of cells, growth factors, or materials. The cartridge is attached to a printing arm, allowing 3D pattern fabrication [350], while printing. Cells are protected from harsh conditions by low-speed and pressure extrusion, which also provides high cell density [351,352].

Although EBB has advantages, it also has drawbacks such as poor resolution, hydrogel deformations, nozzle blockage, and cell death [350]. The time it takes to bioprint complex structures has an impact on cell viability, as high cell concentration affects vitality. Due to the absence of cell culture media, cells also experience dehydration and

nutritional deficiencies.

Extrusion-Based Bioprinting Extrusion-Based Bioprinting is the most popular technique in modern bioprinters, with 57% of commercialized 3D bioprinters worldwide [353]. Create various 3D tissues and biological constructs, including kidneys, liver, blood vessels, and other engineered structures [354].

4.7.1.2. Droplet-based bioprinting. Droplet-based bioprinting techniques (Fig. 31b), first developed in 1988 [355], include electro-hydrodynamic jetting, inkjet, acoustic and microvalve-based methods. Inkjet bioprinting includes continuous and drop-on-demand techniques, using piezoelectric, thermal, and electrostatic methods. Drop-on-demand technology offers affordable prices, fast printing due to parallel print-heads, and high cell viability [356]. However, it has limitations such as limited material selectivity, inconsistent temperatures, and frequent printhead blockage. Hybrid cell printing techniques are being researched to improve performance [357].

Inkjet-based bioprinting is the second most prevalent mode, with 10% of commercial bioprinters worldwide. However, inkjet printing of cells is limited by technical challenges and practical difficulties [358].

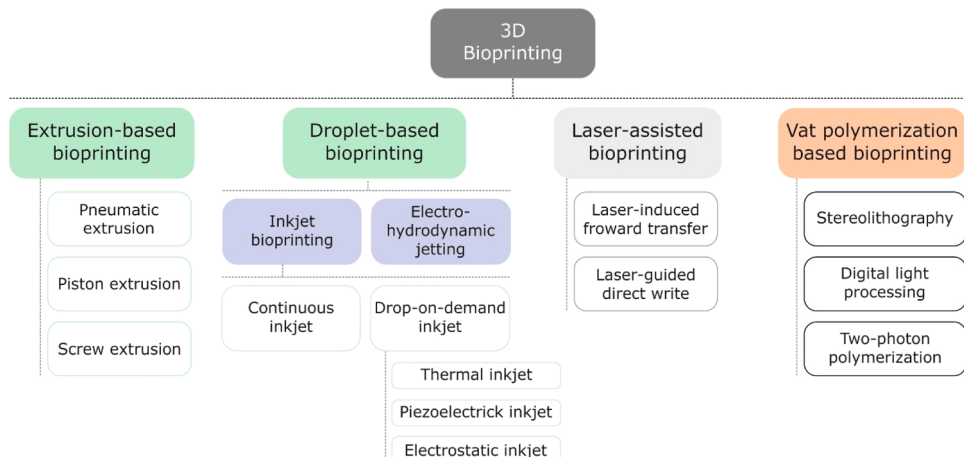


Fig. 30. Categorization of the four-primary scaffold-based 3D bioprinting approaches: extrusion-based, droplet-based, laser-assisted, and vat polymerization-based.

Table 4

Examples of 3D bioprinters used for tissue engineering and regenerative medicine.

Company	Bioprinter	Features	Tissue or Organs	Reference
ORGANOVO (San Diego, CA, USA)	NovoGen MMX™	1. Manufactures biological tissues such as those in the pancreas, liver, kidneys, intestines and skin. 2. Two print-heads are included, one for cell extraction and a second for printing hydrogels, scaffolds, or soft biomaterials.	1. Kidney, tissue-engineered muscle, liver, human intestinal tissue.	[329–331]
ENVISIONTEC (Gladbeck, Germany)	3D Bioplotter®	1. Capable of processing a range of biomaterials (such as hydrogels, soft polymers, bioceramics, etc.). 2. Used in the formation of skin and cartilage, and in the regeneration of bones, cells and organs.	1. Blood vessels, adipose tissue, tracheal graft, tooth tissue, adipose tissue.	[332]
CELLINK (Gothenburg, Sweden)	BIO X™	1. Three print-heads. 2. Built on the extrusion principle. 3. Could create structures from any kind of cell (such as fibroblasts, stem cells, or endothelial cells). 4. Equipped with a UV-C germicide, allows for the sterilization of light in the printing area.	1. Engineered neural tissues, skin constructs, wound dressings, bone tissue.	[333,334]
ASPECT BIOSYSTEMS (Vancouver, BC, Canada)	RX1™	1. Capable of producing diverse, physiologically complicated diverse human tissues. 2. High cell density bioprinting with excellent survivability and phenotypic preservation. 3. Low-viscosity biomaterials are used.	1. Renal tissue, 3D contractile smooth muscle tissues, engineered neural tissues, brain tissue	[335,336]
GESIM (Radeberg, Germany)	BioScaffolder®	1. Printing with or without cells of extremely distinct hard and soft biopolymers. 2. Porous and multi-biomaterial structures can be designed and printed using a bioprinter for tissue engineering. 3. Nanoliter pipetting, coaxial extrusion, and sequential bioprinting.	1. Repair of heart tissue, periodontal tissue, and vaginal wall.	[337,338]
ALLEVI (Philadelphia, USA)	Allevi	1. Contains blue and ultraviolet (UV) light for LED photo curing. 2. Enables the use of several biomaterials, including graphene, matrigel, collagen, and methacrylate.	1. Osteochondral constructions, bone grafts, and veterinary dosages.	[339,340]
REGENHU (Fribourg, Switzerland)	3D Discovery® Evolution	1. Ability to fabricate in both macro and nano dimensions with a single unit. 2. Similar to the tissue architecture found in nature is produced. 3. Uses a single instrument to provide 11 distinct printhead technologies. 4. The specification and configuration can be adjusted and customized.	1. Engineered tissues are produced in cartilage tissue.	[341,342]
REGENHU (Fribourg, Switzerland)	Biofactory ®	1. Modified to work with a variety of bioprinting methods, such as droplet and extrusion methods. 2. Enables working with a wide variety of biomaterials, including high-viscosity biomaterials, proteins, and photo-cross-linkable hydrogels. 3. Gives access to a system integrated inside the laminar flow hood that keeps the air sterile by controlling the temperature, humidity, and gas composition.	1. Skin, air–blood tissue barrier, skin tissue regeneration, 3D tubular construction.	[335,343, 344]
CLUSTER TECHNOLOGY (Osaka, Japan)	DeskViewer™	1. Using the underlying technology of piezoelectric inkjet printing. 2. The unit contains four injectors with various sized nozzles. 3. Capable of printing various cell or protein solutions. 4. The drop that emerges from the nozzle can be adjusted and varied in terms of both volume and diameter.	1. Human tissue chips.	[345]
REGEFAT (Granada, Spain)	Bio V1	1. Suitable for osteochondral tissues and usable in other related applications. 2. A wide range application is made possible by exchangeable printheads.	1. Builds of articular cartilage and bone tissue.	[346,347]
POIETIS (Pessac, France)	NGB-R™	1. Excellent precision and resolution characteristics. 2. Featuring an integrated in-line monitoring system that can regulate the precision of each layer applied, resulting in regulated 3D cellular architectures and repeatable tissue designs.	1. Skin model.	[98]

Inkjet-based bioprinting has created 3D replicas of various tissues [343], including cartilage, neural tissues, the brain, kidney, skin, and liver. This technology could be beneficial in wound healing and layer-by-layer filling of wounds [359].

4.7.1.3. Laser-based bioprinting. Laser-assisted bioprinting (Fig. 31c), introduced in 1999, resembles direct writing techniques and includes matrix-assisted laser evaporation writing, laser-induced forward transfer, and forward transfer supported by an absorption film. Laser-assisted bioprinting is a complex process that uses pulsed laser radiation to transfer materials to a substrate. It requires an objective, beam-delivery optics, a pulsed laser source, and a receiving substrate, and does not require nozzles, making it resistant to clogging problems like extrusion-based bioprinting [356].

Laser-assisted bioprinting offers advantages such as high cell density and viscosity biomaterials, high-resolution printing, and real-time observation of living cells and biomaterials [360]. Commercial laser-assisted bioprinters account for 3% of the total number of

bioprinters in the worldwide 3D bioprinting market. This approach is appealing for multicellular constructions in space-ordered patterns since it is non-contact and orifice-free and permits accurate microscale deposition of biological material. Laser-assisted bioprinting offers precision in microscale structure geometry and higher cell viability compared to extrusion and inkjet processes [358].

Laser-assisted bioprinters have the ability to build intricate 3D tissue constructs, such as hollow tubes, skin, bone, and transplants. They have also been effective in producing patterned liver models that closely resemble the liver lobule structure [361].

4.7.1.4. Vat polymerization-based bioprinting. In 1984, vat polymerization bioprinting was introduced, offering high manufacturing accuracy for tissue engineering applications (Fig. 31d). This technique uses photo initiators for crosslinking, enabling intricate, high-resolution tissue structures [362].

Stereolithography bioprinting is a light-based method for 3D object printing, using layer-by-layer light patterning to photo-crosslink specific

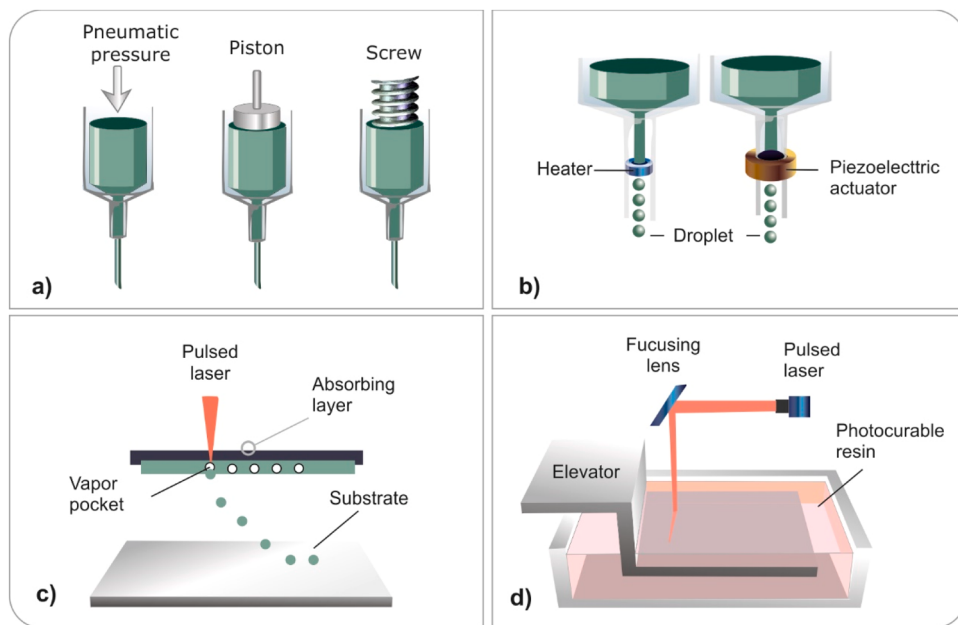


Fig. 31. An outline of the most common scaffold-based 3D bioprinting approaches: Bioprinting techniques include (a) extrusion-based techniques, (b) inkjet-based techniques, (c) laser-assisted techniques, and (d) vat polymerization-based techniques [328].

portions of a photo-sensitive bio-ink [362]. It is nozzle-free, clogging-free, and faster than nozzle-based systems. It offers the highest spatial resolution among current bioprinting techniques [363].

Vat polymerization-based bioprinting enhances tissue engineering by producing materials containing cells, biomaterials, and photo initiators, with potential applications in biomedicine, including aortas, heart valves, and cranial implants [362].

Fig. 32 depicts an overview of the bioprinting manufacturing process, which includes the pre-bioprinting, cell and bioink selection, bioprinting, and post-bioprinting phases. Table 5 lists the advantages and drawbacks of these four types of operation.

4.7.2. Bio-inks

Bioprinting creates 3D tissue buildings with preprogrammed patterns and geometries containing biomaterials and living cells, known as bioink [370]. Bioinks protect cells from damage during printing and have a viscosity similar to that of gel, making them easy to print [371]. Distinguishing between bioink (cell-laden) and biomaterial ink (cell-free) is crucial in bioprinting (Fig. 33). Biomaterials that form bioinks function as cell transporters, allowing cell delivery during the formulation and bioprinting process [372]. Biomaterial inks are not considered bioinks, but they reduce biological limitations that affect ink characteristics and behavior.

Bioinks and biomaterial inks are formulations based on cells, while biomaterial inks are made up of biomaterials, biologically active components, and other elements [373]. 3D bioprinting technology has significant potential in regenerative medicine, with the demand for

bioprinted tissues and organs increasing. An ideal bioink must possess the right mechanical, rheological and biological characteristics for tissue constructs to function properly. Bioinks can be classified into scaffold-free and scaffold-based types. Uniform bioink formulations are essential for various bioprinting tasks, and the selection depends on the specific application, cells, and bioprinter.

4.7.2.1. Scaffold-free bio-inks. There has been a lot of interest in making use of scaffold-free cell suspensions in 3D bioprinting technologies to produce tissues or organs which employ mono- or multicellular aggregations of cells, including cell sheets, pellets, spheroids, and more recently tissue strands (Fig. 34a-c). The basic concept of this approach is the collection, harvest, and extraction of the targeted cells without disrupting the cells or subjecting them to any chemical or enzymatic treatment [374]. Compared to scaffold-based bioinks, these bioinks have a higher starting cell seeding density, cell proliferation, and migration, which reduces the period of time necessary to form a tissue [374]. To enhance cellular interactions, the scaffold-free method involves depositing cell aggregates or multicellular spheroids in 3D models of tissue segments that have already been printed. According to this method, cell-cell interactions lead to self-assembly of cells and the organization of structures [375].

4.7.2.2. Scaffold-based bio-inks. The scaffold-based bioprinting technique (Fig. 34 d,e) involves packing living cells with decellularized matrix components, which are then bioprinted in a specific structure [376]. This method is faster than scaffold-free bioprinting, but requires

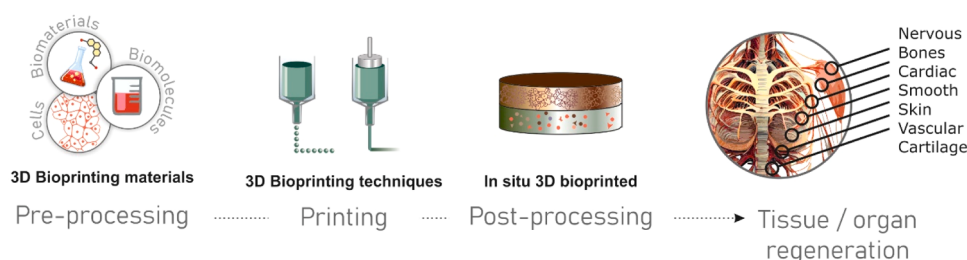
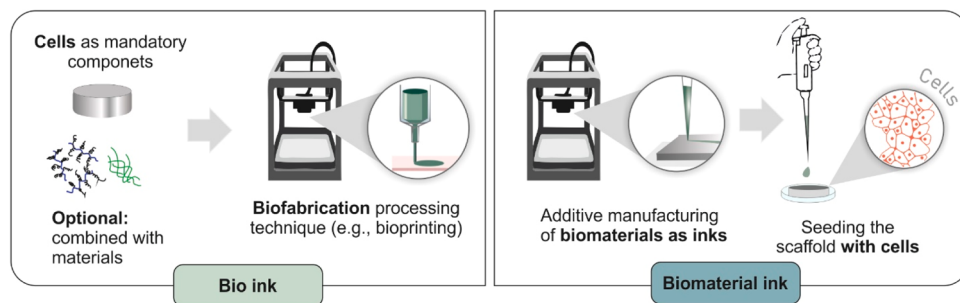
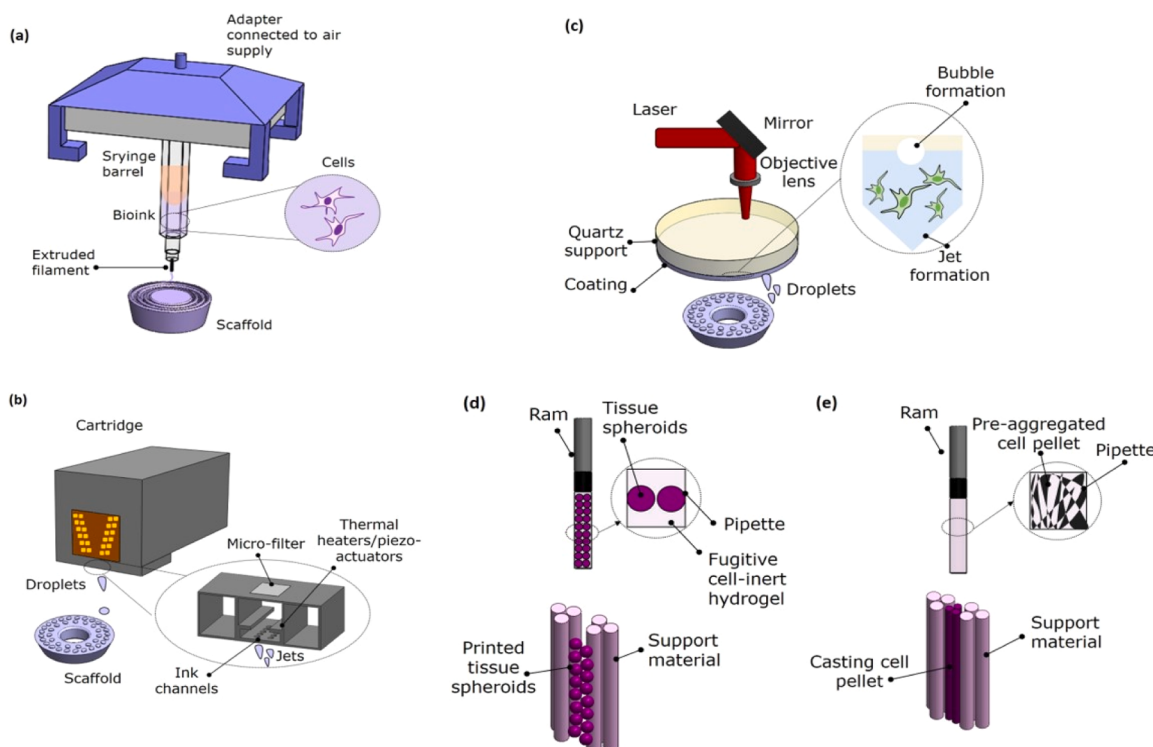


Fig. 32. State-of-the-art 3D bioprinting technology [323].

Table 5

Comparison of parameters based on the bioprinting techniques used: extrusion, droplet, and laser.

Parameter	Extrusion-based	Droplet-based	Laser-based	Vat polymerization	Ref.
Material	various biocompatible materials	Possible to print numerous cells, which is necessary for complex organs.	extremely quick gelation	photo-sensitive bio-ink	[364]
Viscosity	$30 \text{ mPa}\cdot\text{s} \rightarrow 6 \times 10^7 \text{ mPa}\cdot\text{s}$	3.5–12 mPa·s	1–300 mPa·s	No limitation	[322, 365]
Gelation	Shear thinning, temperature, photo-crosslinking, and chemical	Chemical, photo-crosslinking	Chemical, photo-crosslinking	photo-crosslinking	[365]
Resolution	5 μm to a few millimeters	< 1 pl to > 300 pl droplets, 50 μm wide Cell	Possibility of manipulating a single cell	< 50 μm	[366]
Print Speed	Slow (10–50 $\mu\text{m}/\text{s}$)	Fast (1–10,000 droplets per second)	Medium-fast (200–1600 mm/s)	Fast multi layers / s	[322]
Nozzle Dynamics	Shear stress caused by the nozzle wall and extrusion pressure	Non-contact Nozzle, however it might get obstructed	Nozzle Free	Nozzle-Free	[367, 368]
Cell Viability	40–80%	>85%	>95%	>85%	[369]
Cell Density	High, cell spheroids	Low, <10 ⁶ cells/ml	Medium, 10 ⁸ cells/ml	Medium, 10 ⁸ cells/ml	[360]

**Fig. 33.** Difference between a bioink (i.e., cell-laden) and a biomaterial ink (i.e., cell-free).**Fig. 34.** Scaffold-based and scaffold-free bioprinting technologies: (a) extrusion-based bioprinting, (b) droplet-based bioprinting, (c) laser-based bioprinting, (d) bioprinting tissue spheroids, and (e) bioprinting cell pellet collapse.

more time [377]. The bioprinting medium is a soft biomaterial that allows living cells to be deposited as tissue-like replicas. Ideal bioinks should have significant bioprintability, in situ gelation, accuracy, mechanical and structural strength, cytocompatibility, tissue regeneration, permeability, oxygen, nutrients, metabolic waste, and controlled biodegradability. However, producing fully functional organs is challenging due to the lack of a suitable bioink, as conventional materials lack essential characteristics [378].

4.7.3. Hydrogels for 3D bioprinting

Hydrogels are essential components for 3D bioprinting as they incorporate water while remaining impermeable to it in their three-dimensional networks [379]. They have a high-water absorption capacity and can change from a gel to a solid state under certain conditions. These cross-linked polymeric materials are vital for maintaining the mechanical and 3D stability of printed tissue. Hydrogels can be used with a variety of 3D bioprinting techniques, including inkjet, laser-assisted printing, microextrusion, and stereolithography [380]. Advances in 3D bioprinting techniques have made hydrogel-based materials suitable for various uses, including tissue engineering, stem cell therapy, and immunomodulation. However, uses related to biomedical engineering demand more than just mechanical and chemical adaptability from hydrogels; they also require cell compatibility and simulation of the extracellular matrix environment for cell functions [381].

Novel manufacturing methods have been developed to address dynamic modulation of hydrogels, allowing control of spatial heterogeneity and enabling specific biological interactions within printed cells. Some hydrogels also have different cell-binding sites, which makes it easier to bind printed cells for spread, growth, and differentiation [382].

Bioprintable hydrogels can be derived naturally or synthetically. Natural hydrogels, such as collagen, fibrin, and gelatin, have signaling molecules for cell attachment [383]. Synthetically produced hydrogels such as Poly-D, L-Lactic Acid (PLA), Acrylonitrile Butadiene Styrene (ABS), polyethylene glycol (PEG), Poly(glycolic acid) (PGA), polycaprolactone (PCL), Polybutylene Terephthalate (PBT), Poly(vinyl alcohol) (PVA) and Poly(lactic-co-glycolic acid) (PLGA) are also widely used [384]. Natural hydrogels have limitations due to their low mechanical strength and rapid biodegradability. To get around these restrictions, hybrid bioinks comprised of both organic and synthetic hydrogels have been created.

4.7.3.1. Natural polymer-based bioinks. Due to their ability to provide specialized scaffolding systems for the cellular structure and functional arrangement of cells, natural polymers such as collagen, agarose, gelatin, alginic acid, chitosan, etc., have assumed significant roles as bioinks for 3D bioprinting of tissues and organs [385]. They have unique characteristics like nontoxicity, biocompatibility, and biodegradability that make them ideal for a range of tissue engineering applications. Table 6 lists the disadvantages as well as advantages of bioinks made from natural ingredients. Table 7 shows the regeneration of several types of wounded tissues using natural hydrogel-based bioinks.

a) Collagen-Based Hydrogel

Collagen (Fig. 35), is the most common extracellular matrix (ECM) molecule in adult mammals, accounting for 30% of protein composition in multicellular animals [386]. It has 29 subtypes, with type I, type II, and type III variants accounting for 90% of collagen [387]. The primary structural component is a 300 nm protein consisting of three braided α -subunits, each with a repeating motif. These strands form a distinctive triple helix structure, with every residue containing glycine (Gly), forming an Aaa-Baa-Gly-Caa-Daa-Gly repeat unit [387]. The right-handed triple helix is formed by coiling and wrapping parallel chains, creating a left-handed polyproline II-type (PPII) helix supported by 360-degree intra- and interstrand hydrogen bonds [388].

Table 6

Drawbacks and advantages of bioinks made of natural polymers.

Natural-based Bio-inks	Advantages	Disadvantages	Ref.
Collagen	This hydrogel might improve cell adhesion and function because of the ability of collagen to connect with elastin fibers to provide recoil to fibronectin and the extracellular matrix.	Poor mechanical characteristics. Its usefulness could be restricted by rapid degradation. Thrombogenicity, contamination, and source and batch variability are just a few more concerns with the hydrogel.	[432, 433]
Gelatin	Biocompatible and non-immunogenic.	The quick degradation rates and weak mechanical characteristics of the bioink make it inapplicable for the development of stable scaffolds and hydrogels.	[434, 435]
Fibrin	Superior biocompatibility and biodegradation.	Weak mechanical characteristics.	[436]
Silk	Highly printable and have outstanding resolution. Furthermore, cell viability can be preserved.	Poor mechanical characteristics and adverse swelling behavior.	[432]
Alginate	Non-toxic, biocompatibility, biodegradability, and hydrophilic.	Bio-ink might not be very stable and have inadequate mechanical characteristics.	[437]
Hyaluronic acid	The bioink has advantages including inherent bifunctionality, non-immunogenicity, flexibility, and biological degradation.	Fast degradation and weak mechanical characteristics define the bioink. Enzymatic degradation and oxidant species both contribute to degradation.	[438, 439]
Chitosan	In addition to being non-toxic, the bioink offers good flexibility characteristics.	Weak mechanical characteristics, poor stability, and difficulty controlling the pore size.	[440]
Cellulose	After printing, the final construct can have good cell viability and favorable water retention. Additionally, the bioink has high crystallinity, acceptable biocompatibility, low toxicity, and high tensile strength.	Some application restrictions result from poor dissolution.	[441]
Agarose	The bioink only needs relatively low gelation temperatures (40 °C). Additionally, the constructions produced by the bio-ink have good shape accuracy.	Agarose is not frequently used as a material for bioprinting methods because of restrictions associated with viscosity clogging. The construction may be constrained by difficulties with brittleness, even though structures made with this bioink have good shape preservation.	[442, 443]
dECM-based bio-inks	Superior cell viability.	The higher price compared to other bioinks derived from natural sources might be a drawback.	[444]

The right-handed triple helix is created by these parallel chains that coil and wrap around one another to form a left-handed polyproline II type (PPII) helix, which is held in place by hydrogen bonds and interstrand intrastrand $n \rightarrow \pi^*$ interactions [388]. A nucleophile provides the electron density to the vacant π^* orbital * of a neighboring carbonyl group in an $n \rightarrow \pi^*$ interaction. Energy is released as these orbitals combine, leading to an attractive interaction.

Table 7

Use of natural hydrogel-based bioinks in the regeneration of several types of injured tissues.

Tissue or organ	Bio-inks	Reference
Skin Tissue	<ul style="list-style-type: none"> - Nanocellulose alginate with Fibroblasts. - dECM hydrogel containing various cell types. - Collagen with keratinocytes and fibroblasts. - Gelatin-methacryloyl with human fibroblasts. - Fibrin containing human-induced pluripotent stem cells. - Schwann cells containing methacrylated hyaluronic acid. - Fibrin containing neural progenitor cells. - Fibrin-containing neural cells. 	[445] [416] [446] [447] [448] [333] [449] [450]
Neural tissue		
Periodontal tissue	<ul style="list-style-type: none"> - Gelatin-alginate-containing stem cells from human dental pulp. - Cells containing gelatin methacrylate from human primary periodontal ligaments. 	[449] [337]
Renal tissue	<ul style="list-style-type: none"> - Photo-cross-linked dECM in human kidney cells that have undergone methacrylation modification. - Epithelial endothelial cells embedded in an alginate-gelatin-pectin hydrogel. 	[451] [336]
Adipose tissue	<ul style="list-style-type: none"> - Gelatin-alginate containing mesenchymal tissue from human adipose tissue. - dECM hydrogel containing human adipose-derived stem cells. 	[452] [453]
Tracheal graft	- Fibrin hydrogel containing mesenchymal stem cells.	[454]
Chondral tissue	<ul style="list-style-type: none"> - Collagen-supramolecular hyaluronic acid incorporated human mesenchymal stromal cells. - Silk with stem cells. - Hyaluronic acid containing gelatin-methacrylamide-methacrylated hyaluronic acid containing human adipose stem cells. - Alginate with human chondrocytes and osteogenic progenitors. 	[455] [339] [456] [457]
Vaginal wall	- Alginate contains endometrial mesenchymal stem cells.	[338]
Bone tissue	<ul style="list-style-type: none"> - Alginate-gelatinagarose hydrogel seeded with SaOS-2 cells. - The bone-like hybrid hydrogel comprises chitosan-hydroxyapatite nanocrystals seeded with human osteosarcoma cells. - Chitosan contains osteoblast cells. - Silk-gelatin hydrogel seeded with mesenchymal stem cells. 	[419] [458] [334] [459]
Breast tissue	- dECM hydrogel containing human adipose-derived stem cells.	[460]
Muscle tissue	<ul style="list-style-type: none"> - dECM hydrogel seeded with human skeletal muscle cells. - The dECM hydrogel contains progenitor cells. - The alginate-collagen hydrogel contains intestinal smooth muscle cells. 	[461] [330] [462]
Vascular constructs	- Fibrinogen-gelatin hydrogel containing primary neonatal human dermal fibroblasts.	[463]
Cardiac tissue	<ul style="list-style-type: none"> - The dECM hydrogel contains human-induced pluripotent and mesenchymal stem cells. - Alginate contains human cardiac-derived cardiomyocyte progenitor cells. 	[464] [465]
Menisci	- Silk-gelatin hydrogel containing fibrochondrocytes.	[414]
Biological engineered tissues	<ul style="list-style-type: none"> - Alginate-chitosan-agarose contains induced pluripotent stem cells. - Platelet-rich plasma embedded in an alginate-gelatin hydrogel. - Human mesenchymal stem cells seeded in agarose. - The collagen hyaluronic acid hydrogel contains human bone marrow-derived mesenchymal stromal cells. 	[466] [467] [468] [342]
Spinal cord	- Collagen-silk hydrogel containing neural stem cells.	[469]
Blood vessels	- Polyethylene glycol-hyaluronic acid-gelatin contains fibroblasts.	[470] [332] [471]

Table 7 (continued)

Tissue or organ	Bio-inks	Reference
	<ul style="list-style-type: none"> - vascular smooth muscle cell-laden hydrogel comprising gelatin methacryloyl, Polyethylene(glycol) diacrylate and alginate. - Gelatin methacryloyl contains multiple cell types. 	

Collagen is a hierarchical biomaterial that self-assembles into fibrils about 1 cm long and 500 nm in diameter. It is biodegradable, biocompatible, and low immunogenic, making it popular in 3D bioprinting for tissue engineering applications [389]. Collagen has been used in 3D bioprinted thyroid gland, skin healing, and cornea fabrication [390]. Commercial collagen is obtained primarily from mammalian sources, such as pig hide and bone, but can spread diseases. Marine collagen, found in fish by-products such as skin, scales, and bone, offers advantages over land-based mammalian collagen, including its abundance, low melting point, low viscosity, good water solubility, and low risk of disease transmission [391].

b) Fibrin-Based Hydrogels

Fibrin (Fig. 36), a biopolymer generated during blood coagulation, is crucial for wound healing by inhibiting blood leakage and facilitating tissue regeneration. Its 3D network of randomly placed fibers inhibits blood leakage and helps platelets and leukocytes produce soluble components [392]. Fibrin's *in vivo* approach is straightforward and repeatable *in-vitro*. Its amino acid sequences facilitate cell attachment, proliferation, and differentiation, and its biocompatibility makes it a popular scaffold for 3D cell culture in tissue engineering applications.

In limited proteolysis by thrombin, fibrinogen, a plasma glycoprotein 340 kDa, is transformed into fibrin [393]. Due to changes in partial proteolysis, phosphorylation or sulfation of amino acids, genetic polymorphisms, and alternative splicing, the protein is quite diverse [394]. Fibrinogen is made up of 29 disulfide bonds that connect its $2\alpha_1$, $2\beta_1$, and 2γ -chains together to form a dimeric structure [394]. The D-region is made up of the β_1 - and C-termini, while the N-termini of all 6 chains are found in the E-region. $2\alpha_1$ -helical coiled coil segments link the D-regions to the E-region. In fibrinogen, the α_1 C-termini are globular and adjacent to the E region [395].

The physical, mechanical, and rheological characteristics of bio-inks are crucial for 3D bioprinting's effectiveness. Fibrinogen bioink cannot maintain a stable shape due to its Newtonian fluid behavior [396]. To overcome this issue, methods such as combining fibrinogen with printable materials such as gelatin and PEG have been developed. These techniques create tissue-like structures, simulating complex soft tissues with mechanical stiffness, and improving hard-like tissues by enhancing cell survival in stiffer microenvironments [397].

c) Hydrogels based on hyaluronic acid

HA (Fig. 37), is a naturally occurring polymer composed of negatively charged glycosaminoglycans (GAGs) found in all vertebrate tissues [398]. It is biodegradable and biocompatible but can be broken down by enzymes or free radicals. HA contributes to tissue preservation, homeostasis, viscoelasticity, and lubrication, and plays an essential role in inflammation, wound healing, tissue repair, morphogenesis, tumor proliferation, and metastasis [399]. Its 3D cross-linked network promotes cell attachment and hydrophilicity, allowing molecules to diffuse within its matrix. HA-based hydrogels are ideal for 3D bioprinting due to their biomechanical stability, printability, and degradation rate [400].

To ensure smooth flow and easy printing, bio-inks with suitable viscosity and shear thinning are used [400]. Low-viscosity bioinks cause sagging and floppy 3D structures, while shear thinning materials maintain long-lasting 3D pattern preservation [401].

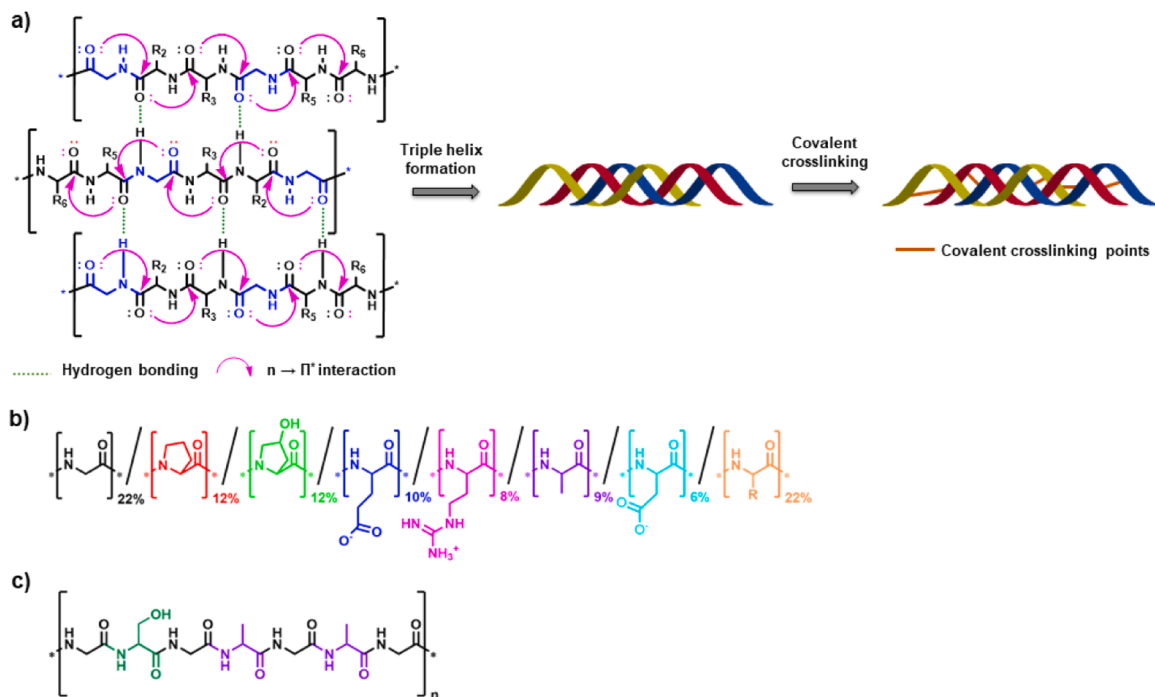


Fig. 35. Chemical structure of collagen.

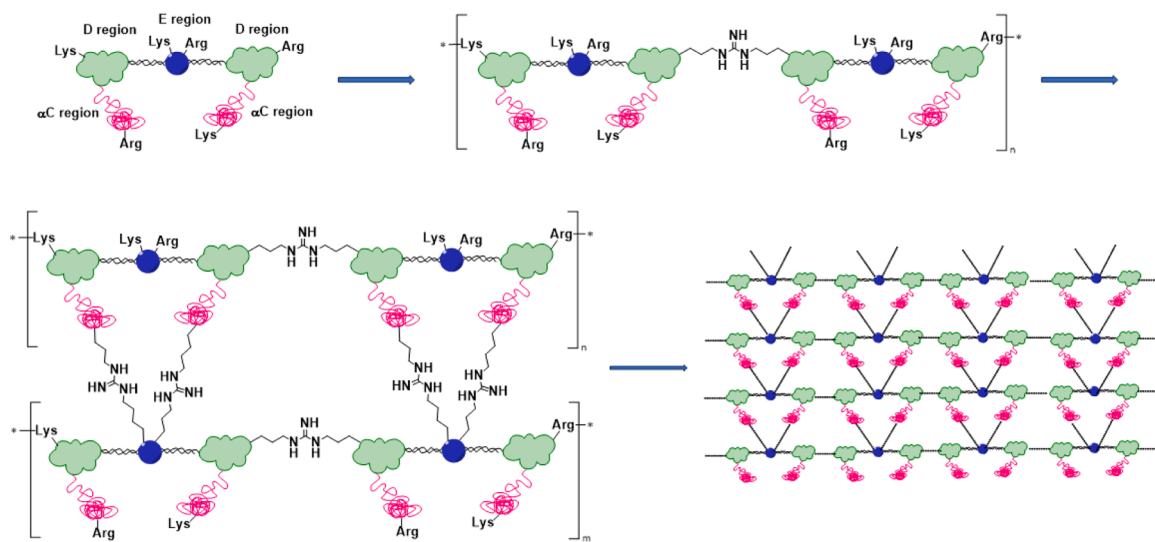


Fig. 36. Diagram showing the structure of fibrinogen, which is stabilized by activated factor XIII and cross-linked by thrombin.

Pentenoate-functionalized HA has shear thinning capabilities, making it a more useful material for bioinks [402]. Improved viscoelasticity of hydrogels can be achieved by combining HA with chitosan, alginate, and other materials [403]. Cross-linking processes also impact printability and physico-rheological characteristics [403]. The process employed to cross-link the material also has a substantial impact on the hydrogel's printability, in addition to its physico-rheological characteristics. Additionally, a stepwise multiple cross-linking method was presented for pure HA hydrogel precursors. For consistent and stable filament extrusion, a chemical pre-cross-linking using a Michael addition reaction is advantageous during the mixing stage. Thiol-acrylate or acrylate-acrylate photopolymerization was used during the extrusion stage to improve the mechanical characteristics of the 3D printed hydrogel and preserve the geometry of the 3D pattern [404].

d) Alginate-Based Hydrogels

Alginate (Fig. 37), is a low-cost biopolymer made from calcium, magnesium, and sodium alginate ions, is a biomaterial commonly used in bioprinting applications [405]. It is a polyanionic linear block copolymer with longer M or G blocks, with G blocks responsible for strength and stiffness and M blocks for elasticity [406]. Alginate is biocompatible and minimally cytotoxic, making it suitable for use in bioinks. However, pure alginate has limitations as a bioink due to lack of binding spots and slow biodegradation [370]. Due to its excellent biocompatibility and minimal cytotoxicity, alginate is a biological polymer that is frequently used in applications involving generic biomaterials [370]. Uses of alginate-based hydrogels for 3D bioprinting are limited by their low viscosity and poor adhesive property.

To improve performance as a bioink, alginate can be mixed with

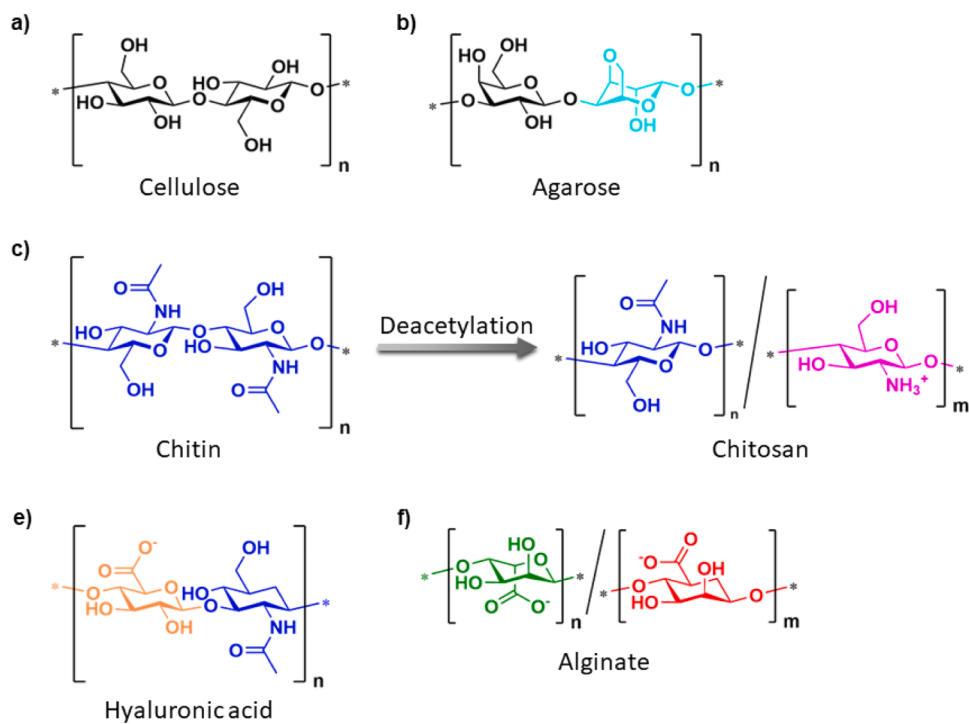


Fig. 37. Chemical structure of cellulose, agarose, chitin, chitosan, HA, and alginate.

other substances such as gelatin, gelatin methacrylate, PVA, hyaluronic acid, collagen, and nanocellulose [407]. Alginate mixed with gelatin improves cell attachment and proliferation, as collagen is hydrolyzed to produce gelatin, which promotes cell adhesion, proliferation, migration, and differentiation [408].

e) Gelatin-based Hydrogels

Gelatin is a water-soluble protein with molecular weights ranging from 20 to 250 kDa, made by partially hydrolyzing collagen from bones, skin, and connective tissues [409]. It forms simple gels at low temperatures through hydrophobic crosslinking and is soluble in warm water solutions [409]. Gelatin gels can only be used at physiological temperatures or higher because of their low melting point. Gelatin can contain biomolecules, allowing for adjustments in crosslinking and molecular weight to control drug loading and release kinetics [409]. Gelatin-based hydrogels are used in various biological applications, including cell encapsulation, wound healing, soft tissue restoration, nerve regeneration, and 3D bioprinting [410].

Gelatin is a well-known candidate for bioinks because of its biocompatibility and biodegradability, but its application is constrained by its low printability [411]. Combining gelatin with other ingredients can improve its rheological characteristics, such as adding hyaluronan and glycerol [411]. A consistent bioink with outstanding printing resolution can be produced using a mixture of 10 mg and 20 ml of gelatins, hyaluronic acid and 10% v/v glycerol [412].

f) Silk-based Hydrogels

Silk, a fibrous protein produced by arachnids and myriapods, has amphiphilic properties and can create semicrystalline structures through hydrophobic reactions and cross-linking [413]. Silk-based hydrogels, a natural hydrogel, have potential applications in tissue engineering, wound healing, bone regeneration, drug release regulation, and 3D bioprinting [413]. Bandyopadhyay and Mandal used an innovative silk-based bioink with superior print accuracy and shear-thinning capabilities [414]. Rodriguez et al. found that silk-based bioinks can be used in soft tissue reconstruction, maintaining structural integrity under

physiological conditions and encouraging cellular infiltration and tissue integration [415]. The bioink is biocompatible and promotes cellular infiltration and tissue integration.

a) dECM-based bioinks

dECM-based bioinks are used in tissue engineering to improve biocompatibility and create 3D bioprinted constructions [416]. These bioinks induce cell-matrix interactions and organ-specific differentiation techniques, preserving normal tissue function and incorporating cell surface receptors [417]. These hydrogels retain essential structural and stimulating features of the extracellular matrix (ECM), attracting interest for recellularization, cell differentiation, and proliferation. Studies have shown that dECM bioinks have the right mechanical characteristics for 3D bioprinting technology and can increase tissue-specific differentiation over traditional bioinks.

g) Agarose-Based Hydrogels

Agarose (Fig. 37), a non-ionic linear copolymer derived from red seaweed, is a biocompatibility factor in biomedical applications [418]. The polymer agarose is derived from agar-agar, which is made from red seaweed. It is a non-ionic linear copolymer that is held together by alternating glycosidic links (14) and (13) made up of repeated units of -D-galactose and - 3, 6-anhydro-L-galactopyranose residues [418].

It can form hydrogels without hazardous catalysts or cross-linking agents and is used for self-healing materials, cell culture, cartilage tissue engineering, drug release, and 3D bioprinting [419]. Gu et al. produced a unique agarose-based bioink, using native and carboxylated agarose [420]. The bioink exhibits sol-gel transition at 37 °C and supports high cell density without sacrificing printability [420].

h) Chitosan-based hydrogels

Chitosan (Fig. 37), an aminopolysaccharide with molecular weights ranging from 50 to 2000 kDa, is found in crustaceans, invertebrates, and fungi [421]. It is a cationic heteropolymer made up of D-glucuronic acid and N-acetyl-D-glucosamine disaccharide linked by alternating β -(1→4) and β -(1→3) glycosidic bonds [421].

Chitosan is insoluble in neutral and basic environments, but can be dissolved in an aqueous acidic environment [422]. Researchers have explored chitosan modification approaches to improve the quality of bioinks. Roehm et al. used ethylenediaminetetraacetic acid (EDTA) to modify chitosan, increasing the expression of chondrogenic chondrocyte genes and cell attachment [423].

They also demonstrated the viability of fabricating structures with chitosan-based bioink composed of chitosan and gelatin [423]. Another study examined a bioink based on nanocellulose / chitosan made from chitosan, glycerophosphate, and hydroxyethylcellulose and embedded with cellulose nanocrystals (CNCs), improving its viscosity and improving the mechanical properties of scaffolds containing cells [424].

i) Cellulose-Based Hydrogels

Cellulose (Fig. 37), a widely used biopolymer, is produced by algae, fungi, and bacteria [425]. It is a linear homopolymer with a 3D matrix and crystalline structure [425]. Several cellulose derivatives have been produced to increase water solubility, such as hydroxypropylmethylcellulose (HPMC) and carboxymethylcellulose (CMC) [426]. These materials are widely used in the pharmaceutical industry for drug administration in oral tablet and capsule formulations [427].

Cellulose has the potential to be a biomaterial for bioprinting due to its 400 biocompatibility traits [428]. Researchers have attempted to overcome its mechanical limitations by creating bio-inks with improved printability and shape accuracy [429]. One such bioink was created by replacing the hydroxyl group in glucopyranose chains with carboxymethyl groups [429]. Another bioink was developed using gelatin, chitosan, carboxymethyl cellulose, and hydroxyapatite. Another study found an antagonistic relationship between sodium alginate and cell viability, with bioinks containing 1% and 2.5% sodium alginate that did not affect cell viability [430].

Another study by Zhang et al. explored the use of bioink based on cellulose for the regeneration of articular cartilage and stem cell therapy [431]. A cellulose-based hydrogel was produced, which displayed shear-thinning and self-healing properties and demonstrated higher elastic modulus in comparison to cellulose-based hydrogels.

4.7.3.2. Synthetic polymer-based bioink. The most practical thermoplastic polymers are synthetic polymers, which offer better structural and mechanical characteristics. Natural polymers have low solubility and high viscosity, whereas synthetic polymers offer high strength, dominating microstructure, and regulated degradability [472]. There are fewer constraints on how synthetic polymers are produced and they have better structural and mechanical characteristics. Given their massive molecular weight, natural polymers are low solubles and have high viscosities [473]. Synthetic polymers have contributed significantly to advances as high applicability materials in 3D bioprinting due to the characteristics they provide, including high strength, dominant microstructure, and controlled degradability [472]. A list of several significant synthetic polymers is provided below, along with a brief description: Fig. 38 shows the chemical structure of various synthetic polymers used as bioink.

1) Polylactic acid (PLA)

A popular polymeric bioink, PLA (Fig. 38), is a hydrolytically degradable aliphatic polyester with features that include biocompatibility, degradability, and printing capability [474]. It is the primary polymer employed in the FDM process, as a precursor, PLA. To replace ligaments and non-biodegradable fibers, PLA-generated filaments can be employed in musculoskeletal tissue engineering. The breakdown of PLA results in the production of acidic by-products, which compromises its long-term biocompatibility by causing tissue inflammation and cell death [475]. Furthermore, PLA fragility limits its application because it reduces its overall strength relative to bone. By combining it with inexpensive ceramics, such as calcium phosphate, the restriction can be bypassed. Create stronger bone scaffolds and reduce undesirable acid production [475].

2) Poly-D,L-Lactic Acid

Lactic acid is the source of the polymer known as Poly-D,L-lactic acid (PDLLA) (Fig. 38), which has an amorphous structure. Natural hydrophobicity, practical biocompatibility, and durable mechanical properties make it well suited for biomedical applications, particularly in SLA methods. Polymers are among the most frequently utilized to produce porous and biocompatible scaffolds. As a result, it is

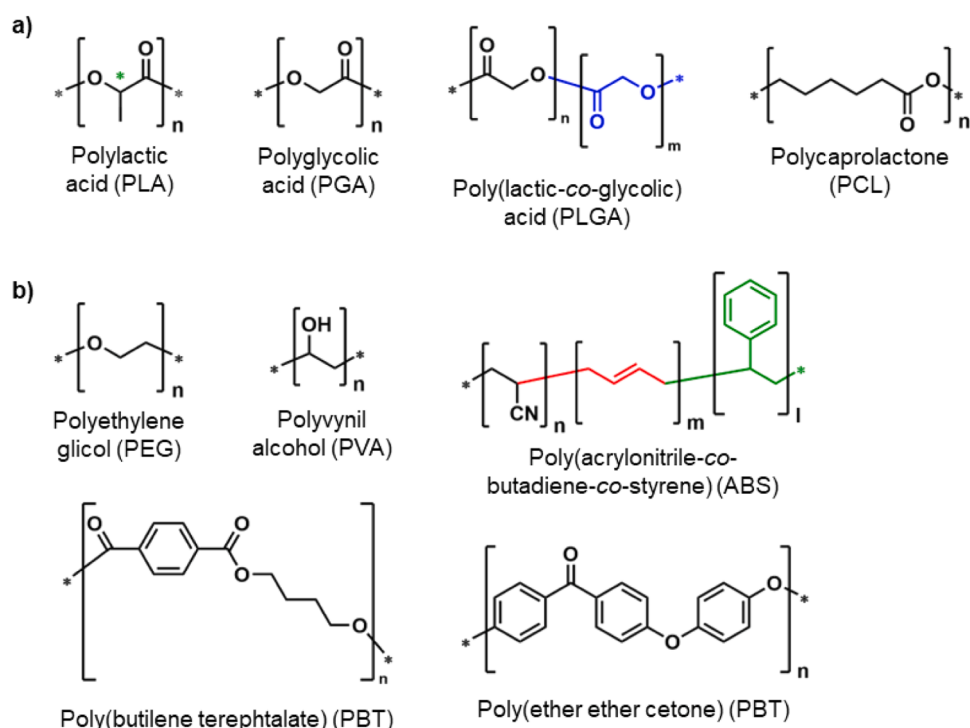


Fig. 38. Chemical structure of various synthetic polymers used as bioink.

used in resorbable orthopedic rehabilitation devices and tissue engineering [476]. Due to its hydrophobicity, PDLLA prevents water from diffusing through its matrix, which slows its breakdown. Hydrophilic groups, on the other hand, increase water absorption. While this is going on, the presence of hydrophilic groups might lower the pH, which will cause the polymer to break down into monomers, as well as produce undesirable allergic and inflammatory reactions in the body [477].

3) Acrylonitrile Butadiene Styrene (ABS)

The triblock copolymer Acrylonitrile Butadiene Styrene (ABS) (Fig. 38) has petrochemical origins. The styrene terpolymer chemical family, which has adequate strength and toughness, is related to ABS. Applications for this material are expanded by its low melting point (105 °C). ABS is composed of three separate monomers, including acrylonitrile, butadiene, and styrene, which together contribute to the material's heat resistance, powerful impact strength, and rigidity. ABS is employed as a precursor in processes such as fused deposition modeling (FDM) and selective laser sintering (SLS) printing. In cartilage technology, it is also employed. However, the material's biodegradability, identical cell integration, and processability to polylactic acid (PLA) limit its usefulness [475].

4) Polyethylene Glycol (PEG)

Radical polymerization is a method employed to create polyethylene glycol (PEG), a hydrophilic polymer (Fig. 38). Its structure is either branched or linear, and its tail groups are hydroxyl ions that are asymmetric or dissymmetric. Nowadays, PEG is used increasingly frequently in drug delivery approaches the creation of scaffolds for tissue engineering, and surface changes that result in amphiphilic block copolymers and ionomers [478]. PEG naturally produces hydrogels and is resistant to protein adsorption and cell adhesion. They lack mechanical strength and are not biodegradable. Their inability to degrade is also linked to the presence of a cyclic carbon (C-C) polymer backbone. However, hydrolytic and enzymatic degradation frequently contribute to the degradability [478].

5) Poly(glycolic acid) (PGA)

Poly(glycolic acid) (PGA), a key synthetic polymer used in the 3D scaffold design (Fig. 38), is thought to be tissue compatible due to its chemical diversity, ease of production, and biological properties. Glycolic acid monomer is produced during PGA biodegradation of PGA and is easily excreted from the body via certain catabolic pathways such as carbon dioxide and water [479]. Additionally, PGA copolymers can preserve their mechanical and physical characteristics. PGA is used to make resorbable sutures and internal fixation devices for bones. The decomposition products of PGA are less hazardous than those of PDLLA. When the PGA surface is functionalized through hydrolysis of ester linkages, the seeding density and cell spread can be enhanced. Although the hydrolysis method has important advantages, its surface morphology and mechanical strength can limit it. It is sensitive to bulk erosion, which can cause the scaffold to collapse and release harmful acidic degradation products [479].

6) Poly Caprolactone (PCL)

In addition to being a more affordable polymer, polycaprolactone (PCL) (Fig. 38), has excellent bioink properties like rigidity, biocompatibility, and degradability [480]. PCL is among the non-toxic polymers that can withstand significant stability [481]. Typically, stability lasts for six months with a biological half-life. SLS-printed PCL scaffolds have features such as a porous structure that promotes connectivity, a rough surface, and compaction that is comparable to bone that promotes bone regeneration and cell ingrowth. Although scaffolds for uses other than bone tissue engineering, their extended biological half-life provides a secondary barrier. Additionally, due to its hydrophobicity, it has low bioactivity, which slows tissue adhesion and cell proliferation [482].

7) Polybutylene Terephthalate (PBT)

Thermoplastic polyester made of polybutylene terephthalate

(PBT) (Fig. 38), is biocompatible and used in FDM printing techniques [482]. PBT exhibits high elasticity, simple processing, and reasonable strength and toughness. PBT is a typical polymer that is frequently used in the biomedical field for *in-vivo* and *in-vitro* biocompatibility [483]. The printing of canine trabecular bone scaffolds and tissue regeneration continue to be two uses for it. Orthopedic surgery also uses it as a filler. It has physical and chemical characteristics similar to PCL or PLA and has no distinguishable advantages [484]. Like other polymers, PBTs decompose under aqueous conditions via oxidation or hydrolysis. Its limited use is due to its high melting point (225 °C) and non-biodegradable nature, which results in the development of crystalline residues during *in-vivo* application [485].

8) Polyvinyl alcohol (PVA)

In the presence of vinyl alcohol and acetate, polyvinyl alcohol (PVA) (Fig. 38) is produced synthetically. These monomers are what make these polymers biocompatible, biodegradable, bioinert, and semicrystalline. A water-soluble polymer called PVA is used in SLS printing technology. Similarly to human articular cartilage, PVA has tensile strength. PVA can produce complex structures when used with the right glue and can also act as an ideal matrix for bone cells [486]. While its semicrystalline shape enables effective transport of oxygen and nutrients to the cell, its preferred hydrophilicity and chemical stability allow it to withstand severe pH and temperature. PVA has many uses in load-bearing procedures, including as the treatment of craniofacial deformities and bone tissue engineering uses [487].

9) Polylactic glycolic acid (PLGA)

The polymer known as polylactic glycolic acid (PLGA) (Fig. 38), is remarkably cytocompatible and has a dependable biodegradable nature [488]. It is osteoconductive and has mechanical characteristics similar to those of human calcareous bone. In several tissue restoration systems and animal models for bone regeneration, PLGA is also employed. However, the hydrophobic property delays its application. In addition, linear structures result in weak mechanical rigidity and a fast deterioration rate, restricting their use as a scaffolding material. When combined with PCL, the fracturing of the fractured PLGA debris can be reduced. This fracturing is vulnerable to increasing inflammatory responses *in-vivo* testing [489].

4.7.4. Key processing factors for 3D bioprinting using hydrogel-based bioinks

Bioinks are essential components of bioprinting, consisting of cells and biomaterials formed through automated biofabrication methods [490]. Cells are crucial for precise placement and organ development, while biomaterials ensure stability, activity, and proliferation [379]. Recent research focuses on developing high-precision, stable bioinks with high cell loading and survival rates [491]. Hydrogels, with their high water content, help cells survive and protect them from manufacturing stresses [491]. However, developing a hydrogel that supports and protects cells while providing a stable structural basis can be challenging because of its varying mechanical requirements. Stiff hydrogels must strike a balance between structural integrity and cell suspension [491].

The most important characteristics of bioinks are their rheological characteristics, dimensional stability, and biocompatibility, all of which are essential to preserve cell viability and proliferation throughout the printing process [379].

4.7.4.1. Nozzle aperture size, geometry, and applied pressure. Previous research indicates that the nozzle aperture size and shape, applied pressure, and cell viability of printed cell-laden hydrogels all have a significant impact on the printing process's success. In fact, the pressure of the system and the nozzle size that are used affect the percentage of

cell death rates, with lower cell viability being seen as the printing pressure and the aperture of the nozzle increase [492].

4.7.4.2. Printing rate. Given how difficult it is to maintain cell viability after prolonged printing, the printing speed has an impact on the way well millimeter- or centimeter-scale biostructures are built. From picoliter to nanoliter per minute, the printing rate can be electronically controlled. It affects both the overall printing time as well as the final dimensions of the filament or droplet and is dictated by the robot motors' motion capability [493].

4.7.4.3. Volumetric flow rate. The volume of printed bioink that passes through the nozzle per unit of time, is essential for determining the shape of bioprinted filaments or droplets [494]. The size of the droplet might be calculated using a straightforward mathematical model that takes into account the relationship between the volumetric flow rate and the printing speed, as long as the effects of swelling and deformation are minimal [494]. The diameter of the droplet is maximized when the flow rate is high and the printing speed is low, while the diameter is decreased when the flow rate is low and the printing speed is high [495].

4.7.4.4. Rheological characteristics of bio-Ink. The printing accuracy and cell lifespan of bioinks are influenced by their rheological characteristics. Rheology will be a more crucial variable when hydrogel-based bioinks are optimized as bioprinting technology develops. Flow behavior, viscosity, shear stress, and viscoelasticity are some of the key rheological variables that influence the final features of 3D bioprinted tissues and biological structures [496].

The fluidity of the bioinks is essential in extrusion bioprinting, as the bioinks must be ejected via an injection port and built one on top of the other on a substrate. A rheometer can be used to test rheological characteristics, which can be identified by variables such as viscosity, storage modulus, and loss modulus. To maintain their shape and stability, bioinks need to gel or cross-link immediately after extrusion. Viscosity is a crucial characterization criterion for bioinks, since they are typically in a non-cross-linked or pre-cross-linked form prior to extrusion. High viscosity is advantageous for maintaining shape and improving mechanical stability; however, it might result in obstruction and uneven buildup. Uneven cell dispersion and deposition are the result of low viscosity [379].

Because of the higher extrusion force caused by high viscosity, shear-thinning materials with rheological attributes have gained interest in bioinks. Non-covalent cross-linked bonds of hydrogel materials break down reversibly, causing shear thinning [379]. Non-covalent links sever under strong shear forces, reducing the viscosity of the bioink. After the shear force, the bonds reunite under the influence of noncovalent forces, enhancing the viscosity and preserving the form stability.

Three phases can be used to examine the rheological characteristics of bioinks (see Fig. 39) [497]. The static viscosity at the beginning of the

initial outflow stage corresponds to the minimum force needed for the bioink to flow and the yield stress is that minimum force. Because high-yield stresses might harm cells and devices, these can be used to assess the suitability of the material for extrusion printing. Viscosity decreases with shear rate during the shear thinning stage, allowing continued extrusion and improving cell survival. However, instead of being a uniform thread, the bioink might become droplets if the viscosity falls below a particular threshold. Post-print curing ability is determined during the post-print recovery stage by interaction between viscosity and time, which has an impact on stability and cell dispersion. Cell sedimentation can be caused by slow viscosity recovery [379].

4.7.4.5. Flow behavior. The correlation between shear stress (also referred to as viscosity) and shear rate affects the flow property of hydrogels, that reveal their resistance to shear deformation. This flow divides behavior into Newtonian and non-Newtonian types [498]. The characterization of bioink flow dynamics is crucial for 3D bioprinting. The preferred bioinks have been stated to exhibit shear-thinning behavior that allows the bioink to flow readily with no clogging [497] while additionally enhancing the printing fidelity and stability of 3D bioprinted structures [498]. Hydrogel-based bioinks typically exhibit non-Newtonian flow.

4.7.4.6. Viscosity. Viscosity is a crucial rheological characteristic of bioinks, as lower viscosities give the cells a favorable environment but impair the printability, whereas higher viscosities may increase the stability of the bioprinted construct at the expense of cell viability. Additionally, a high viscosity could lead to clogging at the nozzle tip, so the amount should be changed depending on the size of the tip of the nozzle. The molecular weight, polymer concentration, mass of additives, temperature, and pre-crosslinking can all be adjusted for the bioink formulations to manage viscosity [499].

4.7.4.7. Shear stress. During bioprinting procedures, shear stress is determined by the viscosity of the bioinks, which might affect cell survival and proliferation. This is due to the possibility of cell injury at higher shear stress levels [500]. Since they provide optimal printing fidelity and the capacity to retain cells viable under *in vitro* and *in-vivo* conditions, hydrogel-based bioinks with low shear stress rates at moderate pressures are chosen [500].

4.7.4.8. Viscoelasticity. To calculate the viscoelasticity, the storage and loss coefficient is dynamically monitored as a function of shear stress, strain, frequency, or time. The energy that a material may retain or recover after each cycle of deformation is indicated by the elastic modulus (G'), also known as the storage modulus. The loss modulus, also known as the modulus of viscosity (G), on the other hand, expresses the energy dissipated through viscous dissipation per cycle of deformation. As a result, in 3D bioprinting, G' and G are associated with elastic form

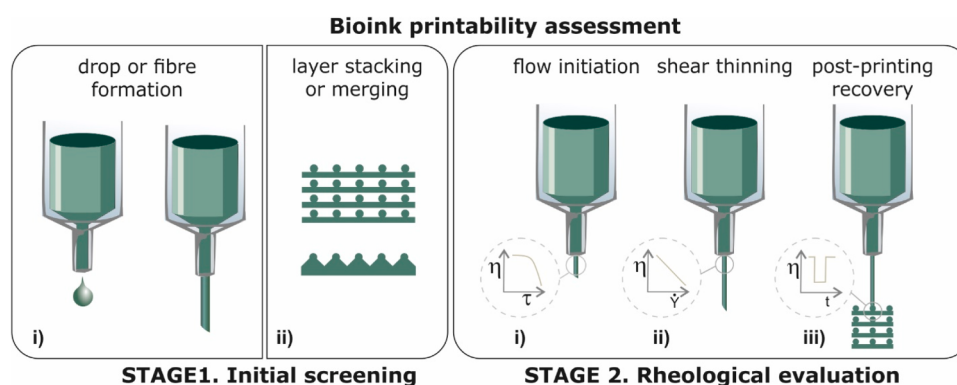


Fig. 39. Rheological assessment of Bio-ink [497].

retention and viscous flow [501].

Viscoelasticity is essential for cell-hydrogel interactions, porosity, and the degeneration of 3D bioprinted structures. It can be considerably altered by the type, concentration, and crosslinking of the hydrogels employed. Additionally, it affects cell differentiation and proliferation along with the structural integrity of hydrogels [502]. Furthermore, bioinks with larger storage moduli exhibit more solid-like behaviour, providing structural stability while additionally running the risk of breaking and clogging filaments. Nevertheless, although being easier to work with, hydrogel-based bioinks with higher loss moduli might produce less stable 3D structures [502].

An additional viscoelastic metric, the damping factor ($\tan(\delta) = G''/G'$) or loss tangent, offers important insights into the interaction between viscous and elastic deformational characteristics. With your help, the structural integrity and homogeneity of the bioprinting procedure can be predicted both during and after the procedure. The damping factor should be between 0.2 and 0.6 for an ideal hydrogel-based bioink to produce a balanced relationship between the hydrogel's structural integrity and the bioink's uniformity during bioprinting. On the other hand, when $\tan(\delta)$ is less than 0.2 or greater than 0.6, we see nozzle blockage and poor form retention, respectively [502].

4.7.5. Cells

Dispersed cells, cell spheroids, and tissue strands can all be part of bioinks employed in extrusion printing due to a broad spectrum of injection port widths (between 50 μm and 1000 μm [503]). At present, scattered cells and biomaterials are widely used in the development of complex 3D tissue structures. The poor intercellular connection, which triggers cell function, poor anti-inflammatory ability, and low immunological resistance *in vivo*, limits its usage in clinical medicine and other biomedical fields. Therefore, innovative bioink designs that can maneuver around these constraints are required [379].

During 3D bioprinting, cell aggregation in the form of cell spheroids possesses several benefits, since it provides a microenvironment that is comparable to that of natural tissue and has properties including anti-inflammatory capacity, tissue regeneration, immunological effects, as well as elevated survival rates [504]. Cell spheroids, which generally consist of spherical aggregates of cells around 200–400 μm in diameter, are being used in ongoing investigations to generate bioinks for printing. For example, Kelm et al. printed the vascular network of renal tissue using cell spheroids made of human umbilical vein endothelial cells coated over human aortic fibroblasts as cores [505]. Researchers have developed a different approach to 3D bioprinting, which has been developed by researchers using tissue strands, which are cylindrical newborn tissues. Using an alginate catheter to culture cell aggregates, Akkouch et al. were able to produce a full tissue strand using ionic decrosslinking [506]. While this was going on, Gabor et al. used multicellular cylinders as printing units to make scaffolds for vessels with tiny diameters [507].

5. 4D bioprinting technology

While 3D bioprinting has revolutionized biomedical applications, its complexity in tissue engineering has led to the development of 4D printing, which adds time as a fourth geometric dimension and addresses its drawbacks as well [508]. In 2013, MIT professor Skylar Tibbits developed 4D printing, which enables objects to change their physical form, properties, and functions in response to surrounding stimuli like water, pH, heat, electric or magnetic fields, or light [509]. Fig. 40 demonstrates how 4D printing, an innovative form of 3D printing, considers the materials and type of stimuli [508]. Due to its advantages over traditional additive manufacturing (AM), 4D printing, is becoming more and more common in a variety of industries like electronics, soft robotics, and particularly biomedical applications like tissue engineering, drug delivery, and wound repair [510]. 4D printing uses the same fabrication processes as 3D printing, such as SLA, DLP, FDM,



Fig. 40. Diagrams for 4D bioprinting. A stimulation externally can cause the printed bioconstruct to change in size, shape, or functionality.

and PolyJet, but with time as a modulating factor for specific constructions [511]. EBB, which is sometimes referred to as DIW in the literature, is the technology of choice for 4D bioprinting since it has several advantages over other AM techniques used in the biomedical sector [512]. EBB offers advantages such as suitable printing resolution, material selection freedom, minimal raw material requirements, economic effectiveness, and viability for composite printing, making it a lab-friendly technique [512].

4D bioprinting allows biomedical devices to communicate with their physiological environment, enhancing sensitivity [513]. Responsiveness involves using materials that can change shape in response to external stimuli. Common materials include shape-memory polymers (SMPs) and shape-changing materials (SCMs). SMPs have a temporary shape and a recovery process, while SCMs, such as liquid crystal elastomers (LCEs) or hydrogels, gradually change shape and return to their original states [514].

As shown in Fig. 40, the main characteristic of 4D bioprinting is "change" in terms of dimension, shape, or functionality. The items may expand or shrink depending on the size change. In the majority of 4D bioprinting uses, the printed objects have the potential to change shape in response to external stimulus. One such example is the controllable evolution of a flat structure into a variety of shapes (such as a self-folding, flower-like, cubic box, and other forms). Another sort of 4D bioprinting is the modification of functionality, that involves the evolution of living cells, comprising cell fusion, cell assembly, and a variety of biological activities [515].

5.1. Potential bioinks for 4D bioprinting

Materials that are stimulus-responsive adjust their conformation in response to particular stimuli, such as temperature, pH, humidity, electricity, magnetic fields, light, acoustics, or a combination of these stimuli [516]. There is great potential for stimuli-responsive materials to be used as 4D bioprinting bioinks. Their capacity to be printed and biocompatibility are key factors in how well these materials work in 4D bioprinting. The safety of the stimulation procedure should also be evaluated with regard to the tissues and cells that were created. Here, we look at a few different types of stimuli-responsive materials that can be used for 4D bioprinting [516].

a) Thermo-responsive materials

Materials that are temperature-responsive can modify their physicochemical characteristics in response to temperature changes. The materials that respond to temperature have been investigated the most are those made of poly(*N*-isopropylacrylamide, or PNIPAM) based polymers [517]. Due to their superior printability, processing ease, and glass transition temperature, these thermally sensitive solid-state polymers (SMPs) are frequently utilized in 4D printing [518]. Only a few of synthetic-based SMPs have the intrinsic characteristics needed to fabricate bio-inks for 4D printing, however most exhibit thermally responsive behavior. Biomedical uses are not possible with materials that have high glass transition temperatures.

In order to use PNIPAM for TERM applications, scientists have developed synthetic materials that are thermo-responsive. Changes in wettability and deformation are caused by bioactive materials' contraction or expansion [519].

Bakarich et al. designed a smart valve using Alg/PNIPAm ionic covalent entanglement gel ink, which automatically closes under hot water and opens in cold water, potentially enhancing soft robotics and smart sensing applications [520]. These 4D-printed actuation hydrogel materials have potential to be used in numerous soft robotics and smart sensing applications. The research conducted by Liu et al. on a zinc, metformin, and F127-based thermosensitive hydrogel showed how well it could cure burn wounds and traumatic skin defects [521].

b) Magneto-responsive materials

Research on electric and magnetic fields has shown the potential of magneto-sensitive materials like para- and ferro-magnetic nanoparticles (MNPs) in the biomedical sector. These materials offer controlled therapeutic action and minimal invasiveness, such as in the development of magneto-responsive DDS for treating soft tissues. Magnetized bio-inks also help control NP direction during bioprinting [522]. By incorporating Fe-based NPs into poly(dimethylsiloxane), Zhu et al. produced magneto-responsive driven 4D-printed bioproducts. Furthermore, the magnetized bio-inks can aid in regulating the direction of NPs throughout the bioprinting process, resulting in scaffolds with anisotropic characteristics [523]. Further examples of magneto-sensitive polymeric materials produced for TE uses include scaffolds made of $\text{Fe}_3\text{O}_4/\text{PCL}$ /mesoporous bioactive glass (MBG) [524], scaffolds made of iron-doped hydroxyapatite (HAP)/PCL [525], and magneto-nanocomposite scaffolds made of $\text{Fe}_3\text{O}_4/\text{polyethylene glycol diacrylate}$ (PEGDA) and $\text{Fe}_3\text{O}_4/\text{PCL}$ [526]. By means of demonstration, Kuhnt et al. investigated the use of anisotropic Fe_3O_4 magnetic NPs with PEGDA hydrogel using a DLP-based 3D printing technique. When these magnetic NPs were added to polymeric nanocomposites, they displayed exceptional viability more than 95% of human dermal fibroblasts and outstanding biocompatibility when directly planted on top of human mesenchymal stem cells (MSCs) [527]. Later, unpaired movements are made possible by aligning magnetic NPs with the appropriate scaffold orientations. Due to this, these magnetic NPs are particularly well suited for TE in a variety of biomedical uses.

c) Electro-responsive materials

Electro-responsive materials, including polymers, are bioactive materials that can be stimulated by electric fields to adjust their behavior. These materials can also contain additives like carbon nanotubes and graphene [528]. They are being explored for muscle and neural tissue engineering applications, with conductive polymer-based hydrogels being a potential choice. In this regard, Okuzaki et al. constructed an origami robot using 4D printing and an organic polymer with electro-sensitive polypyrrole [529]. These bioactive materials are currently being researched in order to produce constructions for brain and muscular TE applications [530]. Additionally, conductive polymer-based hydrogels have great printing capabilities and are biocompatible, making them a potential choice for biomaterials to be printed in 4D.

d) Photo-responsive materials

A light stimulation can be used to change the size or shape of the structures using photo-responsive materials, involving volume changes, contraction, and bending. These substances include photosensitive nanomaterials, nitrobenzene, azobenzene, fulgide, or polymers containing stilbene [531]. Chromophores are incorporated into polymer resins to produce photo-responsive polymeric products. The development of these materials is also possible by incorporating photosensitive nanoparticles into polymers [532]. Depending on the type of chromophore, the response could be either irreversible or reversible [533]. Thoughtful investigation for TE applications is

necessary for 4D bioprinting of polymeric materials that contract, expand, or self-assemble following photo-triggering.

e) Moisture-responsive materials

Moisture-responsive materials can expand, fold, twist, or deform in humid situations. Examples include microcrystalline cellulose (MCC) and silk fibroin [534]. Applications in soft robotics and actuation are aided by these characteristics. Microcrystalline cellulose was utilized by Zhang et al. to build materials that are sensitive to moisture [535], while Kim et al. employed 3D printing with UV-assisted direct-ink writing to make smart structures that might change shape when exposed to moisture [536]. Humidity is a driving force in the actuation of other polymeric materials as cellulose, silk fibroin, PU, and PEGDA. Cui et al. created tendril-inspired hydrogel artificial muscles that demonstrated shape memory behavior and a high actuation rate in response to certain stimuli [537].

f) pH-responsive materials

pH-responsive biomaterials are biologically active materials with different chemical groups that respond to environmental pH changes by releasing or gaining protons, causing them to collapse or swell [538,539]. Materials that are pH-responsive alter chemically and/or structurally in response to pH variations in their environment [540]. When the pH changes, these materials' chemical groups, such as carboxyl, pyridine, sulfonic, phosphate, and tertiary amines, release or receive protons. These materials are divided into basic and acidic polymers, and are used in biomedical applications like gene delivery systems, and glucose sensors. The sensitivity of these materials can also be utilized in tissue engineering applications due to the differences in pH levels. In reaction to variations in the pH of the environment, biomolecules stored in these materials can be released in a targeted manner. The 3D bioprinting process frequently employs alginate [541,542]. As a result, materials based on alginate that are pH sensitive may be employed in 4D bioinks.

g) Biological-responsive materials

Biological-responsive materials use bio-enzymes, glucose, and biomolecules to cleave peptide sequences and biomolecules, causing polymers to swell. This shape-morphing effect can be applied in tissue engineering applications [543]. As an example, Devillard et al. developed bioinspired hydrogels that were activated by the bio-enzymes thrombin and alkaline phosphatase [544]. This caused the 4D-printed object to develop fibrin deposition and calcification.

5.2. Applications of 4D bioprinting

4D bioprinting offers significant potential for various biomedical applications, including tissue engineering, biosensors, bioactuators, and biorobotics, by fabricating smart, multifunctional materials that enhance current materials' functionality.

a) Tissue Engineering

Four-dimensional bioprinting is crucial for fabricating hierarchically complex and dynamic tissues, such as shape-memory and cell-laden scaffolds [545]. These constructs can adapt to conformational changes, accelerating their regenerative potential [546]. In situ unfolding of 4D bioprinted scaffolds can be used for cell delivery in narrow spaces, such as subretinal spaces. Bioelectronic and biodegradable devices can control delivery procedures wirelessly. These smart constructs enable effective communication with the body's natural environment and use natural forces or stimuli for desired changes [547].

b) Biosensors

Four-dimensional bioprinting can open up fresh possibilities for the creation of biosensors that track the activity and functioning of cells. Biosensors have already been developed via three-dimensional printing technology. In order to create molecularly imprinted polymer-based microcantilever-based biosensors, Gomez et al.

employed a two-photon stereolithography technique [548]. Similar to Credi et al., cantilevers containing magnetic nanocomposites were developed using the stereolithography technology [549]. Cell activity and function can be investigated using these cantilevers. For instance, Cui et al. bioprinted mouse myoblasts (C2C12 cell line) for use in biosensing on extremely small cantilevers [550]. When exposed to an exogenous chemical toxins (veratridine), the myotubes on the cantilevers changed their rate of contraction and responded synchronously to electrical stimulation.

c) Bioactuators and Biorobotics

4D printed actuators and robots have been developed, including mechanically strong alginate/PNIPAM hydrogels, airway stents, and stimuli-responsive structures. Cross-linkable liquid crystal polymers were used to print elastomers that change shape in response to thermal stimuli [551]. Laser writing methods were used to create self-folding constructs, which can curve, fold, or roll up as exposed to external stimuli [552].

6. Conclusion and future scope

This bibliographic overview emphasizes how 3D printing has the ability to accomplish tasks that are impossible to carry out using conventional manufacturing techniques. The freedom to create and customize items as well as the on-demand fabrication of intricate components, offers significant benefits to the end user. Greater environmentally friendly operations are also aided by decreased material waste and the need for transporting and storing manufactured products. In this context, the wide range of distinct techniques with such diverse printing characteristics allows a good adaptation to highly different sectors, applications, and materials. With the application of numerical modeling, machine learning, and artificial intelligence to 3D-fabricated components, future applications are entering a new era. Nevertheless, each of them has positive and negative aspects depending on the intended use or the material that needs to be printed. Therefore, in the deliberation preceding the selection of a specific 3D printing technique, it becomes imperative to contemplate several essential aspects: which materials—metals, ceramics, or polymers—shall be employed for the printing process? Is the envisaged component to be manufactured from a singular material or shall it necessitate a multi-material approach? What are the key characteristics of the chosen material for the printing process? Answering these questions could lead the user to select the most adequate technique to be utilized. In the biomedical field, it is quite frequent to need to create a multi-material or multifunctional device, either because it is necessary to use various materials with distinct properties or because it is necessary to apply the same material with various concentrations of its components in order to create concentration gradients. In this sense, although they present excellent resolutions, techniques such as VAT polymerization or laser sintering would not be adequate. Printing multiple inks in one printing step is limited to material jetting and material extrusion. However, material jetting presents an important constraint related to the narrow range of printable viscosities allowed, what makes this technique more appropriate for printing small molecules or precursors, or low-concentration nanoparticle suspensions. Among the material extrusion technologies, DIW stands out for the possibility it offers to print fluid materials with a broad spectrum of viscosities. Selecting the most appropriate printing strategy and nozzle diameter, it can span from relatively low viscosities (for example, Lewis et al. [553] printed a soft polydimethylsiloxane-based ink reducing the nozzle diameter to 30 μm) to very high viscous pastes (for example, Biasetto et al. printed a Ti6Al4V ink containing a 72% of metallic particles increasing the nozzle diameter to 810 μm) [554].

The rise in the global population and longer life expectancies is resulting in a significant uptick in musculoskeletal disorders affecting people of all ages, with varying degrees of disability ranging from short-term to chronic conditions. Among the various musculoskeletal

disorders affecting bones and joints, notable examples include osteoporosis, osteochondral defects (OCD), osteoarthritis, rheumatoid arthritis, and injuries resulting from accidents. Regardless of the underlying cause of these disorders, the demand for implants to replace damaged bone and/or joint structures has emerged as a pressing public health concern in today's society. Diseases affecting both bone and cartilage, such as OCD, necessitate the development of treatments that involve the replacement of both tissue types. While treatments based on autograft or allograft transplants, as well as bioengineered tissues, have already been implemented, they primarily address the issue of articular cartilage. Consequently, there has been a recent focus on exploring biphasic implants as a solution for simultaneously substituting both bone and cartilage tissues in a single surgical procedure. Typically, these implants comprise a rigid section designed to replace bone and a soft outer layer that mimics cartilage tissue. The advantages DIW technology offer of printing multi-materials in just one printing step and the wide range of printable inks points this technique as the ideal option to fabricate biphasic implants, since a metal-based ink could be printed to fabricate the bone replacements and a polymer-based ink could be used as the cartilage tissue substitute. In the scenario of osteochondral defects, we will introduce new developments and trends, when proposing a biphasic implant design ("tailored-made materials") with a better and balanced tribo-mechanical and biofunctional behaviour.

Some of these approaches are related to the replace of subchondral bone defect via printing β titanium alloys and Alumina/Zirconia-based ceramic composites, with controlled porosity (content, size, morphology, and distribution), or the surface modification treatments of the implant area that will be in contact with the host bone tissue, to implement better antibacterial behaviour and/or promote osseointegration. In this sense, among the most promising treatments are the following:

- a) Bioactive glass coatings (BGs) serve as intriguing scaffold materials for bone regeneration owing to their realized superior osteoconductivity, controlled biodegradability, capacity to activate osteogenic gene expression, and angiogenic potential for promoting bone mineral via the release of various charged particles which influence gene expression in osteogenic procedures and vascularization rates that merely lead to the afterwards the encouragement of bone formation [247,555,556].
- b) Sol-gel deposition of hydroxyapatite coatings can be used to prevent the release of metal ions and to implement more resistance to corrosion as well as increment of bioactivity [136,141,225,557,558].
- c) Manipulation of roughness and texture of the implant surface using Femtosecond laser [559]. Laser texturing is a potential method that has numerous advantages than other conventional procedures since it is clean, fast, contactless, and, most importantly, it can be used outside and has remarkable precision [560]. The micro machining by femtosecond laser allows for a wide variety of surface structures, ranging from the nanometric to the micron-scale, so it is necessary to precisely select the appropriate processing parameters [561]. In this context, it's crucial to keep in mind the Directed Irradiation Synthesis (DIS) [561,562]. DIS is a novel method that allows for not only the control and adjustment of both surface topography (nanoscale), but also the chemistry of the surface by controlling the parameters of the ion beam, providing biomaterials with advanced and multi-functional bio-interfaces in order to provide new biological functions [563].
- d) Porous β titanium alloys reinforced by carbon nanotubes, could be an alternative when using 5% and 10% w/w, to obtain nanocomposite entities that display lower stiffness, higher mechanical strength and implemented bioactivity [564].
- e) A significant alternative to address concerns about antibiotic resistance is the deposition of silver nanoparticles, which can stop bacterial growth caused by the release of Ag⁺ [565].

- f) Sulfonated Polyetheretherketone Coatings are an effective anti-biofouling synthetic material that serves as an alternative to conventional antibacterial treatments since it provides a straightforward chemical surface modification for preventing MRSA adherence and growth [566].
- g) Materials with encapsulated Rose Bengal Microspheres is an example of an approximation based on chemical entities extracted from nature with anti-inflammatory pharmacological properties to tackle inflammation produced in these types of surgeries [567].
- h) In order to give cutting-edge treatment choices for a variety of diseases, especially those related with bone tissue, like osteosarcomas, bone cavities, or trauma, customized healthcare and the use of minimally invasive surgery call for new biomedical devices. The therapeutic advantages of local hyperthermia in these pathologies are right now being studied in a number of biological and clinical investigations, as moderate controlled hyperthermia (42°C) prevents bacterial infections, encourages vascularization of bone tissue, and encourages the development of new bone and osseointegration, whereas intense controlled hyperthermia ($>42^{\circ}\text{C}$) leads to apoptosis in cancer cells and enables novel approaches for the treatment of osteosarcoma [568,569]. This technique has the potential to be effective since graphene oxide has exceptional photothermal properties, particularly when subjected to near-infrared laser light [570]. The ability to control localized hyperthermia and modify the biological response of the bone tissue would be made possible by remote heating of the implants [570].
- i) Antibacterial materials with customized poly(acrylic acid) based hydrogels could be used as coatings with the appropriate cross-linking grade to implement antibacterial properties and enhancement of osseointegration rates [571].
- j) The stimulation, proliferation and differentiation of bone cells, especially osteoblasts, through the use of electromagnetic fields, whether static or pulsed, has been a growing source of interest for researchers. The most studied method is the static magnetic field, which uses low-intensity fields to activate biological processes and promote the formation of various tissues, including bone tissue. Studies show that the use of this technique has the potential to help regenerate bone [572,573], increase bone density, decrease pain and improve mobility. Pulsed magnetic fields also present themselves as a promising route for applications in bone regeneration. In addition, some studies combine the use of materials with magnetic properties and the application of magnetic fields to obtain better results. Research carried out by Yun et. al., combine a static magnetic field with a magnetic nanocomposite scaffold made from polycaprolactone/magnetic nanoparticles to evaluate their osteoblastic functions and bone formation, their results indicate that this can be a promising technique for bone regenerative engineering [574]. In this context, a particle of a soft ferromagnetic material with an elongated geometry (rod, thread, tube) tends to orient its magnetization along the geometric axis of symmetry. For high magnetization saturation values, a strong field is generated at the tips of these elongated geometries, facilitating preferential growth of new bone tissue in the direction of the axis of symmetry of the particles.
- k) Integrating micro- and nanoscale- modifications and functionalization with protein, peptides, and bioactive agents improved the wettability and biological activity of titanium implant surfaces. This morphological and chemical modifications of titanium surfaces lead to the migration and differentiation of osteogenic cells, which is followed by an improvement in the production of the mineral matrix, which quickens the osseointegration activity. Additionally, a possible method to prevent early and late implant failures brought on by the formation of biofilm is the inclusion of bioactive compounds into nanostructured surfaces [575]. The hLf1-11 peptide, a potent AMP derived from the human protein lactoferrin, that we showed drastically reduced the adhesion of diverse bacterial strains to the titanium surface [576–578]. With the goal of increasing TiO_2

implant sensitization and promote quicker and more effective osseointegration, which in some cases has been explored using molecular docking and dynamics simulations, the incorporation of various peptides is a time- and money-saving type of method. Additionally, the bio-functionalization of the surface, which promotes cell adhesion and mineralization of newly produced tissue by using certain proteins (bovine serum albumin) and BMPs [579].

On the other hand, to replace damaged cartilage (chondral tissue) is tricky since it possesses a low ability for endogenous repair and unfortunately there are no efficient treatments to repair this specific tissue that degrade when increasing age population that suffers from osteoarthritis. Cartilage tissue engineering aims to develop efficient treatments to provide a 3D environment to provide a space for correct cell proliferation. in the joint area the materials needed could be approached using different chemical entities such as the use of chitosan, alginate, collagen, silk, gelatin or hyaluronan. They promote the development of cartilage at the same time as promote biocompatibility, better biodegradability, convenient mechanics, and cellular adhesion. For the non-natural materials, examples that could be used are polymers are Polyglycolic Acid (PGA) or Polyethylene glycol (PEG) that display ad hoc biodegradability via a chemical tailor-made design [19]. Among the most significant approaches are the following:

- a. In Bioactive Gelatin-Alginate-Bioactive Glass Composite Coatings, the biomaterial shown a greater elastic recovery when utilizing 50% alginate and 50% gelatin, providing evidence that this method might imitate soft tissue activities in the joint regions [234].
- b. Porous silver nanoparticle/polycaprolactone/polyvinyl alcohol coatings exhibit antibacterial properties along as porous networks to allow convenient vascularization. In this case silver cation and AgNPs released from the composite to show a perfect antimicrobial behaviour against *P. aeruginosa* and *S. aureus*. For this study, 50/50 and 80/20 PCL/PVA composites containing 0.4% AgNPs have been used to offer a short-term or longer-term antimicrobial release model. Interestingly, 50/50 PCL/PVA polymer composite was able of creating larger pores while the 80/20 material with pores of approximately $14\ \mu\text{m}$ enhances fibroblast growth factor. If needed this biomaterial is capable of release Ag cation after 21 days [580].
- c. The approach concerning hydrogels materials created using Interpenetrating polymer network hydrogels has been also efficient to generate bioactive scaffolds for tissue engineering and needs to be explored further. This is based on the search for convenient 3D microenvironments that mimic the real tissue concerning not only architectural and physical properties such as mechanical integrity to withstand physiological forces, but also key characteristics such as adhesion or degradability. The great advantage of this chemical entities is since the properties can be easily adjusted via a convenient organic chemistry synthesis. Simple reactions are often used in this kind of transformation such as click reactions that exhibits excellent chemical yields and no further purification is required [581].
- d. Other materials are based on the combination of various types of natural or non-natural chemical entities with gradient composition such as chitosan, hydroxypropyl methyl cellulose, PCL, PVA, hyaluronic acid, collagen, depending on the native osteochondral tissue, also taking into account that crosslinking grade could be an exceptional tool to control mechanical properties associated to cartilage [582–585].

Declaration of Competing Interest

The authors declare the following financial interests/personal relationships which may be considered as potential competing interests: Yadir Torres reports financial support was provided by University of

Seville. Yadir Torres reports a relationship with University of Seville that includes: employment. Yadir Torres has patent #2632888. issued to N/A. Yadir Torres has patent # EP16382069.9 issued to N/A. Yadir Torres has patent #PCT/US18/26567 issued to N/A.

Data availability

No data was used for the research described in the article.

Acknowledgements

This publication is part of the R+D+i projects [PDC2022-133369-I00 and PID2022-137911OB-I00], both funded by MCIN/AEI/10.13039/501100011033.

References

- [1] A. Bandyopadhyay, S. Bose, *Additive Manufacturing*, CRC Press., 2019.
- [2] B. Lyons, *Bridge* 44 (2014).
- [3] A.A. El Hadad, E. Peón, F.R. García-Galván, V. Barranco, J. Parra, A. Jiménez-Morales, J.C. Galván, *Materials* 10 (2017) 94.
- [4] J.S. Akmal, M. Salmi, A. Mäkitie, R. Björkstrand, J. Partanen, *J. Funct. Biomater.* 9 (2018) 41.
- [5] E. Huotilainen, M. Salmi, J. Lindahl, *Knee* 26 (2019) 923–932.
- [6] S.S. Shipp, N. Gupta, B. Lal, J.A. Scott, C.L. Weber, M.S. Fiminin, M. Blake, S. Newsome, S. Thomas, *Emerging Global Trends in Advanced Manufacturing*, Institute for Defense Analyses Alexandria VA, 2012.
- [7] C.W. Hull, United States Patent, Appl., No. 638905, Filed (1984).
- [8] B.C. Gross, J.L. Erkal, S.Y. Lockwood, C. Chen, D.M. Spence, Evaluation of 3D printing and its potential impact on biotechnology and the chemical sciences, *ACS Publ.* (2014).
- [9] V.G. Gokhare, D. Raut, D. Shinde, *Int. J. Eng. Res. Technol.* 6 (2017) 953–958.
- [10] S.S. Crump, *Apparatus and method for creating three-dimensional objects*, Google Patents, 1992.
- [11] C.K. Chua, K.F. Leong, *3D Printing and Additive Manufacturing: Principles and Applications* (With Companion Media Pack)-of Rapid Prototyping, World Scientific Publishing Company., 2014.
- [12] H. Dodziuk, *Kardiocirurgia i Torakochirurgia Pol. /Pol. J. Thorac. Cardiovasc. Surg.* 13 (2016) 283–293.
- [13] N. Shahruhudin, T.C. Lee, R. Ramlan, *Procedia Manuf.* 35 (2019) 1286–1296.
- [14] J.I. Lipton, M. Cutler, F. Nigl, D. Cohen, H. Lipson, *Trends Food Sci. Technol.* 43 (2015) 114–123.
- [15] T. Spahiu, E. Canaj, E. Shehi, *J. Eng. Fibers Fabr.* 15 (2020), 1558925020948216.
- [16] P. Wu, J. Wang, X. Wang, *Autom. Constr.* 68 (2016) 21–31.
- [17] I.G. Ian Gibson, *Additive Manufacturing Technologies 3d Printing, Rapid Prototyping, and Direct Digital Manufacturing*, Springer., 2015.
- [18] S. Saleh Alghamdi, S. John, N. Roy Choudhury, N.K. Dutta, *Polymers* 13 (2021) 753.
- [19] A.A. Elhadad, A. Alcudia, B. Begines, E.M. Pérez-Soriano, Y. Torres, *Appl. Mater. Today* 29 (2022), 101603.
- [20] F. Rengier, A. Mehndiratta, H. Von Tengg-Kobligk, C.M. Zechmann, R. Unterhinninghofen, H.-U. Kauczor, F.L. Giesel, *Int. J. Comput. Assist. Radiol. Surg.* 5 (2010) 335–341.
- [21] N. Wake, H. Chandarana, W. Huang, S. Taneja, A. Rosenkrantz, *Clin. Radiol.* 71 (2016) 610–614.
- [22] T. Friedman, M. Michalski, T.R. Goodman, J.E. Brown, *Skelet. Radiol.* 45 (2016) 307–321.
- [23] M. Blaszczyk, R. Jabbar, B. Szmyd, M. Radek, *J. Clin. Med.* 10 (2021) 1201.
- [24] A. Davids, L. Apfelbacher, L. Hitzler, C. Krempaszky, *Lect. Notes Adv. Struct. Mater.* (2022) 99–117.
- [25] M. Whitaker, *Bull. R. Coll. Surg. Engl.* 96 (2014) 228–229.
- [26] O. Gülcen, K. Güneydin, A. Tamer, *Polymers* 13 (2021) 2829.
- [27] J. Gardan, *Int. J. Prod. Res.* 54 (2016) 3118–3132.
- [28] L. Yang, K. Hsu, B. Baughman, D. Godfrey, F. Medina, M. Menon, S. Wiener, *Additive Manufacturing of Metals: The Technology, Materials, Design and Production*, Springer., 2017.
- [29] H. Yang, J.C. Lim, Y. Liu, X. Qi, Y.L. Yap, V. Dikshit, W.Y. Yeong, J. Wei, *Virtual Phys. Prototyp.* 12 (2017) 95–103.
- [30] A. Pugalendhi, R. Ranganathan, S. Ganesan, *Mater. Today.: Proc.* 46 (2021) 9139–9144.
- [31] J. Edgar, S. Tint, *Johns. Matthey Technol. Rev.* 59 (2015) 193–198.
- [32] I. Gibson, D.W. Rosen, B. Stucker, M. Khorasani, D. Rosen, B. Stucker, M. Khorasani, *Additive Manufacturing Technologies*, Springer., 2021.
- [33] Z. Rahman, N.A. Charoo, M. Kuttolamadom, A. Asadi, M.A. Khan, Chapter 46 - Printing of personalized medication using binder jetting 3D printer, in: J. Faintuch, S. Faintuch (Eds.), *Precision Medicine for Investigators, Practitioners and Providers*, Academic Press, 2020, pp. 473–481.
- [34] E. Sachs, M. Cima, J. Cornie, *CIRP Ann.* 39 (1990) 201–204.
- [35] H. Miyanaji, M. Orth, J.M. Akbar, L. Yang, *Front. Mech. Eng.* 13 (2018) 504–512.
- [36] M. Ziaeef, N.B. Crane, *Addit. Manuf.* 28 (2019) 781–801.
- [37] J. Gonzalez, J. Mireles, Y. Lin, R.B. Wicker, *Ceram. Int.* 42 (2016) 10559–10564.
- [38] A. Mostafaei, E.L. Stevens, J.J. Ference, D.E. Schmidt, M. Chmielus, *Addit. Manuf.* 21 (2018) 63–68.
- [39] D.A. Snelling, C.B. Williams, C.T. Suchicital, A.P. Druschitz, *Int. J. Adv. Manuf. Technol.* 92 (2017) 531–545.
- [40] T. Dahmen, N. Henriksen, K. Dahl, A. Lapina, D. Pedersen, J. Hattel, T. Christiansen, M. Somers, *Addit. Manuf.* 39 (2021), 101912.
- [41] D. Behera, M. Cullinan, *Precis. Eng.* 68 (2021) 326–337.
- [42] R.K. Enneti, K.C. Prough, T.A. Wolfe, A. Klein, N. Studley, J.L. Trasorras, *Int. J. Refract. Met. Hard Mater.* 71 (2018) 28–35.
- [43] B. Zhang, Z. Zhan, Y. Cao, H. Gulau, P. Linner, J. Sun, T. Zwick, H. Zirath, *IEEE Trans. Terahertz Sci. Technol.* 6 (2016) 592–600.
- [44] B. Utela, D. Storti, R. Anderson, M. Ganter, *J. Manuf. Process.* 10 (2008) 96–104.
- [45] S. Masia, P.D. Calvert, W.E. Rhine, H.K. Bowen, *J. Mater. Sci.* 24 (1989) 1907–1912.
- [46] A. Mostafaei, A.M. Elliott, J.E. Barnes, F. Li, W. Tan, C.L. Cramer, P. Nandwana, M. Chmielus, *Prog. Mater. Sci.* 119 (2021), 100707.
- [47] S.J. Trenfield, A. Awad, C.M. Madla, G.B. Hatton, J. Firth, A. Goyanes, S. Gaisford, A.W. Basit, *Expert Opin. Drug Deliv.* 16 (2019) 1081–1094.
- [48] J. Deckers, J. Vleugels, J.-P. Kruth, J. Ceram. Sci. Technol. 5 (2014) 245–260.
- [49] A. Mostafaei, J. Toman, E.L. Stevens, E.T. Hughes, Y.L. Krimer, M. Chmielus, *Acta Mater.* 124 (2017) 280–289.
- [50] R. Trombetta, J.A. Inzana, E.M. Schwarz, S.L. Kates, H.A. Awad, *Ann. Biomed. Eng.* 45 (2017) 23–44.
- [51] R. Bogue, *Assem. Autom.* 33 (2013) 307–311.
- [52] G.X. Gu, M. Takaffoli, A.J. Hsieh, M.J. Buehler, *Extrem. Mech. Lett.* 9 (2016) 317–323.
- [53] F. Calignano, D. Manfredi, E.P. Ambrosio, S. Biamino, M. Lombardi, E. Atzeni, A. Salmi, P. Minetola, L. Iuliano, P. Fino, *Proc. IEEE* 105 (2017) 593–612.
- [54] H. Mostafaei, *IEEE Trans. Ind. Electron.* 66 (2018) 5567–5575.
- [55] A. Katz-Demanyet, V.V. Popov Jr, A. Kovalevsky, D. Safranchik, A. Kozioug, *Manuf. Rev.* 6 (2019).
- [56] Z. Chen, F. Li, W. Chen, D. Zhu, Z. Fu, *J. Mater. Eng. Perform.* 30 (2021) 3705–3717.
- [57] T. Colton, C. Inkley, A. Berry, N.B. Crane, *J. Manuf. Process.* 71 (2021) 187–196.
- [58] T. Singh, S. Kumar, S. Sehgal, *Mater. Today.: Proc.* 28 (2020) 1927–1931.
- [59] W. Piedra-Cascón, V.R. Krishnamurthy, W. Att, M. Revilla-León, *J. Dent.* 109 (2021), 103630.
- [60] R. Palucci Rosa, G. Rosace, *Macromol. Mater. Eng.* 306 (2021), 2100345.
- [61] A. Medellin, W. Du, G. Miao, J. Zou, Z. Pei, C. Ma, *J. Micro Nano-Manuf.* 7 (2019).
- [62] S. Sahin, *A New Approach to Vat Polymerization Additive Manufacturing*, Universitat Politècnica de Catalunya., 2022.
- [63] W.L. Ng, J.M. Lee, M. Zhou, Y.-W. Chen, K.-X.A. Lee, W.Y. Yeong, Y.-F. Shen, *Biofabrication* 12 (2020), 022001.
- [64] W. Li, L.S. Mille, J.A. Robledo, T. Uribe, V. Huerta, Y.S. Zhang, *Adv. Healthc. Mater.* 9 (2020), 2000156.
- [65] C.I. Higgins, T.E. Brown, J.P. Killgore, *Addit. Manuf.* 38 (2021), 101744.
- [66] M. Wiese, A. Kwauka, S. Thiede, C. Herrmann, *CIRP J. Manuf. Sci. Technol.* 35 (2021) 268–280.
- [67] T.D. Ngo, A. Kashani, G. Imbalzano, K.T. Nguyen, D. Hui, *Compos. Part B: Eng.* 143 (2018) 172–196.
- [68] M. Vaezi, S. Chianrabutra, B. Mellor, S. Yang, Multiple material additive manufacturing-Part 1: a review: this review paper covers a decade of research on multiple material additive manufacturing technologies which can produce complex geometry parts with different materials, *Virtual Phys. Prototyp.* 8 (2013) 19–50.
- [69] N. Guo, M.C. Leu, *Front. Mech. Eng.* 8 (2013) 215–243.
- [70] A. Awad, F. Fina, A. Goyanes, S. Gaisford, A.W. Basit, *Int. J. Pharm.* 586 (2020), 119594.
- [71] V. Chastand, P. Quaegebeur, W. Maia, E. Charkaluk, *Mater. Charact.* 143 (2018) 76–81.
- [72] K.C. Kolan, M.C. Leu, G.E. Hilmas, R.F. Brown, M. Velez, *Biofabrication* 3 (2011), 025004.
- [73] T.G. Spears, S.A. Gold, *Integr. Mater. Manuf. Innov.* 5 (2016) 16–40.
- [74] E. Louis, P. Fox, C.J. Sutcliffe, J. Mater. Process. Technol. 211 (2011) 275–284.
- [75] M. Vaezi, S. Chianrabutra, B. Mellor, S. Yang, *Virtual Phys. Prototyp.* 8 (2013) 19–50.
- [76] C.A. Terrazas, J. Mireles, S.M. Gaytan, P.A. Morton, A. Hinojos, P. Frigola, R. B. Wicker, *Int. J. Adv. Manuf. Technol.* 84 (2016) 1115–1126.
- [77] V.A. Matviychuk, V. Nesterenkov, M. Rusynik, *Электротехника и электроника* 53 (2018) 69–73.
- [78] W.J. Sames, F. List, S. Pannala, R.R. Dehoff, S.S. Babu, *Int. Mater. Rev.* 61 (2016) 315–360.
- [79] R. Galante, C.G. Figueiredo-Pina, A.P. Serro, *Dent. Mater.* 35 (2019) 825–846.
- [80] M. Ueda, D. Carter, K. Yamazaki, Y. Kakinuma, *Journal of Advanced Mechanical Design, Systems, and Manufacturing* 14 (2020) JAMDSM0015–JAMDSM0015.
- [81] I. Mathoho, E. Akinlabi, N. Arthur, M. Tlottengl, *CIRP J. Manuf. Sci. Technol.* 31 (2020) 450–458.
- [82] B. Lu, H. Lan, H. Liu, *Opto-Electron. Adv.* 1 (2018), 170004.
- [83] E.S. Rosker, R. Sandhu, J. Hester, M.S. Goorsky, J. Tice, *Int. J. Antennas Propag.* 2018 (2018) 1–19.
- [84] B. Bliim, F. Krebs, M. Ley, C. Gläßner, M. Smaga, J.C. Aurich, R. Teutsch, T. Beck, *Metals* 9 (2019) 1285.
- [85] J. Halo, 2021.

- [86] B. Baufeld, R. Widdison, T. Dutilleul, Wire based electron beam additive manufacturing, 70th IIW assembly and international conference Shanghai, China, 2017.
- [87] V. Bharav, P. Kattire, S. Thakare, R. Singh, A review on functionally gradient materials (FGMs) and their applications, in: IOP conference series: materials science and engineering, vol 229, IOP Publishing, 2017, 012021.
- [88] B. Dermeik, N. Travitzky, Adv. Eng. Mater. 22 (2020), 2000256.
- [89] I. Gibson, D. Rosen, B. Stucker, M. Khorasani, D. Rosen, B. Stucker, M. Khorasani, Additive Manufacturing Technologies, Springer, 2021.
- [90] D.T. Pham, R.S. Gault, Int. J. Mach. Tools Manuf. 38 (1998) 1257–1287.
- [91] A. Babbar, A. Sharma, V. Jain, D. Gupta, Additive Manufacturing Processes in Biomedical Engineering: Advanced Fabrication Methods and Rapid Tooling Techniques, CRC Press, 2022.
- [92] N.T. Aboulkhair, F. Bosio, N. Gilani, C. Phutela, R.J.M. Hague, C.J. Tuck, Chapter Six - Additive manufacturing processes for metals, in: J. Kadkhodapour, S. Schmauder, F. Sajadi (Eds.), Quality Analysis of Additively Manufactured Metals, Elsevier, 2023, pp. 201–258.
- [93] F. Xu, H. Loh, Y. Wong, Rapid Prototyp. J. 5 (1999) 54–60.
- [94] W. Wu, X. Li, Q. Liu, J.Y.H. Fu, A. Zheng, Y. Zhou, L. Ren, G. Li, Mater. Today Adv. 16 (2022), 100319.
- [95] S. Niyanth, (2016).
- [96] C. Hopkins, M. Dapino, S. Fernandez, J. Eng. Mater. Technol. 132 (2010).
- [97] I. Buj-Corral, A. Tejo-Otero, F. Fenollosa-Artés, Fused Depos. Model. Based 3D Print. (2021) 277–297.
- [98] I.T. Ozbolat, M. Hospidouk, Biomaterials 76 (2016) 321–343.
- [99] Z. Gu, J. Fu, H. Lin, Y. He, Asian J. Pharm. Sci. 15 (2020) 529–557.
- [100] C. Suwanpreecha, A. Manonukul, Metals 12 (2022) 429.
- [101] O. Mlicete, R. Côté, V. Demers, V. Brailovski, Addit. Manuf. 60 (2022), 103252.
- [102] J.M. Justino Netto, H.T. Idogava, L.E. Frezzatto Santos, Zd.C. Silveira, P. Romio, J.L. Alves, Int. J. Adv. Manuf. Technol. 115 (2021) 2711–2727.
- [103] D.L. Bourell, W.E. Frazier, H.A. Kuhn, M. Seifi, ASM Handbook: Additive Manufacturing Processes, ASM International, 2020.
- [104] W. Li, A. Ghazanfari, M.C. Leu, R.G. Landers, Virtual Phys. Prototyp. 12 (2017) 193–205.
- [105] M.P. Serdeczny, R. Comminal, D.B. Pedersen, J. Spangenberg, Addit. Manuf. 32 (2020), 100997.
- [106] A. Ferrández-Montero, M. Lieblich, R. Benavente, J.L. González-Carrasco, B. Ferrari, Addit. Manuf. 33 (2020), 101142.
- [107] L. Xie, H. Guo, Y. Song, C. Liu, Z. Wang, L. Hua, L. Wang, L.-C. Zhang, Mater. Charact. 161 (2020), 110137.
- [108] N. Pirch, S. Linnenbrink, A. Gasser, H. Schleifenbaum, Int. J. Heat. Mass Transf. 143 (2019), 118464.
- [109] P. Li, Y. Gong, Y. Xu, Y. Qi, Y. Sun, H. Zhang, Arch. Civ. Mech. Eng. 19 (2019) 820–831.
- [110] J. Dilag, T. Chen, S. Li, S.A. Bateman, Addit. Manuf. 27 (2019) 167–174.
- [111] Y. He, F. Zhang, E. Saleh, J. Vaithilingam, N. Aboulkhair, B. Begines, C.J. Tuck, R. J. Hague, I.A. Ashcroft, R.D. Wildman, Addit. Manuf. 16 (2017) 153–161.
- [112] J.-Y. Lee, J. An, C.K. Chua, Appl. Mater. Today 7 (2017) 120–133.
- [113] W. Zhang, M. Tong, N.M. Harrison, Data Brief. 27 (2019), 104559.
- [114] L.E. Murr, J. Mater. Res. Technol. 9 (2020) 1087–1103.
- [115] M.A. Dechet, A. Demina, L. Römling, J.S. Gómez Bonilla, F.J. Lanyi, D. W. Schubert, A. Bück, W. Peukert, J. Schmidt, Addit. Manuf. 32 (2020), 100966.
- [116] F. Verga, M. Borlaf, L. Conti, K. Florio, M. Vetterli, T. Graule, M. Schmid, K. Wegener, Addit. Manuf. 31 (2020), 100959.
- [117] P.A. Morton, H.C. Taylor, L.E. Murr, O.G. Delgado, C.A. Terrazas, R.B. Wicker, J. Mater. Sci. Technol. 45 (2020) 98–107.
- [118] Y.-H. Chueh, C. Wei, X. Zhang, L. Li, Addit. Manuf. 31 (2020), 100928.
- [119] I. Gibson, D. Rosen, B. Stucker, M. Khorasani, Sheet Lamination, in: I. Gibson, D. Rosen, B. Stucker, M. Khorasani (Eds.), Additive Manufacturing Technologies, Springer International Publishing, Cham, 2021, pp. 253–283.
- [120] D.L. Naik, R. Kiran, Addit. Manuf. 23 (2018) 181–196.
- [121] L. SMITH, Arch. Surg. 87 (1963) 653–661.
- [122] F. Baino, Ceramics for bone replacement: Commercial products and clinical use, in: P. Palmero, F. Cambier, E. De Barra (Eds.), Advances in Ceramic Biomaterials, 7, Woodhead Publishing, 2017, pp. 249–278.
- [123] M. Vallet-Regi, A.J. Salinas, Ceramics as bone repair materials, in: K.M. Pawelec, J.A. Planell (Eds.), Bone Repair Biomaterials (Second Edition), 6, Woodhead Publishing, 2019, pp. 141–178.
- [124] A. Mansour, L. Abu Nada, A.A. El-hadad, M.A. Mezour, A. Ersheidat, A. Al-Subaie, H. Moussa, M. Laurenti, M.T. Kaartinen, F. Tamimi, J. Biomed. Mater. Res. Part A 109 (2021) 666–681.
- [125] Q. Chen, G.A. Thouas, Mater. Sci. Eng.: R: Rep. 87 (2015) 1–57.
- [126] R. Murugan, S. Ramakrishna, Compos. Sci. Technol. 65 (2005) 2385–2406.
- [127] J.H. Martin, B.D. Yahata, J.M. Hundley, J.A. Mayer, T.A. Schaeder, T.M. Pollock, Nature 549 (2017) 369–369.
- [128] A. Jiménez-Morales, A.A. El hadad, E. Peón, F.R. García-Galván, V. Barranco, J. C. Galván, Study of the Biocompatibility and Corrosion Resistance of Hydroxyapatite Sol-Gel Thin Coatings on Ti6Al4V Alloy, Electrochemical Society Meeting Abstracts 230, The Electrochemical Society, Inc., 2016, p. 1365.
- [129] F.R. García-Galván, A.A. El hadad, A. Jiménez-Morales, G.J. Hickman, C.C. Perry, J.C. Galván, Sol-Gel TiO₂ and ZrO₂-Nanocomposite Thin Films for Enhancing in Vitro Biocompatibility and Bio-Corrosion Resistance of Ti6Al4V Orthopaedic Implants. Electrochemical Society Meeting Abstracts 230, The Electrochemical Society, Inc., 2016, p. 1364.
- [130] L. Hitzler, F. Alifui-Segbaya, P. Williams, B. Heine, M. Heitzmann, W. Hall, M. Merkel, A. Öchsner, Adv. Mater. Sci. Eng. 2018 (2018) 1–12.
- [131] L.E. Murr, J. Mater. Sci. Technol. 32 (2016) 987–995.
- [132] T. DebRoy, H. Wei, J. Zuback, T. Mukherjee, J. Elmer, J. Milewski, A.M. Beese, Ad Wilson-Heid, A. De, W. Zhang, Prog. Mater. Sci. 92 (2018) 112–224.
- [133] E. Uhlmann, R. Kersting, T.B. Klein, M.F. Cruz, A.V. Borille, Procedia Cirp 35 (2015) 55–60.
- [134] D.J. Horst, C.A. Duvoisin, R. de Almeida Vieira, Int. J. Eng. Tech. Res. 8 (2018).
- [135] F. Trevisan, F. Calignano, A. Aversa, G. Marchese, M. Lombardi, S. Biamino, D. Ugués, D. Manfredi, J. Appl. Biomater. Funct. Mater. 16 (2018) 57–67.
- [136] F. García-Galván, M. Mezour, G. Hickman, I. Soliman, A. Jiménez-Morales, V. Barranco, J. Galván, C. Perry, Prog. Org. Coat. 148 (2020), 105834.
- [137] F.R. García-Galván, M.Á. Pacha-Olivenza, A.A. El hadad, A. Páez-Pavón, S. Fajardo, V. Barranco, J.C. Galván, Enhanced Antibacterial Capability and Corrosion Resistance of Ti6Al4V Implant Coated with ZrO₂/Organosilica Nanocomposite Sol-Gel Films, Electrochemical Society Meeting Abstracts 236, The Electrochemical Society, Inc., 2019, p. 825.
- [138] A. El Hadad, B. Barranco, A. Jiménez-Morales, E. Peón, J.C. Galván Sierra, (2010).
- [139] A.A. El Hadad, D. Carbonell, V. Barranco, A. Jiménez-Morales, B. Casal, J. C. Galván, Colloid Polym. Sci. 289 (2011) 1875–1883.
- [140] E.J. Delgado-Pujol, A. Alcudia, A.A. Elhadad, L.M. Rodríguez-Albelo, P. Navarro, B. Begines, Y. Torres, Mater. Chem. Phys. 300 (2023), 127559.
- [141] V. Barranco, A. Jiménez-Morales, G. Hickman, J. Galván, C. Perry, J. Mater. Chem. B 2 (2014) 7955–7963.
- [142] A. Abdelsami El-Hadad, F. García Galván, M.A. Mezour, G.J. Hickman, I.E. Soliman, A. Jiménez Morales, V. Barranco, J.C. Galván, C.C. Perry, (2020).
- [143] A. Bandyopadhyay, S. Ciliveri, S. Bose, J. Indian Inst. Sci. 102 (2022) 561–584.
- [144] H. Sahasrabudhe, A. Bandyopadhyay, J. Mech. Behav. Biomed. Mater. 85 (2018) 1–11.
- [145] M. Dumas, P. Terriault, V. Brailovski, Mater. Des. 121 (2017) 383–392.
- [146] A. Bandyopadhyay, A. Shivaram, I. Mitra, S. Bose, Acta Biomater. 96 (2019) 686–693.
- [147] Y. Iwaya, M. Machigashira, K. Kanbara, M. Miyamoto, K. Noguchi, Y. Izumi, S. Ban, Dent. Mater. J. 27 (2008) 415–421.
- [148] A. Ataee, Y. Li, C. Wen, Acta Biomater. 97 (2019) 587–596.
- [149] H.K. Rafi, T.L. Starr, B.E. Stucker, Int. J. Adv. Manuf. Technol. 69 (2013) 1299–1309.
- [150] M. Khan, R.L. Williams, D. Williams, Biomaterials 20 (1999) 631–637.
- [151] K. Bordji, J. Jouzeau, D. Mainard, E. Payan, P. Netter, K. Rie, T. Stucky, M. Hage-Ali, Biomaterials 17 (1996) 929–940.
- [152] B. Wang, L. Li, Y. Zheng, Biomed. Mater. 5 (2010), 044102.
- [153] D. Terada, M. Inoue, H. Kitahara, N. Tsujii, Mater. Trans. 49 (2008) 41–46.
- [154] Y.-L. Chen, Y.-W. Cui, L.-C. Zhang, Metals 10 (2020) 1139.
- [155] L. Zhang, D. Klemm, J. Eckert, Y. Hao, T. Sercombe, Scr. Mater. 65 (2011) 21–24.
- [156] M. Fischer, P. Laheurte, P. Acquier, D. Joguet, L. Peltier, T. Petithory, K. Anselme, P. Mille, Mater. Sci. Eng.: C. 75 (2017) 341–348.
- [157] W. Xue, B.V. Krishna, A. Bandyopadhyay, S. Bose, Acta Biomater. 3 (2007) 1007–1018.
- [158] E. Sheydaein, Z. Fishman, M. Vlasea, E. Toyserkani, Addit. Manuf. 18 (2017) 40–47.
- [159] A. Bandyopadhyay, F. Espana, V.K. Balla, S. Bose, Y. Ohgami, N.M. Davies, Acta Biomater. 6 (2010) 1640–1648.
- [160] A. Bandyopadhyay, M. Upadhyayula, K.D. Traxel, B. Onuike, Mater. Lett. 255 (2019), 126541.
- [161] S.A. Yavari, S. Ahmadi, R. Wauthle, B. Pouran, J. Schrooten, H. Weinans, A. Zadpoor, J. Mech. Behav. Biomed. Mater. 43 (2015) 91–100.
- [162] V.K. Balla, J. Soderlind, S. Bose, A. Bandyopadhyay, J. Mech. Behav. Biomed. Mater. 32 (2014) 335–344.
- [163] J.D. Avila, Z. Alrawahi, S. Bose, A. Bandyopadhyay, Addit. Manuf. 34 (2020), 101241.
- [164] D. Wang, Y. Wang, S. Wu, H. Lin, Y. Yang, S. Fan, C. Gu, J. Wang, C. Song, Materials 10 (2017) 35.
- [165] K. Gulati, M. Pridieux, M. Kogawa, L. Lima-Marques, G.J. Atkins, D.M. Findlay, D. Losic, J. Tissue Eng. Regen. Med. 11 (2017) 3313–3325.
- [166] Y. Gu, X. Chen, J.-H. Lee, D.A. Monteiro, H. Wang, W.Y. Lee, Acta Biomater. 8 (2012) 424–431.
- [167] F. Yang, C. Chen, Q. Zhou, Y. Gong, R. Li, C. Li, F. Klämpfl, S. Freund, X. Wu, Y. Sun, Sci. Rep. 7 (1) (2017) 12.
- [168] R. Davis, A. Singh, M.J. Jackson, R.T. Coelho, D. Prakash, C.P. Charalambous, W. Ahmed, L.R.R. da Silva, A.A. Lawrence, Int. J. Adv. Manuf. Technol. 120 (2022) 1473–1530.
- [169] S. Mueller, A. Seufert, H. Peng, R. Kovacs, K. Reuss, F. Guimbretière, P. Baudisch, Formfab: Continuous interactive fabrication, Proc. Thirteen. Int. Conf. Tangible, Embed., Embodied Interact. (2019) 315–323.
- [170] G. Manogharan, Hybrid Manufacturing: Analysis of Integrating Additive and Subtractive Methods, North Carolina State University, 2014.
- [171] G. Djogo, J. Li, S. Ho, M. Haque, E. Ertorer, J. Liu, X. Song, J. Suo, P.R. Herman, Int. J. Extrem. Manuf. 1 (2019), 045002.
- [172] N. Zhong, X. Zhao, Eur. Arch. Oto-Rhino-Laryngol. 274 (2017) 4079–4089.
- [173] M. Delić, D.R. Eyers, Int. J. Prod. Econ. 228 (2020), 107689.
- [174] M. Bambach, A. Sviridov, A. Weisheit, J.H. Schleifenbaum, Metals 7 (2017) 113.
- [175] A. Marques, G. Miranda, F. Silva, P. Pinto, Ó. Carvalho, J. Biomed. Mater. Res. Part B: Appl. Biomater. 109 (2021) 377–393.
- [176] A. Nouri, A. Rohani Shirvan, Y. Li, C. Wen, J. Mater. Sci. Technol. 94 (2021) 196–215.
- [177] H. Watschke, M. Goutier, J. Heubach, T. Vietor, K. Leichsenring, M. Böl, Appl. Sci. 11 (2021) 113.

- [178] E. Łyczkowska, P. Szymczyk, B. Dybala, E. Chlebus, *Arch. Civ. Mech. Eng.* 14 (2014) 586–594.
- [179] R. Davis, A. Singh, M.J. Jackson, R.T. Coelho, D. Prakash, C.P. Charalambous, W. Ahmed, L.R.R. da Silva, A.A. Lawrence, *Int. J. Adv. Manuf. Technol.* 120 (2022) 1473–1530.
- [180] E. Liverani, G. Rogati, S. Pagani, S. Brogini, A. Fortunato, P. Caravaggi, *J. Mech. Behav. Biomed. Mater.* 121 (2021), 104608.
- [181] A. Kruusing, *Opt. Lasers Eng.* 41 (2004) 329–352.
- [182] N. Taniguchi, S. Fujibayashi, M. Takemoto, K. Sasaki, B. Otsuki, T. Nakamura, T. Matsushita, T. Kokubo, S. Matsuda, *Mater. Sci. Eng.: C* 59 (2016) 690–701.
- [183] K.-C. Wong, P. Scheinemann, *Sci. China Mater.* 61 (2018) 440–454.
- [184] M. Mezour, Y. Oweis, A. El-Hadad, S. Algizani, F. Tamimi, M. Cerruti, *RSC Adv.* 8 (2018) 23191–23198.
- [185] Ł. Rakoczy, M. Grudzień-Rakoczy, R. Cygan, B. Rutkowski, T. Kargul, T. Dudziak, E. Rząd, O. Milković, A. Zielińska-Lipiec, *Arch. Civ. Mech. Eng.* 22 (2022) 143.
- [186] F.A. España, V.K. Balla, S. Bose, A. Bandyopadhyay, *Mater. Sci. Eng.: C* 30 (2010) 50–57.
- [187] Z. Guo, X. Pang, Y. Yan, K. Gao, A.A. Volinsky, T.-Y. Zhang, *Appl. Surf. Sci.* 347 (2015) 23–34.
- [188] H.M. Ayu, S. Izman, R. Daud, G. Krishnamurthy, A. Shah, S. Tomadi, M. Salwani, *Procedia Eng.* 184 (2017) 399–408.
- [189] G. Cacciamani, G. Roncallo, Y. Wang, E. Vacchieri, A. Costa, *J. Alloy. Compd.* 730 (2018) 291–310.
- [190] A. Bandyopadhyay, B.V. Krishna, W. Xue, S. Bose, *J. Mater. Sci.: Mater. Med.* 20 (2009) 29–34.
- [191] H. Sahasrabudhe, S. Bose, A. Bandyopadhyay, *Acta Biomater.* 66 (2018) 118–128.
- [192] A. Bandyopadhyay, A. Shivaram, M. Isik, J.D. Avila, W.S. Dernell, S. Bose, *Addit. Manuf.* 28 (2019) 312–324.
- [193] L. Wu, H. Zhu, X. Gai, Y. Wang, *J. Prosthet. Dent.* 111 (2014) 51–55.
- [194] S. Mischler, A.I. Munoz, *Wear* 297 (2013) 1081–1094.
- [195] O.M. Posada, R.J. Tate, R.D. Meek, M.H. Grant, *Lubricants* 3 (2015) 539–568.
- [196] R. Li, J. Liu, Y. Shi, M. Du, Z. Xie, *J. Mater. Eng. Perform.* 19 (2010) 666–671.
- [197] N.S. Al-Mamun, K.M. Deen, W. Haider, E. Asselin, I. Shabib, *Addit. Manuf.* 34 (2020), 101237.
- [198] J. Park, R.S. Lakes, *Biomaterials: An Introduction*, Springer Science & Business Media., 2007.
- [199] N. Duraipandy, K.M. Syamala, N. Rajendran, *Appl. Surf. Sci.* 427 (2018) 1166–1181.
- [200] D. McGregor, R. Baan, C. Partensky, J. Rice, J. Wilbourn, *Eur. J. Cancer* 36 (2000) 307–313.
- [201] J.-P. Simon, G. Fabry, *Acta Orthop. Belg.* 57 (1991) 1–5.
- [202] L. Hao, S. Dadbakhsh, O. Seaman, M. Felstead, *J. Mater. Process. Technol.* 209 (2009) 5793–5801.
- [203] B. AlMangour, D. Grzesiak, J.-M. Yang, *J. Alloy. Compd.* 680 (2016) 480–493.
- [204] Y. Shang, Y. Yuan, D. Li, Y. Li, J. Chen, *Int. J. Adv. Manuf. Technol.* 92 (2017) 4379–4385.
- [205] C.C. Barber, M. Burnham, O. Ojameruaye, M.D. McKee, *OTA Int.* 4 (2021).
- [206] A.A.-S. El-Hadad, (2012).
- [207] S. Dadbakhsh, M. Speirs, J.-P. Kruth, J. Van Humbeeck, *CIRP Ann.* 64 (2015) 209–212.
- [208] M. Speirs, X. Wang, S. Van Baelen, A. Ahadi, S. Dadbakhsh, J.-P. Kruth, J. Van Humbeeck, *Shape Mem. Superelasticity* 2 (2016) 310–316.
- [209] M. Taheri Andani, C. Haberland, J.M. Walker, M. Karamooz, A. Sadi Turabi, S. Saedi, R. Rahamanian, H. Karaca, D. Dean, M. Kadkhodaei, *J. Intell. Mater. Syst. Struct.* 27 (2016) 2661–2671.
- [210] M. de Wild, F. Meier, T. Bormann, C.B. Howald, B. Müller, *J. Mater. Eng. Perform.* 23 (2014) 2614–2619.
- [211] B.V. Krishna, S. Bose, A. Bandyopadhyay, *Metall. Mater. Trans. A* 38 (2007) 1096–1103.
- [212] B.V. Krishna, S. Bose, A. Bandyopadhyay, *J. Biomed. Mater. Res. Part B: Appl. Biomater.*: Off. J. Soc. Biomater., Jpn. Soc. Biomater., Aust. Soc. Biomater. Korean Soc. Biomater. 89 (2009) 481–490.
- [213] J.J. Marattukalam, A.K. Singh, S. Datta, M. Das, V.K. Balla, S. Bontha, S. K. Kalpathy, *Mater. Sci. Eng.: C* 57 (2015) 309–313.
- [214] S. Bernard, V.K. Balla, S. Bose, A. Bandyopadhyay, *J. Mech. Behav. Biomed. Mater.* 13 (2012) 62–68.
- [215] M. Elahinia, N.S. Moghaddam, M.T. Andani, A. Amerinatanzi, B.A. Bimber, R. F. Hamilton, *Prog. Mater. Sci.* 83 (2016) 630–663.
- [216] C. Ma, M.T. Andani, H. Qin, N.S. Moghaddam, H. Ibrahim, A. Jahadakbar, A. Amerinatanzi, Z. Ren, H. Zhang, G.L. Doll, *J. Mater. Process. Technol.* 249 (2017) 433–440.
- [217] H. Ibrahim, A. Jahadakbar, A. Dehghan, N.S. Moghaddam, A. Amerinatanzi, M. Elahinia, *Metals* 8 (2018) 164.
- [218] Z. Gorgin Karaji, M. Speirs, S. Dadbakhsh, J.-P. Kruth, H. Weinans, A. Zadpoor, S. Amin Yavaric, *ACS Appl. Mater. Interfaces* 9 (2017) 1293–1304.
- [219] J. Black, *Clin. Mater.* 16 (1994) 167–173.
- [220] L. Bai, C. Gong, X. Chen, Y. Sun, J. Zhang, L. Cai, S. Zhu, S.Q. Xie, *Metals* 9 (2019) 1004.
- [221] I. Mitra, S. Bose, W.S. Dernell, N. Dasgupta, C. Eckstrand, J. Herrick, M. J. Yaszemski, S.B. Goodman, A. Bandyopadhyay, *Mater. Today* 45 (2021) 20–34.
- [222] N. Soro, H. Attar, E. Brodie, M. Veidt, A. Molotnikov, M.S. Dargusch, *J. Mech. Behav. Biomed. Mater.* 97 (2019) 149–158.
- [223] A. Bandyopadhyay, I. Mitra, A. Shivaram, N. Dasgupta, S. Bose, *Addit. Manuf.* 28 (2019) 259–266.
- [224] M.P. Staiger, A.M. Pietak, J. Huadmai, G. Dias, *Biomaterials* 27 (2006) 1728–1734.
- [225] S. Feliu Jr, A.A. El Hadad, V. Barranco, I. Llorente, F.R. García-Galván, A. Jiménez-Morales, J.C. Galván, *New Trends in Alloy Development, Characterization and Application*, IntechOpen., Rijeka, 2015, pp. 97–123.
- [226] A.A. El-Hadad, V. Barranco, A. Samaniego, I. Llorente, F. García-Galván, A. Jiménez-Morales, J. Galván, S. Feliu Jr, *Prog. Org. Coat.* 77 (2014) 1642–1652.
- [227] S. Feliu Jr, A. Samaniego, E.A. Bermudez, A.A. El-Hadad, I. Llorente, J.C. Galván, *Materials* 7 (2014) 2534–2560.
- [228] S. Feliu Jr, A. Samaniego, V. Barranco, A. El-Hadad, I. Llorente, C. Serra, J. Galván, *Appl. Surf. Sci.* 295 (2014) 219–230.
- [229] S. Feliu Jr, A. Samaniego, V. Barranco, A. El-Hadad, I. Llorente, P. Adeva, *Corros. Sci.* 80 (2014) 461–472.
- [230] Y. Li, J. Zhou, P. Pavaram, M. Leeflang, L. Fockaert, B. Pouran, N. Tiimer, K.-U. Schröder, J. Mol. H. Weinans, *Acta Biomater.* 67 (2018) 378–392.
- [231] M. Caminero, J. Chacón, I. García-Moreno, G. Rodríguez, *Compos. Part B: Eng.* 148 (2018) 93–103.
- [232] J.R.C. Dizon, A.H. Espera Jr, Q. Chen, R.C. Advincula, *Addit. Manuf.* 20 (2018) 44–67.
- [233] X. Wang, M. Jiang, Z. Zhou, J. Gou, D. Hui, *Compos. Part B: Eng.* 110 (2017) 442–458.
- [234] B. Begines, C. Arevalo, C. Romero, Z. Hadzhieva, A.R. Boccaccini, Y. Torres, *ACS Appl. Mater. Interfaces* 14 (2022) 15008–15020.
- [235] M. Cámará-Torres, S. Duarte, R. Sinha, A. Egizabal, N. Álvarez, M. Bastianini, M. Sisani, P. Scopece, M. Scatto, A. Bonetto, *Bioact. Mater.* 6 (2021) 1073–1082.
- [236] A. Mohammed, A. Elshaer, P. Sareh, M. Elsayed, H. Hassanin, *Int. J. Pharm.* 580 (2020), 119245.
- [237] W. Huang, Q. Zheng, W. Sun, H. Xu, X. Yang, *Int. J. Pharm.* 339 (2007) 33–38.
- [238] G. Wu, W. Wu, Q. Zheng, J. Li, J. Zhou, Z. Hu, *Biomed. Eng. Online* 13 (1) (2014) 11.
- [239] J.-H. Shim, S.E. Kim, J.Y. Park, J. Kundu, S.W. Kim, S.S. Kang, D.-W. Cho, *Tissue Eng. Part A* 20 (2014) 1980–1992.
- [240] J.-H. Shim, J.-B. Huh, J.Y. Park, Y.-C. Jeon, S.S. Kang, J.Y. Kim, J.-W. Rhie, D.-W. Cho, *Tissue Eng. Part A* 19 (2013) 317–328.
- [241] D. Yu, Q. Li, X. Mu, T. Chang, Z. Xiong, *Int. J. Oral. Maxillofac. Surg.* 37 (2008) 929–934.
- [242] F. Baldassarre, F. Ricciardi, J. Emerg. Trends Mark. Manag. 1 (2017) 105–115.
- [243] D. Owen, J. Hickey, A. Cusson, O.I. Ayeni, J. Rhoades, Y. Deng, Y. Zhang, L. Wu, H.-Y. Park, N. Hawaldar, *Prog. Addit. Manuf.* 3 (2018) 3–9.
- [244] A. Zocca, P. Lima, J. Günster, J. Ceram. Sci. Technol. 8 (2017) 141–148.
- [245] R. Gmeiner, U. Deisinger, J. Schönherr, B. Lechner, R. Detsch, A. Boccaccini, J. Stampfl, *J. Ceram. Sci. Technol.* 6 (2015) 75–86.
- [246] T. Ianko, S. Panov, O. Sushchyński, M. Pylypenko, O. Dmytrenko, *Вопросы ароматной науки и техники* (2018).
- [247] M.H. Kenawy, A. El-Hadad, I.E. Soliman, K.M. Ereiba, *Middle East J. Appl. Sci.* 6 (2016) 329–340.
- [248] X. Tang, Y. Yu, *Ceram. Int.* 41 (2015) 9232–9238.
- [249] Z. Liu, J. Zhu, Z. Li, H. Liu, C. Fu, *Front. Bioeng. Biotechnol.* 11 (2023), 1140393.
- [250] S. Esslinger, R. Gadow, J. Eur. Ceram. Soc. 40 (2020) 3707–3713.
- [251] Y. Wen, S. Xun, M. Maoye, S. Baichuan, C. Peng, L. Xuejian, Z. Kaihong, Y. Xuan, P. Jiang, L. Shibi, *Biomater. Sci.* 5 (2017) 1690–1698.
- [252] D. Alves Cardoso, J. Jansen, S.G. Leeuwenburgh, J. Biomed. Mater. Res. Part B: *Appl. Biomater.* 100 (2012) 2316–2326.
- [253] E. Vorndran, U. Klammert, A. Ewald, J.E. Barralet, U. Gbureck, *Adv. Funct. Mater.* 20 (2010) 1585–1591.
- [254] U. Gbureck, E. Vorndran, F.A. Müller, J.E. Barralet, *J. Control. Release* 122 (2007) 173–180.
- [255] J.A. Inzana, *Three-dimensional Printing of Antibiotic-laden Calcium Phosphates for Treatment of Orthopaedic Implant-associated Bone Infections*, University of Rochester., 2015.
- [256] S. Bose, D. Banerjee, S. Robertson, S. Vahabzadeh, *Ann. Biomed. Eng.* 46 (2018) 1241–1253.
- [257] S. Bose, S. Vahabzadeh, A. Bandyopadhyay, *Mater. Today* 16 (2013) 496–504.
- [258] F. Baine, J. Minguela-Canel, F. Korkusuz, P. Korkusuz, B. Kankılıç, M.Á. Montealegre, M.A. De los Santos-López, C. Vitale-Brovarone, *Int. J. Mol. Sci.* 20 (2019) 722.
- [259] W. Liu, H. Wu, M. Zhou, R. He, Q. Jiang, Z. Wu, Y. Cheng, X. Song, Y. Chen, S. Wu, *Ceram. Int.* 42 (2016) 17736–17741.
- [260] M. Dehurtevent, L. Robberecht, J.-C. Hornez, A. Thuault, E. Deveaux, P. Béhin, *Dent. Mater.* 33 (2017) 477–485.
- [261] H. Wu, Y. Cheng, W. Liu, R. He, M. Zhou, S. Wu, X. Song, Y. Chen, *Ceram. Int.* 42 (2016) 17290–17294.
- [262] N. Travitzky, A. Bonet, B. Dermeik, T. Fey, I. Filbert-Demut, L. Schlier, T. Schlördt, P. Greil, *Adv. Eng. Mater.* 16 (2014) 729–754.
- [263] W. Hao, Y. Liu, H. Zhou, H. Chen, D. Fang, *Polym. Test.* 65 (2018) 29–34.
- [264] Z. Liu, L. Zhang, E. Yu, Z. Ying, Y. Zhang, X. Liu, W. Eli, *Curr. Org. Chem.* 19 (2015) 991–1010.
- [265] M.J. Imola, D.D. Hamlar, W. Shao, K. Chowdhury, S. Tatum, *Arch. Facial Plast. Surg.* 3 (2001) 79–90.
- [266] J.K. Placone, A.J. Engler, *Adv. Healthc. Mater.* 7 (2018), 1701161.
- [267] S. Bose, N. Sarkar, S. Vahabzadeh, *Mater. Sci. Eng.: C* 105 (2019), 110096.
- [268] B.P. Hung, B.A. Naved, E.L. Nyberg, M. Dias, C.A. Holmes, J.H. Elisseeff, A. H. Dorafshar, W.L. Grayson, *ACS Biomater. Sci. Eng.* 2 (2016) 1806–1816.
- [269] C. Koski, B. Onuike, A. Bandyopadhyay, S. Bose, *Addit. Manuf.* 24 (2018) 47–59.
- [270] N. Sarkar, S. Bose, *ACS Appl. Mater. Interfaces* 11 (2019) 17184–17192.
- [271] Y. Yang, Y. Chen, Y. Wei, Y. Li, *Int. J. Adv. Manuf. Technol.* 84 (2016) 2079–2095.
- [272] J. Van Humbeeck, *Shape Mem. Superelasticity* 4 (2018) 309–312.

- [273] X. Zhang, X. Wu, J. Shi, *J. Mater. Res. Technol.* 9 (2020) 9029–9048.
- [274] S.C. Joshi, A.A. Sheikh, *Virtual Phys. Prototyp.* 10 (2015) 175–185.
- [275] A. Uriondo, M. Esperon-Miguez, S. Perippanayagam, *Proc. Inst. Mech. Eng., Part G: J. Aerosp. Eng.* 229 (2015) 2132–2147.
- [276] N. Guo, M.C. Leu, *Front. Mech. Eng.* 8 (2013) 215–243.
- [277] C.W.J. Lim, K.Q. Le, Q. Lu, C.H. Wong, *IEEE Potentials* 35 (2016) 18–22.
- [278] Y.-C. Wang, T. Chen, Y.-L. Yeh, *Int. J. Adv. Manuf. Technol.* 105 (2019) 4059–4069.
- [279] L.J. Kumar, C.G. Krishnadas Nair, Current trends of additive manufacturing in the aerospace industry, in: D.I. Wimpenny, P.M. Pandey, L.J. Kumar (Eds.), *Advances in 3D Printing & Additive Manufacturing Technologies*, Springer Singapore, Singapore, 2017, pp. 39–54.
- [280] J.C. Vasco, Chapter 16 - Additive manufacturing for the automotive industry, in: J. Pou, A. Riveiro, J.P. Davim (Eds.), *Additive Manufacturing*, Elsevier, 2021, pp. 505–530.
- [281] S.G. Sarvankar, S.N. Yewale, *Int. J. Res. Aeronaut. Mech. Eng.* 7 (2019) 1–10.
- [282] V. Sreehitha, *Int. J. Mech. Prod. Eng.* 5 (2017) 91–94.
- [283] B. Praveena, N. Lokesh, A. Buradi, N. Santhosh, B. Praveena, R. Vignesh, *Mater. Today: Proc.* 52 (2022) 1309–1313.
- [284] M. Petch, *3D Printing Industry* (2018).
- [285] R. Maghnani, *Int. J. Curr. Eng. Technol.* 5 (2015) 1–4.
- [286] J. Lee, H.-C. Kim, J.-W. Choi, I.H. Lee, *Int. J. Precis. Eng. Manuf. -Green. Technol.* 4 (2017) 373–383.
- [287] R.D. Farahani, M. Dubé, D. Therriault, *Adv. Mater.* 28 (2016) 5794–5821.
- [288] C.L. Ventola, *Pharm. Ther.* 39 (2014) 704.
- [289] J.T. Muth, D.M. Vogt, R.L. Truby, Y. Mengüç, D.B. Kolesky, R.J. Wood, J.A. Lewis, *Adv. Mater.* 26 (2014) 6307–6312.
- [290] H. Ota, S. Emaminejad, Y. Gao, A. Zhao, E. Wu, S. Challa, K. Chen, H.M. Fahad, A. K. Jha, D. Kiriya, *Adv. Mater. Technol.* 1 (2016) 1600013.
- [291] C. Sun, Y. Wang, M.D. McMurtrey, N.D. Jerred, F. Liou, J. Li, *Appl. Energy* 282 (2021), 116041.
- [292] J.C. Ruiz-Morales, A. Tarancón, J. Canales-Vázquez, J. Méndez-Ramos, L. Hernández-Afonso, P. Acosta-Mora, J.R. Marín Rueda, R. Fernández-González, *Energy Environ. Sci.* 10 (2017) 846–859.
- [293] A. Paolini, S. Kollmannsberger, E. Rank, *Addit. Manuf.* 30 (2019), 100894.
- [294] I. Gibson, T. Kvan, L. Wai Ming, *Rapid Prototyp. J.* 8 (2002) 91–95.
- [295] S. Lim, R.A. Buswell, T.T. Le, S.A. Austin, A.G.F. Gibb, T. Thorpe, *Autom. Constr.* 21 (2012) 262–268.
- [296] S.H. Ghaffar, J. Corker, M. Fan, *Autom. Constr.* 93 (2018) 1–11.
- [297] M. Sakin, Y.C. Kiroglu, *Energy Procedia* 134 (2017) 702–711.
- [298] I. Hager, A. Golonka, R. Putanowicz, *Procedia Eng.* 151 (2016) 292–299.
- [299] M. Mataneh, S. El-Ashri, (2018).
- [300] I. Ibrahim, F. Eltarabishi, H. Abdalla, M. Abdallah, *Buildings* 12 (2022) 1703.
- [301] V. Kolesnikov, *3D Print. Houses, Build. Constr.*, Актуальные проблемы науки и техники 2020 (2020) 729–730.
- [302] A. Emeloglu, M. Marufuzzaman, S.M. Thompson, N. Shamsaei, L. Bian, *Addit. Manuf.* 11 (2016) 97–113.
- [303] M. Salmi, *Materials* 14 (2021) 191.
- [304] D. Pai, *Allure N.* (2017).
- [305] A. De Mori, M. Peña Fernández, G. Blunn, G. Tozzi, M. Roldo, *Polymers* 10 (2018) 285.
- [306] Y. Liu, Q. Hamid, J. Snyder, C. Wang, W. Sun, *Rapid Prototyp. J.* 22 (2016) 947–955.
- [307] Q. Yan, H. Dong, J. Su, J. Han, B. Song, Q. Wei, Y. Shi, *Engineering* 4 (2018) 729–742.
- [308] C. Hu, W. Zhang, P. Li, *Bioengineering* 10 (2023) 299.
- [309] P. Datta, M. Dey, Z. Ataie, D. Unutmaz, I.T. Ozbolat, *NPJ Precis. Oncol.* 4 (2020), 18.
- [310] V. Baskaran, G. Štrkalj, M. Štrkalj, A. Di Ieva, *Front. Neuroanat.* 10 (2016) 69.
- [311] C.F. Smith, N. Tollemache, D. Covill, M. Johnston, *Anat. Sci. Educ.* 11 (2018) 44–53.
- [312] D. Vlaescanu, F. Baciu, D. Popescu, A. Hadar, R. Marinescu, *Mater. Plast.* 55 (2018).
- [313] C. Schubert, M.C. Van Langeveld, L.A. Donoso, *Br. J. Ophthalmol.* 98 (2014) 159–161.
- [314] G.T. Klein, Y. Lu, M.Y. Wang, *World Neurosurg.* 80 (2013) 233–235.
- [315] How 3D printing is impacting the medical field, in: [\[https://www.med-technnews.com/medtech-insights/medtech-materials-and-assembly-insights/how-3d-printing-is-impacting-the-medical-field/\]](https://www.med-technnews.com/medtech-insights/medtech-materials-and-assembly-insights/how-3d-printing-is-impacting-the-medical-field/) (Ed.) 2022.
- [316] A.H. Association.
- [317] M. Gebler, A.J.S. Uiterkamp, C. Visser, *Energy Policy* 74 (2014) 158–167.
- [318] J. Banks, *IEEE Pulse* 4 (2013) 22–26.
- [319] L. Mertz, *IEEE Pulse* 4 (2013) 15–21.
- [320] I.D. Ursan, L. Chiu, A. Pierce, *J. Am. Pharm. Assoc.* 53 (2013) 136–144.
- [321] M. Abdolahad, H. Taghinejad, A. Saeidi, M. Taghinejad, M. Janmaleki, S. Mohajerzadeh, *RSC Adv.* 4 (2014) 7425–7431.
- [322] S.V. Murphy, A. Atala, *Nat. Biotechnol.* 32 (2014) 773–785.
- [323] S. Vanaei, M.S. Parizi, S. Vanaei, F. Salemirzadehparizi, H.R. Vanaei, *Eng. Regen.* 2 (2021) 1–18.
- [324] W.-C. Yan, P. Davoodi, S. Vijayaventakaraman, Y. Tian, W.C. Ng, J.Y.H. Fuh, K. S. Robinson, C.-H. Wang, *Adv. Drug Deliv. Rev.* 132 (2018) 270–295.
- [325] X. Chen, J.K. Possel, C. Wacongne, A.F. Van Ham, P.C. Klink, P.R. Roelfsema, *J. Neurosci. Methods* 286 (2017) 38–55.
- [326] A. Schwab, R. Levato, M. D'Este, S. Piluso, D. Eglin, J. Malda, *Chem. Rev.* 120 (2020) 11028–11055.
- [327] E.S. Bishop, S. Mostafa, M. Pakvasa, H.H. Luu, M.J. Lee, J.M. Wolf, G.A. Ameer, T.-C. He, R.R. Reid, *Genes Dis.* 4 (2017) 185–195.
- [328] H.-J. Jeong, H. Nam, J. Jang, S.-J. Lee, *Bioengineering* 7 (2020) 32.
- [329] L.R. Madden, T.V. Nguyen, S. Garcia-Mojica, V. Shah, A.V. Le, A. Peier, R. Visconti, E.M. Parker, S.C. Presnell, D.G. Nguyen, *IScience* 2 (2018) 156–167.
- [330] R. Bour, P. Sharma, J. Turner, W. Hess, E. Mintz, C. Latvis, B. Shepherd, S. Presnell, M. McConnell, C. Highley, *Connect. Tissue Res.* 61 (2020) 216–228.
- [331] K.T. Lawlor, J.M. Vanslambrouck, J.W. Higgins, A. Chambon, K. Bishard, D. Arndt, P.X. Er, S.B. Wilson, S.E. Howden, K.S. Tan, F. Li, L.J. Hale, B. Shepherd, S. Pentoney, S.C. Presnell, A.E. Chen, M.H. Little, *Nat. Mater.* 20 (2021) 260–271.
- [332] X. Zhou, M. Nowicki, H. Sun, S.Y. Hann, H. Cui, T. Esworthy, J.D. Lee, M. Plesniak, I.G. Zhang, *ACS Appl. Mater. Interfaces* 12 (2020) 45904–45915.
- [333] T.B. Ngo, B.S. Spearman, N. Hlavac, C.E. Schmidt, *ACS Biomater. Sci. Eng.* 6 (2020) 6819–6830.
- [334] S. Ramesh, V. Kovelaikuntla, A.S. Meyer, I.V. Rivero, *Bioprinting* 24 (2021), e00106.
- [335] W.L. Ng, W.Y. Yeong, M.W. Naing, *Int. J. Bioprinting* 2 (2016).
- [336] G. Addario, S. Djudjaj, S. Farè, P. Boor, L. Moroni, C. Mota, *Bioprinting* 20 (2020), e00108.
- [337] N. Thattaraparambil Raveendran, C. Vaquette, C. Meinert, D. Samuel Ipe, S. Ivanovski, *Dent. Mater.* 35 (2019) 1683–1694.
- [338] K. Paul, S. Darzi, G. McPhee, M.P. Del Borgo, J.A. Werkmeister, C.E. Gargett, S. Mukherjee, *Acta Biomater.* 97 (2019) 162–176.
- [339] J.C. Moses, T. Saha, B.B. Mandal, *Bioprinting* 17 (2020), e00067.
- [340] U.K. Roopavath, R. Soni, U. Mahanta, A.S. Deshpande, S.N. Rath, *RSC Adv.* 9 (2019) 23832–23842.
- [341] L. T. Somasekharan, N. Kasoju, R. Raju, A. Bhatt, Formulation and Characterization of Alginate Dialdehyde, Gelatin, and Platelet-Rich Plasma-Based Bioink for Bioprinting Applications, *Bioengineering* vol 7 (2020).
- [342] A. Schwab, C. Hélary, R.G. Richards, M. Alini, D. Eglin, M. D'Este, *Mater. Today Bio* 7 (2020), 100058.
- [343] W.L. Ng, J.T.Z. Qi, W.Y. Yeong, M.W. Naing, *Biofabrication* 10 (2018), 025005.
- [344] L. Horváth, Y. Umehara, C. Jud, F. Blank, A. Petri-Fink, B. Rothen-Rutishauser, *Sci. Rep.* 5 (2015) 7974.
- [345] M. Matsusaki, K. Sakaue, K. Kadowaki, M. Akashi, *Adv. Healthc. Mater.* 2 (2013) 534–539.
- [346] C. Antich, J. de Vicente, G. Jiménez, C. Chocarro, E. Carrillo, E. Montañez, P. Gálvez-Martín, J.A. Marchal, *Acta Biomater.* 106 (2020) 114–123.
- [347] K. Zafeiris, D. Brasinika, A. Karatza, E. Koumoulos, I.K. Karoussis, K. Kyriakidou, C.A. Charitidis, *Mater. Sci. Eng. C* 119 (2021), 111639.
- [348] R. Landers, U. Hübner, R. Schmelzeisen, R. Mühlaupt, *Biomaterials* 23 (2002) 4437–4447.
- [349] I.T. Ozbolat, M. Hospoduk, *Biomaterials* 76 (2016) 321–343.
- [350] S.A. Irvine, S.S. Venkatraman, *Molecules* 21 (2016) 1188.
- [351] C. Colosi, S.R. Shin, V. Manoharan, S. Massa, M. Costantini, A. Barbetta, M. R. Dokmeci, M. Dentini, A. Khademhosseini, *Adv. Mater.* 28 (2016) 677–684.
- [352] A. Faulkner-Jones, C. Fyfe, D.-J. Cornelissen, J. Gardner, J. King, A. Courtney, W. Shu, *Biofabrication* 7 (2015), 044102.
- [353] I.T. Ozbolat, K.K. Moncal, H. Gudapati, *Addit. Manuf.* 13 (2017) 179–200.
- [354] M.-Y. Shie, J.-J. Lee, C.-C. Ho, S.-Y. Yen, H.Y. Ng, Y.-W. Chen, *Polymers* 12 (2020) 1930.
- [355] R.J. Klebe, *Exp. Cell Res.* 179 (1988) 362–373.
- [356] L. Roseti, C. Cavallo, G. Desando, V. Parisi, M. Petretta, I. Bartolotti, B. Grigolo, *Mater. (Basel)* 11 (2018).
- [357] A.D. Graham, S.N. Olof, M.J. Burke, J.P.K. Armstrong, E.A. Mikhailova, J. G. Nicholson, S.J. Box, F.G. Szele, A.W. Perriman, H. Bayley, *Sci. Rep.* 7 (2017) 7004.
- [358] D. Choudhury, S. Anand, M.W. Naing, *Int. J. Bioprinting* 4 (2018).
- [359] C.C. Chang, E.D. Boland, S.K. Williams, J.B. Hoying, *J. Biomed. Mater. Res. Part B: Appl. Biomater.* 98 (2011) 160–170.
- [360] K. Hözl, S. Lin, L. Tytgat, S. Van Vlierberghe, L. Gu, A. Ovsianikov, *Biofabrication* 8 (2016), 032002.
- [361] X. Ma, X. Qu, W. Zhu, Y.S. Li, S. Yuan, H. Zhang, J. Liu, P. Wang, C.S. Lai, F. Zanella, G.S. Feng, F. Sheikh, S. Chien, S. Chen, *Proc. Natl. Acad. Sci. USA* 113 (2016) 2206–2211.
- [362] F.P.W. Melchels, J. Feijen, D.W. Grijpma, *Biomaterials* 31 (2010) 6121–6130.
- [363] S. Loai, B.R. Kingston, Z. Wang, D.N. Philpott, M. Tao, H.-L.M. Cheng, *Regen. Med. Front.* 1 (2019).
- [364] M. Hospoduk, M. Dey, D. Sosnoski, I.T. Ozbolat, *Biotechnol. Adv.* 35 (2017) 217–239.
- [365] Y. He, F. Yang, H. Zhao, Q. Gao, B. Xia, J. Fu, *Sci. Rep.* 6 (2016), 29977.
- [366] B. Guillotin, M. Ali, A. Ducom, S. Catros, V. Keriquel, A. Souquet, M. Remy, J.-C. Fricain, F. Guillemot, Chapter 6 - Laser-Assisted Bioprinting for Tissue Engineering, in: G. Forgacs, W. Sun (Eds.), *Biofabrication*, William Andrew Publishing, Boston, 2013, pp. 95–118.
- [367] H. Gudapati, M. Dey, I. Ozbolat, *Biomaterials* 102 (2016) 20–42.
- [368] S. Tasoglu, U. Demirci, *Trends Biotechnol.* 31 (2013) 10–19.
- [369] A.C. Daly, S.E. Critchley, E.M. Rencsok, D.J. Kelly, *Biofabrication* 8 (2016), 045002.
- [370] P.S. Gungor-Ozkerim, I. Inci, Y.S. Zhang, A. Khademhosseini, M.R. Dokmeci, *Biomater. Sci.* 6 (2018) 915–946.
- [371] J. Groll, J.A. Burdick, D.W. Cho, B. Derby, M. Gelinsky, S.C. Heilshorn, T. Jüngst, J. Maldá, V.A. Mironov, K. Nakayama, A. Ovsianikov, W. Sun, S. Takeuchi, J. J. Yoo, T.B.F. Woodfield, *Biofabrication* 11 (2019), 013001.
- [372] R. Levato, W.R. Webb, I.A. Otto, A. Mensinga, Y. Zhang, M. van Rijen, R. van Weeren, I.M. Khan, J. Maldá, *Acta Biomater.* 61 (2017) 41–53.

- [373] J. Groll, J.A. Burdick, D.-W. Cho, B. Derby, M. Gelinsky, S.C. Heilshorn, T. Juengst, J. Malda, V.A. Mironov, K. Nakayama, *Biofabrication* 11 (2018), 013001.
- [374] A. Alblawi, A.S. Ranjani, H. Yasmin, S. Gupta, A. Bit, M. Rahimi-Gorji, *Comput. Methods Prog. Biomed.* 185 (2020), 105148.
- [375] A. Ovsianikov, A. Khademhosseini, V. Mironov, *Trends Biotechnol.* 36 (2018) 348–357.
- [376] J. Malda, J. Visser, F.P. Melchels, T. Jüngst, W.E. Hennink, W.J. Dhert, J. Groll, D. W. Hutmacher, *Adv. Mater.* 25 (2013) 5011–5028.
- [377] Y. Yu, I.T. Ozbolat, *Tissue strands as “bioink” for scale-up organ printing*, 2014 36th annual international conference of the IEEE engineering in medicine and biology society, IEEE,, 2014, pp. 1428–1431.
- [378] Z. Wu, X. Su, Y. Xu, B. Kong, W. Sun, S. Mi, *Sci. Rep.* 6 (2016), 24474.
- [379] T. Zhang, W. Zhao, Z. Xiahou, X. Wang, K. Zhang, J. Yin, *Appl. Mater. Today* 25 (2021), 101227.
- [380] D. Seliktar, *Science* 336 (2012) 1124–1128.
- [381] J.A. Burdick, W.L. Murphy, *Nat. Commun.* 3 (2012), 1269.
- [382] S. Das, B. Basu, *J. Indian Inst. Sci.* 99 (2019) 405–428.
- [383] L. Gasperini, J.F. Mano, R.L. Reis, J. R. Soc. Interface 11 (2014) 20140817.
- [384] H. Tan, K.G. Marra, *Materials* 3 (2010) 1746–1767.
- [385] R. Khoeini, H. Nosrati, A. Akbarzadeh, A. Eftekhari, T. Kavetsky, R. Khalilov, E. Ahmadian, A. Nasibova, P. Datta, L. Roshangar, D.C. Deluca, S. Davaran, M. Cucchiarin, I.T. Ozbolat, *Adv. NanoBiomed Res.* 1 (2021) 2000097.
- [386] C. Frantz, K.M. Stewart, V.M. Weaver, J. Cell Sci. 123 (2010) 4195–4200.
- [387] H. Lodish, A. Berk, S.L. Zipursky, P. Matsudaira, D. Baltimore, J. Darnell, *Mol. Cell Biol.* 4 (2000) 145–154.
- [388] L.C. Abraham, E. Zuena, B. Perez-Ramirez, D.L. Kaplan, *J. Biomed. Mater. Res. Part B: Appl. Biomater.: Off. J. Soc. Biomater., Jpn. Soc. Biomater., Aust. Soc. Biomater. Korean Soc. Biomater.* 87 (2008) 264–285.
- [389] M.D. Shoulders, R.T. Raines, *Annu. Rev. Biochem.* 78 (2009) 929–958.
- [390] D.F. Duarte Campos, M. Rohde, M. Ross, P. Anvari, A. Blaeser, M. Vogt, C. Panfil, G.H.F. Yam, J.S. Mehta, H. Fischer, *J. Biomed. Mater. Res. Part A* 107 (2019) 1945–1953.
- [391] F. Subhan, M. Ikram, A. Shehzad, A. Ghafoor, *J. Food Sci. Technol.* 52 (2015) 4703–4707.
- [392] A. Undas, R.A.S. Ariëns, *Arterioscler., Thromb., Vasc. Biol.* 31 (2011) e88–e99.
- [393] K. Pratt, H. Cote, D. Chung, R. Stenkamp, E. Davie, *Proc. Natl. Acad. Sci.* 94 (1997) 7176–7181.
- [394] A.H. HENSCHEN-EDMAN, *Ann. N. Y. Acad. Sci.* 936 (2001) 580–593.
- [395] R.A. Burton, G. Tsurupa, L. Medved, N. Tjandra, *Biochemistry* 45 (2006) 2257–2266.
- [396] B.A.G. de Melo, Y.A. Jodat, S. Mehrotra, M.A. Calabrese, T. Kamperman, B. B. Mandal, M.H.A. Santana, E. Alsberg, J. Leijten, S.R. Shin, *Adv. Funct. Mater.* 29 (2019) 1906330.
- [397] L. De la Vega, D.A. Rosas Gómez, E. Abelseth, L. Abelseth, V. Allisson da Silva, S. M. Willerth, *Appl. Sci.* 8 (2018) 2414.
- [398] C. Buckley, E.J. Murphy, T.R. Montgomery, I. Major, *Polymers* 14 (2022) 3442.
- [399] R.C. Gupta, R. Lall, A. Srivastava, A. Sinha, *Front. Vet. Sci.* 6 (2019).
- [400] Y.-W. Ding, X.-W. Zhang, C.-H. Mi, X.-Y. Qi, J. Zhou, D.-X. Wei, *Smart Mater. Med.* 4 (2023) 59–68.
- [401] C. Xu, G. Dai, Y. Hong, *Acta Biomater.* 95 (2019) 50–59.
- [402] E.A. Kiyotake, A.W. Douglas, E.E. Thomas, S.L. Nimmo, M.S. Detamore, *Acta Biomater.* 95 (2019) 176–187.
- [403] S. Maiz-Fernández, N. Barroso, L. Pérez-Álvarez, U. Silván, J.L. Vilas-Vilela, S. Lánceros-Méndez, *Int. J. Biol. Macromol.* 188 (2021) 820–832.
- [404] T. Wan, P. Fan, M. Zhang, K. Shi, X. Chen, H. Yang, X. Liu, W. Xu, Y. Zhou, *ACS Appl. Bio Mater.* 5 (2022) 334–343.
- [405] H.H. Tønnesen, J. Karlens, *Drug Dev. Ind. Pharm.* 28 (2002) 621–630.
- [406] K.I. Draget, C. Taylor, *Food Hydrocoll.* 25 (2011) 251–256.
- [407] Y. Luo, G. Luo, M. Gelinsky, P. Huang, C. Ruan, *Mater. Lett.* 189 (2017) 295–298.
- [408] M. Ojansuu, A. Rashad, A. Ahlinder, J. Massera, A. Mishra, K. Syverud, A. Finne-Wistrand, S. Miettinen, K. Mustafa, *Biofabrication* 11 (2019), 035010.
- [409] J. Eysturkskarð, I.J. Haug, A.-S. Ulset, K.I. Draget, *Food Hydrocoll.* 23 (2009) 2315–2321.
- [410] M. Santoro, A.M. Tatare, A.G. Mikos, *J. Control. Release* 190 (2014) 210–218.
- [411] D.J. Choi, Y. Kho, S.J. Park, Y.-J. Kim, S. Chung, C.-H. Kim, *Int. J. Biol. Macromol.* 135 (2019) 659–667.
- [412] S. Das, F. Pati, Y.-J. Choi, G. Rijal, J.-H. Shim, S.W. Kim, A.R. Ray, D.-W. Cho, S. Ghosh, *Acta Biomater.* 11 (2015) 233–246.
- [413] C. Vepari, D.L. Kaplan, *Prog. Polym. Sci.* 32 (2007) 991–1007.
- [414] A. Bandyopadhyay, B.B. Mandal, *Biofabrication* 12 (2020), 015003.
- [415] M.J. Rodriguez, J. Brown, J. Giordano, S.J. Lin, F.G. Omenetto, D.L. Kaplan, *Biomaterials* 117 (2017) 105–115.
- [416] N. Khoshnood, A. Zamanian, *Bioprinting* 20 (2020), e00095.
- [417] C.A. DeForest, K.S. Anseth, *Annu. Rev. Chem. Biomol. Eng.* 3 (2012) 421–444.
- [418] K. Rotjanasuworapong, N. Thummarungsan, W. Lerdwijitjarud, A. Sirivat, *Carbohydr. Polym.* 247 (2020), 116709.
- [419] M. Neufurth, X. Wang, H.C. Schröder, Q. Feng, B. Diehl-Seifert, T. Ziebart, R. Steffen, S. Wang, W.E.G. Müller, *Biomaterials* 35 (2014) 8810–8819.
- [420] Y. Gu, B. Schwarz, A. Forget, A. Barbero, I. Martin, V.P. Shastri, *Bioengineering* 7 (2020) 141.
- [421] N. Ruocco, S. Costantini, S. Guariniello, M. Costantini, *Molecules* 21 (2016) 551.
- [422] A. Chenite, M. Buschmann, D. Wang, C. Chaput, N. Kandani, *Carbohydr. Polym.* 46 (2001) 39–47.
- [423] K.D. Roehm, S.V. Madihally, *Biofabrication* 10 (2018), 015002.
- [424] P. Maturavongsadit, L.K. Narayanan, P. Chansoria, R. Shirwaiker, S. R. Benhabbour, *ACS Appl. Bio Mater.* 4 (2021) 2342–2353.
- [425] O.V. Okoro, A. Amenaghawon, D. Podstawczyk, H. Alimoradi, M.R. Khalili, M. Anwar, P.B. Milan, L. Nie, A. Shavandi, J. Clean. Prod. 328 (2021), 129498.
- [426] D. Haldar, M.K. Purkait, *Carbohydr. Polym.* 250 (2020), 116937.
- [427] K.J. Edgar, *Cellulose* 14 (2007) 49–64.
- [428] M.A. Habib, B. Khoda, *Procedia Manuf.* 26 (2018) 846–856.
- [429] T. Heinze, K. Pfeiffer, *Die Angew. Makromol. Chem.* 266 (1999) 37–45.
- [430] A. Gospodinova, V. Nankov, S. Tomov, M. Redzhev, P.D. Petrov, *Carbohydr. Polym.* 260 (2021), 117793.
- [431] S. Zhang, D. Huang, H. Lin, Y. Xiao, X. Zhang, *Biomacromolecules* 21 (2020) 2400–2408.
- [432] J. Gopinathan, I. Noh, *Biomater. Res.* 22 (2018), 11.
- [433] S.R. Caliari, M.A. Ramirez, B.A. Harley, *Biomaterials* 32 (2011) 8990–8998.
- [434] X. Wang, Q. Ao, X. Tian, J. Fan, H. Tong, W. Hou, S. Bai, *Polym. (Basel)* 9 (2017).
- [435] R. Guizzardi, L. Vaghi, M. Marelli, A. Natalello, I. Andreosso, A. Papagni, L. Cipolla, *Molecules* 24 (2019) 589.
- [436] X. Cui, T. Boland, *Biomaterials* 30 (2009) 6221–6227.
- [437] F. Abasalizadeh, S.V. Moghaddam, E. Alizadeh, E. akbari, E. Kashani, S.M. B. Fazljou, M. Torbati, A. Akbarzadeh, *J. Biol. Eng.* 14 (2020) 8.
- [438] L.A. Pérez, R. Hernández, J.M. Alonso, R. Pérez-González, V. Sáez-Martínez, *Biomedicines* 9 (2021) 1113.
- [439] S. Trombino, C. Servidio, F. Curcio, R. Cassano, *Pharmaceutics* 11 (2019) 407.
- [440] F. Croisier, C. Jérôme, *Eur. Polym. J.* 49 (2013) 780–792.
- [441] S.H. Zainal, N.H. Mohd, N. Suhaili, F.H. Anuar, A.M. Lazim, R. Othaman, *J. Mater. Res. Technol.* 10 (2021) 935–952.
- [442] M. Yamada, H. Imaishi, K. Morigaki, *Langmuir* 29 (2013) 6404–6408.
- [443] M. Tako, S. Nakamura, *Carbohydr. Res.* 180 (1988) 277–284.
- [444] J. Jang, H.-J. Park, S.-W. Kim, H. Kim, J.Y. Park, S.J. Na, H.J. Kim, M.N. Park, S. H. Choi, S.H. Park, S.W. Kim, S.-M. Kwon, P.-J. Kim, D.-W. Cho, *Biomaterials* 112 (2017) 264–274.
- [445] P.S. Au - Thayer, L.S. Au - Orrhult, H. Au - Martínez, *JoVE* (2018), e56372.
- [446] B.S. Kim, Y.W. Kwon, J.-S. Kong, G.T. Park, G. Gao, W. Han, M.-B. Kim, H. Lee, J. H. Kim, D.-W. Cho, *Biomaterials* 168 (2018) 38–53.
- [447] *Tissue Eng. Part C: Methods* 20 (2014) 473–484.
- [448] E. Abelseth, L. Abelseth, L. De la Vega, S.T. Beyer, S.J. Wadsworth, S.M. Willerth, *ACS Biomater. Sci. Eng.* 5 (2019) 234–243.
- [449] R. Sharma, I.P. Smits, L. De La Vega, C. Lee, S.M. Willerth, *Front. Bioeng. Biotechnol.* 8 (2020), 57.
- [450] C. Lee, E. Abelseth, L. de la Vega, S.M. Willerth, *Mater. Today Chem.* 12 (2019) 78–84.
- [451] M. Ali, A.K. Pr, J.J. Yoo, F. Zahran, A. Atala, S.J. Lee, *Adv. Healthc. Mater.* 8 (2019), 1800992.
- [452] X.-F. Wang, Y. Song, Y.-S. Liu, Y.-c Sun, Y.-g Wang, Y. Wang, P.-J. Lyu, *PLOS ONE* 11 (2016), e0157214.
- [453] F. Pati, J. Jang, D.-H. Ha, S. Won Kim, J.-W. Rhie, J.-H. Shim, D.-H. Kim, D.-W. Cho, *Nat. Commun.* 5 (2014) 3935.
- [454] J.W. Chang, S.A. Park, J.K. Park, J.W. Choi, Y.S. Kim, Y.S. Shin, C.H. Kim, *Artif. Organs* 38 (2014) E95–E105.
- [455] J.-H. Shim, K.-M. Jang, S.K. Hahn, J.Y. Park, H. Jung, K. Oh, K.M. Park, J. Yeom, S.H. Park, S.W. Kim, J.H. Wang, K. Kim, D.-W. Cho, *Biofabrication* 8 (2016), 014102.
- [456] C.D. O'Connell, C. Di Bella, F. Thompson, C. Augustine, S. Beirne, R. Cornock, C. J. Richards, J. Chung, S. Gambhir, Z. Yue, J. Bourke, B. Zhang, A. Taylor, A. Quigley, R. Kapsa, P. Choong, G.G. Wallace, *Biofabrication* 8 (2016), 015019.
- [457] N.E. Fedorovich, W. Schuurman, H.M. Wijnberg, H.J. Prins, P.R. van Weeren, J. Malda, J. Alblas, W.J. Dhert, *Tissue Eng. Part C. Methods* 18 (2012) 33–44.
- [458] K. Zafeiris, D. Brasniká, A. Karatza, E. Koumoulos, I.K. Karoussis, K. Kyriakidou, C.A. Charitidis, *Mater. Sci. Eng. C. Mater. Biol. Appl.* 119 (2021), 111639.
- [459] S. Chawla, A. Sharma, A. Bandyopadhyay, S. Ghosh, *ACS Biomater. Sci. Eng.* 4 (2018) 3545–3560.
- [460] C. Cleversey, M. Robinson, S.M. Willerth, *Micromachines* 10 (2019) 501.
- [461] Y.-J. Choi, Y.-J. Jun, D.Y. Kim, H.-G. Yi, S.-H. Chae, J. Kang, J. Lee, G. Gao, J.-S. Kong, J. Jang, W.K. Chung, J.-W. Rhie, D.-W. Cho, *Biomaterials* 206 (2019) 160–169.
- [462] C.T.D. Dickman, V. Russo, K. Thain, S. Pan, S.T. Beyer, K. Walus, S. Getsios, T. Mohamed, S.J. Wadsworth, *Faseb J.* 34 (2020) 1652–1664.
- [463] S. Freeman, R. Ramos, P. Alexis Chando, L. Zhou, K. Reeser, S. Jin, P. Soman, K. Ye, *Acta Biomater.* 95 (2019) 152–164.
- [464] S.J. Park, R.Y. Kim, B.W. Park, S. Lee, S.W. Choi, J.H. Park, J.J. Choi, S.W. Kim, J. Jang, D.W. Cho, H.M. Chung, S.H. Moon, K. Ban, H.J. Park, *Nat. Commun.* 10 (2019) 3123.
- [465] R. Gaetani, P.A. Doevedans, C.H.G. Metz, J. Alblas, E. Messina, A. Giacomello, J. P.G. Sluijter, *Biomaterials* 33 (2012) 1782–1790.
- [466] Q. Gu, E. Tomaskovic-Crook, G.G. Wallace, J.M. Crook, *Adv. Healthc. Mater.* 6 (2017), 1700175.
- [467] L. T. Somasekharan, N. Kasoju, R. Raju, A. Bhatt, *Bioengineering* 7 (2020) 108.
- [468] A. Forget, A. Blaeser, F. Miessmer, M. Köpf, D.F.D. Campos, N.H. Voelcker, A. Blencowe, H. Fischer, V.P. Shastri, *Adv. Healthc. Mater.* 6 (2017) 1700255.
- [469] J.-P. Jiang, X.-Y. Liu, F. Zhao, X. Zhu, X.-Y. Li, X.-G. Niu, Z.-T. Yao, C. Dai, H.-Y. Xu, K. Ma, X.-Y. Chen, S. Zhang, *Neural Regen. Res.* 15 (2020) 959–968.
- [470] A. Skardal, J. Zhang, G.D. Prestwich, *Biomaterials* 31 (2010) 6173–6181.
- [471] Y. Wang, R.K. Kankala, K. Zhu, S.B. Wang, Y.S. Zhang, A.Z. Chen, *ACS Biomater. Sci. Eng.* 5 (2019) 5514–5524.
- [472] T. Kojima, K. Higashi, T. Suzuki, K. Tomono, K. Moribe, K. Yamamoto, *Pharm. Res.* 29 (2012) 2777–2791.

- [473] H. Zhang, X. Mao, Z. Du, W. Jiang, X. Han, D. Zhao, D. Han, Q. Li, *Sci. Technol. Adv. Mater.* 17 (2016) 136–148.
- [474] D. Garlotta, J. Polym. Environ. 9 (2001) 63–84.
- [475] M. Guvendiren, J. Molde, R.M. Soares, J. Kohn, *ACS Biomater. Sci. Eng.* 2 (2016) 1679–1693.
- [476] F.P. Melchels, J. Feijen, D.W. Grijpma, *Biomaterials* 30 (2009) 3801–3809.
- [477] H.-J. Sung, C. Meredith, C. Johnson, Z.S. Galis, *Biomaterials* 25 (2004) 5735–5742.
- [478] J. Zhu, *Biomaterials* 31 (2010) 4639–4656.
- [479] X. Liu, P.X. Ma, *Ann. Biomed. Eng.* 32 (2004) 477–486.
- [480] C. Murphy, K. Kolan, W. Li, J. Semon, D. Day, M. Leu, *Int J. Bioprint* 3 (2017) 005.
- [481] Q. Pan, C. Gao, Y. Wang, Y. Wang, C. Mao, Q. Wang, S.N. Economidou, D. Douroumis, F. Wen, L.P. Tan, H. Li, *Bio-Des. Manuf.* 3 (2020) 396–409.
- [482] M. Guvendiren, J. Molde, R.M.D. Soares, J. Kohn, *ACS Biomater. Sci. Eng.* 2 (2016) 1679–1693.
- [483] B.C. Tellis, J.A. Szivek, C.L. Bliss, D.S. Margolis, R.K. Vaidyanathan, P. Calvert, *Mater. Sci. Eng.: C* 28 (2008) 171–178.
- [484] J.M. Bezemer, D.W. Grijpma, P.J. Dijkstra, C.A. van Blitterswijk, J. Feijen, *J. Control.* Release 62 (1999) 393–405.
- [485] A.A. Deschamps, A.A. van Apeldoorn, H. Hayen, J.D. de Bruijn, U. Karst, D. W. Grijpma, J. Feijen, *Biomaterials* 25 (2004) 247–258.
- [486] C.K. Chua, K.F. Leong, K.H. Tan, F.E. Wiria, C.M. Cheah, *J. Mater. Sci.: Mater. Med.* 15 (2004) 1113–1121.
- [487] M. Oka, T. Noguchi, P. Kumar, K. Ikeuchi, T. Yamamuro, S.H. Hyon, Y. Ikada, *Clin. Mater.* 6 (1990) 361–381.
- [488] Z.G. Tang, J.T. Callaghan, J.A. Hunt, *Biomaterials* 26 (2005) 6618–6624.
- [489] Z. Ge, X. Tian, B.C. Heng, V. Fan, J.F. Yeo, T. Cao, *Biomed. Mater.* 4 (2009), 021001.
- [490] J. Groll, T. Boland, T. Blunk, J.A. Burdick, D.-W. Cho, P.D. Dalton, B. Derby, G. Forgacs, Q. Li, V.A. Mironov, *Biofabrication* 8 (2016), 013001.
- [491] A.K. Miri, D. Nieto, L. Iglesias, H. Goodarzi Hosseiniabadi, S. Maharjan, G.U. Ruiz-Esparza, P. Khoshakhlagh, A. Manbachi, M.R. Dokmeci, S. Chen, *Adv. Mater.* 30 (2018) 1800242.
- [492] A. El Magri, K. El Mabrouk, S. Vaudreuil, M. Ebn Touhami, *J. Appl. Polym. Sci.* 138 (2021), 49625.
- [493] K. Nair, M. Gandhi, S. Khalil, K.C. Yan, M. Marcolongo, K. Barbee, W. Sun, *Biotechnol. J.* 4 (2009) 1168–1177.
- [494] M. Sarker, X.B. Chen, *J. Manuf. Sci. Eng.* 139 (2017).
- [495] X.B. Chen, M.G. Li, H. Ke, *J. Manuf. Sci. Eng.* 130 (2008).
- [496] A. Ribeiro, M.M. Blokzijl, R. Levato, C.W. Visser, M. Castilho, W.E. Hennink, T. Vermonden, J. Malda, *Biofabrication* 10 (2018), 014102.
- [497] N. Paxton, W. Smolan, T. Böck, F. Melchels, J. Groll, T. Jungst, *Biofabrication* 9 (2017), 044107.
- [498] L. Ning, H. Sun, T. Lelong, R. Guilloteau, N. Zhu, D.J. Schreyer, X. Chen, *Biofabrication* 10 (2018), 035014.
- [499] A.L. Rutz, K.E. Hyland, A.E. Jakus, W.R. Burghardt, R.N. Shah, *Adv. Mater.* 27 (2015) 1607–1614.
- [500] A. Blaeser, D.F. Duarte Campos, U. Puster, W. Richtering, M.M. Stevens, H. Fischer, *Adv. Healthc. Mater.* 5 (2016) 326–333.
- [501] A. Skardal, M. Devarasetty, H.-W. Kang, I. Mead, C. Bishop, T. Shupe, S.J. Lee, J. Jackson, J. Yoo, S. Soker, A. Atala, *Acta Biomater.* 25 (2015) 24–34.
- [502] O. Chaudhuri, *Biomater. Sci.* 5 (2017) 1480–1490.
- [503] K.A. Deo, K.A. Singh, C.W. Peak, D.L. Alge, A.K. Gaharwar, *Tissue Eng. Part A* 26 (2020) 318–338.
- [504] Y. Hong, J. Chen, H. Fang, G. Li, S. Yan, K. Zhang, C. Wang, J. Yin, *ACS Appl. Mater. Interfaces* 12 (2020) 11375–11387.
- [505] J.M. Kelm, W. Moritz, D. Schmidt, S.P. Hoerstrup, M. Fussenegger, *Tissue Eng.* (2007) 153–166.
- [506] A. Akkouch, Y. Yu, I.T. Ozbolat, *Biofabrication* 7 (2015), 031002.
- [507] C. Norotte, F.S. Marga, L.E. Niklason, G. Forgacs, *Biomaterials* 30 (2009) 5910–5917.
- [508] M. Kameoka, *SPAST Abstr.* (2021) 1.
- [509] M.C. Biswas, S. Chakraborty, A. Bhattacharjee, Z. Mohammed, *Adv. Funct. Mater.* 31 (2021), 2100257.
- [510] S.Y. Hann, H. Cui, M. Nowicki, L.G. Zhang, *Addit. Manuf.* 36 (2020), 101567.
- [511] X. Chen, S. Han, W. Wu, Z. Wu, Y. Yuan, J. Wu, C. Liu, *Small* 18 (2022), 2106824.
- [512] K. Agarwal, V. Srinivasan, V. Lather, D. Pandita, K.S. Vasanthan, *J. Mater. Res.* (2022) 1–30.
- [513] W. Zhou, Z. Qiao, E. Nazarzadeh Zare, J. Huang, X. Zheng, X. Sun, M. Shao, H. Wang, X. Wang, D. Chen, *J. Med. Chem.* 63 (2020) 8003–8024.
- [514] M.Y. Khalid, Z.U. Arif, R. Noroozi, A. Zolfagharian, M. Bodaghi, *J. Manuf. Process.* 81 (2022) 759–797.
- [515] J. An, C.K. Chua, V. Mironov, *Int. J. Bioprinting* 2 (2016).
- [516] C. Lin, L. Liu, Y. Liu, J. Leng, *Compos. Struct.* 279 (2022), 114729.
- [517] H. Wei, S.-X. Cheng, X.-Z. Zhang, R.-X. Zhuo, *Prog. Polym. Sci.* 34 (2009) 893–910.
- [518] P. Rastogi, B. Kandasubramanian, *Biofabrication* 11 (2019), 042001.
- [519] S.R. Derkach, N.G. Voron'ko, Y.A. Kuchina, D.S. Kolotova, *Polymers* 12 (2020) 3051.
- [520] S.E. Bakarich, R. Gorkin III, M.I.H. Panhuis, G.M. Spinks, *Macromol. rapid Commun.* 36 (2015) 1211–1217.
- [521] Z. Liu, W. Tang, J. Liu, Y. Han, Q. Yan, Y. Dong, X. Liu, D. Yang, G. Ma, H. Cao, *Bioact. Mater.* 20 (2023) 610–626.
- [522] K. Ulbrich, K. Hola, V. Subr, A. Bakandritsos, J. Tucek, R. Zboril, *Chem. Rev.* 116 (2016) 5338–5431.
- [523] P. Zhu, W. Yang, R. Wang, S. Gao, B. Li, Q. Li, *ACS Appl. Mater. Interfaces* 10 (2018) 36435–36442.
- [524] Y. Zhang, L. Ionov, *ACS Appl. Mater. Interfaces* 6 (2014) 10072–10077.
- [525] U. D'Amora, T. Russo, A. Gloria, V. Rivieccio, V. D'Antò, G. Negri, L. Ambrosio, R. De Santis, *Bioact. Mater.* 2 (2017) 138–145.
- [526] R. De Santis, U. D'Amora, T. Russo, A. Ronca, A. Gloria, L. Ambrosio, *J. Mater. Sci.: Mater. Med.* 26 (2015) 1–9.
- [527] T. Kuhnt, S. Camarero-Espinosa, M. Takhsa Ghahfarokhi, M. Arreguin, R. Cabassi, F. Albertini, D. Nieto, M.B. Baker, L. Moroni, *Adv. Funct. Mater.* 32 (2022) 2202539.
- [528] H. Ding, X. Zhang, Y. Liu, S. Ramakrishna, *Int. J. Adv. Manuf. Technol.* 105 (2019) 4633–4649.
- [529] H. Okuzaki, T. Kuwabara, K. Funasaka, T. Saido, *Adv. Funct. Mater.* 23 (2013) 4400–4407.
- [530] S. Miao, H. Cui, M. Nowicki, L. Xia, X. Zhou, S.J. Lee, W. Zhu, K. Sarkar, Z. Zhang, L.G. Zhang, *Adv. Biosyst.* 2 (2018) 1800101.
- [531] J. Patdiya, B. Kandasubramanian, *Polym. -Plast. Technol. Mater.* 60 (2021) 1845–1883.
- [532] H. Shi, C. Wang, Z. Ma, *APL Bioeng.* 5 (2021).
- [533] M. Amer, X. Ni, M. Xian, R.K. Chen, *J. Eng. Sci. Med. Diagn. Ther.* (2021).
- [534] C. Maraveyas, I.S. Bayer, T. Bartzanas, *Biotechnol. Adv.* 54 (2022), 107785.
- [535] K. Zhang, A. Geissler, M. Standhardt, S. Mehlhase, M. Gallei, L. Chen, C. Marie Thiele, *Sci. Rep.* 5 (2015) 11011.
- [536] K. Kim, Y. Guo, J. Bae, S. Choi, H.Y. Song, S. Park, K. Hyun, S.K. Ahn, *Small* 17 (2021) 2100910.
- [537] Y. Cui, D. Li, C. Gong, C. Chang, *ACS nano* 15 (2021) 13712–13720.
- [538] M. Danish, P. Vijay Anirudh, C. Karunakaran, V. Rajamohan, A.T. Mathew, K. Koziol, V.K. Thakur, C. Kannan, A. Balan, *J. Appl. Polym. Sci.* 138 (2021) 50903.
- [539] K. Hussain, Z. Aslam, S. Ullah, M.R. Shah, *Chem. Phys. Lipids* 238 (2021), 105101.
- [540] G. Kocak, C. Tuncer, V. Büttün, *Polym. Chem.* 8 (2017) 144–176.
- [541] M. Du, B. Chen, Q. Meng, S. Liu, X. Zheng, C. Zhang, H. Wang, H. Li, N. Wang, J. Dai, *Biofabrication* 7 (2015), 044104.
- [542] K. Markstedt, A. Mantas, I. Tournier, H. Martínez Ávila, D. Hagg, P. Gatenholm, *Biomacromolecules* 16 (2015) 1489–1496.
- [543] J. Hill, R. Wildman, A. Mata, *Curr. Opin. Biotechnol.* 74 (2022) 42–54.
- [544] C.D. Devillard, C.A. Mandon, S.A. Lambert, L.J. Blum, C.A. Marquette, *Biotechnol. J.* 13 (2018) 1800098.
- [545] M. Montgomery, S. Ahadian, L. Davenport Huyer, M. Lo Rito, R.A. Civitarese, R. D. Vanderlaan, J. Wu, L.A. Reis, A. Momen, S. Akbari, *Nat. Mater.* 16 (2017) 1038–1046.
- [546] B. Gao, Q. Yang, X. Zhao, G. Jin, Y. Ma, F. Xu, *Trends Biotechnol.* 34 (2016) 746–756.
- [547] A. Zhang, C.M. Lieber, *Chem. Rev.* 116 (2016) 215–257.
- [548] L.P.C. Gomez, A. Spangenberg, X.A. Ton, Y. Fuchs, F. Bokeloh, J.P. Malval, B. Tse Sum Bui, D. Thuau, C. Ayela, K. Haupt, *Adv. Mater.* 28 (2016) 5931–5937.
- [549] C. Credi, A. Fiorese, M. Tironi, R. Bernasconi, L. Magagnin, M. Levi, S. Turri, *ACS Appl. Mater. Interfaces* 8 (2016) 26332–26342.
- [550] X. Cui, G. Yao, Y. Qiu, *Biotechnol. Lett.* 35 (2013) 315–321.
- [551] M. López-Valdeolivas, D. Liu, D.J. Broer, C. Sánchez-Somolinos, *Macromol. Rapid Commun.* 39 (2018), 1700710.
- [552] A. Nishiguchi, A. Mourran, H. Zhang, M. Möller, *Adv. Sci.* 5 (2018), 1700038.
- [553] J.U. Lind, T.A. Busbee, A.D. Valentine, F.S. Pasqualini, H. Yuan, M. Yadid, S.-J. Park, A. Kotikian, A.P. Nesmith, P.H. Campbell, *Nat. Mater.* 16 (2017) 303–308.
- [554] H. Elsayed, P. Rebesan, G. Giacomello, M. Pasetto, C. Gardin, L. Ferroni, B. Zavan, L. Biasetto, *Mater. Sci. Eng.: C* 103 (2019), 109794.
- [555] C. Domínguez-Trujillo, F. Terner, J.A. Rodríguez-Ortiz, S. Heise, A.R. Boccaccini, J. Lebrero, Y. Torres, *Surf. Coat. Technol.* 349 (2018) 584–592.
- [556] A.M. Beltrán, B. Begines, A. Alcidia, J.A. Rodríguez-Ortiz, Y. Torres, *ACS Appl. Mater. Interfaces* 12 (2020) 30170–30180.
- [557] V. Barranco, A. Jimenez-Morales, E. Peón, G. Hickman, C. Perry, J. Galvan, J. Mater. Chem. B 2 (2014) 3886–3896.
- [558] C. Domínguez-Trujillo, E. Peón, E. Chicardi, H. Pérez, J.A. Rodríguez-Ortiz, J. Pavón, J. García-Couce, J. Galván, F. García-Moreno, Y. Torres, *Surf. Coat. Technol.* 333 (2018) 158–162.
- [559] P. Trueba, M. Giner, A. Rodríguez, A.M. Beltrán, J.M. Amado, M.J. Montoya-García, L.M. Rodriguez-Albelo, Y. Torres, *Surf. Coat. Technol.* 422 (2021), 127555.
- [560] R. Vilar, (2016).
- [561] B.E. Lee, H. Exir, A. Weck, K. Grandfield, *Appl. Surf. Sci.* 441 (2018) 1034–1042.
- [562] A. Civantos, A. Mesa-Restrepo, Y. Torres, A.R. Shetty, M.K. Cheng, C. Jaramillo-Correia, T. Aditya, J.P. Allain, J. Biomed. Mater. Res. Part A (2023).
- [563] J. Allain, M. Echeverry-Rendón, J. Pavón, S. Arias, *Nanostructured biointerfaces Nanopatterning and Nanoscale Devices for Biological Applications (p)*, CRC Press., Boca Raton, FL, 2014.
- [564] J.J. Pavón, D. López, F. Mondragón, J. Gallego, S.L. Arias, K. Luitjohan, B. Holybee, Y. Torres, J.A. Rodríguez, M. Echeverry-Rendón, *J. Biomed. Mater. Res. Part A* 107 (2019) 719–731.
- [565] J. Gaviria, A. Alcidia, B. Begines, A.M. Beltrán, J. Villarraga, R. Moriche, J. A. Rodríguez-Ortiz, Y. Torres, *Surf. Coat. Technol.* 406 (2021), 126667.
- [566] A.M. Beltrán, A. Civantos, C. Domínguez-Trujillo, R. Moriche, J.A. Rodríguez-Ortiz, F. García-Moreno, T.J. Webster, P.H. Kamm, A.M. Restrepo, Y. Torres, *Metals* 9 (2019) 995.

- [567] F. Accioni, G. Rassu, B. Begines, L.M. Rodríguez-Albelo, Y. Torres, A. Alcudia, E. Gavini, *Pharmaceutics* 14 (2022) 1244.
- [568] I.S. Bayer, *Materials* 10 (2017) 748.
- [569] A.M. Pinto, S. Moreira, I.C. Gonçalves, F.M. Gama, A.M. Mendes, F.D. Magalhães, *Colloids Surf. B: Biointerfaces* 104 (2013) 229–238.
- [570] Y. Yang, A.M. Asiri, Z. Tang, D. Du, Y. Lin, *Mater. Today* 16 (2013) 365–373.
- [571] G. Martínez, B. Begines, E. Pajuelo, J. Vázquez, L.M. Rodriguez-Albelo, D. Cofini, Y. Torres, A. Alcudia, *Biomacromolecules* (2023).
- [572] J. Yang, J. Wu, Z. Guo, G. Zhang, H. Zhang, *Cells* 11 (2022) 3298.
- [573] J. Zhang, C. Ding, L. Ren, Y. Zhou, P. Shang, *Prog. Biophys. Mol. Biol.* 114 (2014) 146–152.
- [574] H.-M. Yun, S.-J. Ahn, K.-R. Park, M.-J. Kim, J.-J. Kim, G.-Z. Jin, H.-W. Kim, E.-C. Kim, *Biomaterials* 85 (2016) 88–98.
- [575] J.C. Souza, M.B. Sordi, M. Kanazawa, S. Ravindran, B. Henriques, F.S. Silva, C. Aparicio, L.F. Cooper, *Acta Biomater.* 94 (2019) 112–131.
- [576] Y. Zhang, P. Xiu, Z. Jia, T. Zhang, C. Yin, Y. Cheng, H. Cai, K. Zhang, C. Song, H. Leng, *Colloids Surf. B: Biointerfaces* 169 (2018) 366–374.
- [577] M. Hoyos-Nogués, J. Buxadera-Palomero, M.-P. Ginebra, J.M. Manero, F. Gil, C. Mas-Moruno, *Colloids Surf. B: Biointerfaces* 169 (2018) 30–40.
- [578] M. Hoyos-Nogués, F. Velasco, M.-P. Ginebra, J.M. Manero, F.J. Gil, C. Mas-Moruno, *ACS Appl. Mater. Interfaces* 9 (2017) 21618–21630.
- [579] A. Agrelli, N.F. Vasconcelos, R.C.Sd Silva, C.L. Mendes-Marques, I.R.D.S. Arruda, P.S.S.D. Oliveira, L.R.L. Santos, A.N.D. Andrade, R.R.D. Moura, L.C. Bernardo-Menezes, *Int. J. Mol. Sci.* 23 (2022) 14048.
- [580] X. Duan, X. Zhu, X. Dong, J. Yang, F. Huang, S. Cen, F. Leung, H. Fan, Z. Xiang, *Mater. Sci. Eng.: C* 33 (2013) 3951–3957.
- [581] C.O. Crosby, B. Stern, N. Kalkunte, S. Pedahzur, S. Ramesh, J. Zoldan, *Rev. Chem. Eng.* 38 (2022) 347–361.
- [582] A.E. Erickson, J. Sun, S.K. Lan Levengood, S. Swanson, F.-C. Chang, C.T. Tsao, M. Zhang, *Biomed. Micro* 21 (2019) 1–16.
- [583] S. Korpayev, G. Kaygusuz, M. Şen, K. Orhan, Ç. Oto, A. Karakeçili, *Int. J. Biol. Macromol.* 156 (2020) 681–690.
- [584] A. Roffi, E. Kon, F. Perdisa, M. Fini, A. Di Martino, A. Parrilli, F. Salamanna, M. Sandri, M. Sartori, S. Sprio, *Int. J. Mol. Sci.* 20 (2019) 2227.
- [585] C. Boyer, G. Réthoré, P. Weiss, C. d'Arros, J. Lesoeur, C. Vinatier, B. Halgand, O. Geffroy, M. Fusellier, G. Vaillant, *Front. Bioeng. Biotechnol.* 8 (2020), 23.



Amir Elhadad received his Ph.D. from Carlos III university of Madrid, Spain. His thesis focused on designing novel coatings for biomedical applications. He is currently working as a Research associate at College of dental medicine, Qatar university.



Ana Rosa Sainz earned her Ph.D. in the Department of Mechanical Engineering and Manufacturing at the University of Seville. Her doctoral thesis focused on analyzing conventional and incremental forming of polymeric sheets. The research explored the manufacturing of various medical prostheses using single-point incremental forming with biocompatible polymeric sheets. Her main research interests revolve around manufacturing processes, with a particular emphasis on incremental forming and additive manufacturing, as well as materials science. Her investigations have resulted in multiple publications in international journals and conferences.



Raquel Cañete is an industrial design engineer and interaction designer, currently pursuing a Ph.D. and working as a pre-doctoral researcher at the Higher Polytechnic School of the University of Seville. She works in the Department of Design Engineering and the Department of Materials and Transportation Engineering and Science. Raquel's research is focused on social sustainability and inclusive design, designing and developing assistive technology and smart products for children with autism, highlighting the importance of materials and sensoriality. Her results have led to several publications in international journals and conferences, and have earned her distinctions such as a Fulbright Scholarship.



Estela Peralta is an Associate Professor of Project Engineering and Product Design in the Department of Engineering Design at the University of Seville. She earned her degree in Industrial Design Engineering in 2009, followed by a Master's in Environmental Engineering in 2011. In 2016, she successfully completed her Doctoral Degree in Manufacturing Engineering, and her doctoral thesis was recognized with the Doctoral Extraordinary Award. Peralta's research interest and expertise lie in the field of designing and manufacturing sustainable products and systems tailored to the human factor and environmental context.



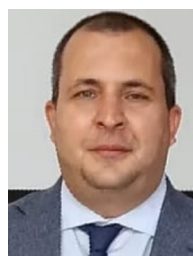
Dr. Belén Begines holds an MSc in Chemistry (2005) and a PhD in Organic Chemistry (2011) from the University of Seville. Her doctoral work focused on biodegradable polyurethanes and polyureas derived from carbohydrates for biomedical applications. After a postdoctoral stint at the University of Seville, she joined the Additive Manufacturing Centre at the University of Nottingham as a Research Fellow, exploring 3D printing of biocompatible polymeric materials. She returned to the University of Seville as an Assistant Professor in Organic and Medicinal Chemistry in 2017. Currently, she is part of the Applied Medicinal Chemistry Group, researching surface modification of Ti-based implants and developing polymeric composite and Ti-based biphasic implants for osteochondral injury treatment.



Mario Balbuena completed his Master's in Biomaterials at the Complutense University of Madrid, Spain, where he studied the effect of microfluidics on the adhesion, proliferation, and osteogenic differentiation of mesenchymal stem cells on Ti6Al4V scaffolds. Currently, he works in the Applied Pharmaceutical Chemistry Research Group at the University of Seville, Spain, studying the fabrication of personalized biphasic implants for the treatment of osteochondral defects.



Ana Alcudia's research journey began after graduating in Chemical Sciences from the University of Seville in 1994, eventually leading to her current position as an Associate Professor in Organic and Medicinal Chemistry since 2011. She pursued her PhD in "Optimally Pure N-sulfonilimines: Application to the Synthesis of Aziridines and Aminoalcohols," earning outstanding qualifications and an Extraordinary Doctorate Award in 1999. Following this, she undertook a postdoctoral stay at Emory University, focusing on molybdenum complex synthesis and its applications to biological products. Her research took her to Johnson and Johnson Pharmaceuticals Laboratories and PharmaMar S.A. Later, she secured a postdoctoral research contract at CSIC.



Dr. Torres is a Full Professor at Seville University, serving as the Deputy Director of Postgraduate Studies and R&D+i at the Polytechnic School, and leading the research line on Advanced Porous Applications. His primary research areas and expertise lie in the design and manufacturing of custom-made porous materials, surface modification, as well as the bio-functional and tribomechanical behavior of materials for biomedical applications.